UNIVERSITAT DE BARCELONA

Implications of Structural Stability for Drug Design

Maciej Majewski

Universitat de Barcelona
Facultat de Farmàcia i Ciències de l'Alimentació

Implications of Structural Stability for Drug Design

Maciej Majewski

2020

Programa de Doctorat en Biomedicina, Universitat de Barcelona
Director de Tesi: Dr. Xavier Barril Alonso

UNIVERSITAT DE BARCELONA

FACULTAT DE FARMÀCIA I CIÈNCIES DE L'ALIMENTACIÓ

DEPARTAMENT DE FARMÀCIA I TECNOLOGIA FARMACÈUTICA I FISICOQUÍMICA

PROGRAMA DE DOCTORAT EN BIOMEDICINA

IMPLICATIONS OF STRUCTURAL STABILITY FOR DRUG DESIGN

Aquesta tesi ha estat realitzada per Maciej Majewski sota la direcció del Dr. Xavier Barril Alonso, Professor d'Investigació ICREA en el Departament de Farmàcia i Tecnologia Farmacèutica i Fisicoquímica de la Facultat de Farmàcia i Ciències de l'Alimentació de la Universitat de Barcelona. Es presenta aquesta memòria per optar al títol de doctor per la Universitat de Barcelona en el Programa de Doctorat en Biomedicina.

Xavier Barril Alonso	Maciej Majewski
Director de tesi	Doctorand

Maciej Majewski
Marzo 2020

Mamo, Tato, Agnieszko,
To dla was

Acknowledgements

It has been a long journey getting to this point. I have always wanted to get a PhD, so four years ago I packed my bags and moved to Spain. At first it was easy and exciting, but then, life happened and through all the struggle and self-doubt I started to believe I would never manage to achieve this goal. But here I am doing it. And it feels great!

This is my small contribution to scientific world and it would not be possible without an input and support of many amazing people. First, a to all members of Barril lab: Andrea, Marina, Miriam, Moira, Morena, Serena, Álvaro, Alex, Carles, Dylan, Guillermo, Juan and Salvo. Thank you for creating a friendly and stimulation environment. Also former members Peter and Sergio, who had a major input in this work as well as my initial training. Also Sharon and Janet for being the best work companion I could ever imagine.

I would like to also acknowledge EU Horizon 2020 program, Marie Skłodowska-Curie ITN FRAGNET for funding my salary and giving me best conditions possible to complete a PhD project. Thanks to all the PIs, ESRs and partners involved in the network, especially Chris de Graaf and Sosei Heptares, Ben Davies and Vernalis Research, and David. This was truly an amazing opportunity in every aspect possible. I had a blast.

Most importantly Xavi, the best supervisor one could ever wish for. Thank you for taking a chance on me, for believing in me and for your constant support. Gràcies.

It is also the place to acknowledge my own privilege. I grew up in a stable home, had an access to free education, including the University, and it would be unfair of me an all people without same opportunities, to claim I achieved it all on my own.

Najwieksze podziekowania naleza sie rowniaz mojej rodzinie: Renacie, Jarolawowi i Agnieszcze Majewskim. Rowniez dziadkom Urszuli, Jurkowi, Janinie i Zenonowi. Dziekuje za sworzenie stabilnego domu, wolnego od stresu gdzie moglem sie skupic na nauce i rozwinac swoj prawdziwy potencial. Bez waszego wspacia, szczegulnie w ciezkich miesiacach doktoratu, powstanie tej pracy nie byloby mozliwe.

And finally the two reasons I wake up every morning; Louis and Lito. Thank you for making every day a little brighter.

Table of contents

Chapter 1

Introduction

1.1 Overview of Drug Discovery

Finding new drugs and therapies for a disease, that has effective treatment, is an extremely challenging task. The process starting from target identification to drug's approval takes around 12-15 years and cost billions of euros,[1] with the success rate of such process being less than 10%.[2] Figure 1.1 illustrates the stages of the process.

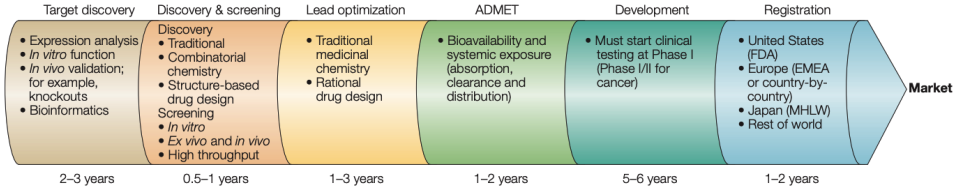

Fig. 1.1 Stages of the drug development process from target discovery to registration. Graphics adapted from [3]

The first and one of the essential steps in drug development is target identification and validation. Target is a biological entity (protein, gene or RNA) that causes a disease. It can be identified using experimental techniques (biochemical methods, genetic manipulation or phenotypic screening) or by data-mining of available biological data. The use of bioinformatics in prioritizing potential targets has improved the process significantly.[4] Next, the target needs to be validated, to confirm that targeting it will cause a desired pharmacological effect. Validation can be achieved in various ways starting from *in vitro* knockouts to use of whole animal models. The target, except for playing a vital role in the causation and progression of the disease, should also be "druggable". This means that it can be bound by a drug molecule, that influences its function and causes an observable effect.[5, 6]

The next step is hit identification and lead discovery. A "hit" molecule is a compound with the desired activity against the tested target. Many experimental techniques exist for screening chemical libraries to find hits, with most popular being high throughput screening[7] and fragment screening.[8]

Detected hits are later validated with complementary assays and become a starting point for the lead discovery phase. At this step, each hit is refined to produce more potent compounds, suitable for *in vivo* experiments - leads.

In the lead optimization step, candidate molecules undergo extensive medicinal chemistry optimization in order to maintain desirable properties and improve on lacking ones. This step is a series of iterations of chemical synthesis, producing series of analogues with a particular focus on improving pharmacokinetic and ADMET properties (Absorption, Distribution, Metabolism, Excretion and Toxicity), and ends with a clinical candidate.

Successful clinical candidates are taken to clinical trials. There are four phases of clinical trials. The objective of phase I is to determine the safety and dosing on healthy volunteers. Phase II includes patients affected by the disease and is used to study safety, side effects and measure the efficacy of the drug. In phase III, the effectiveness of the drug is measured on a large group of affected patients. If the drug proves to be successful, it gets approved and registered by appropriate organs and enters the market. The last phase VI of the process monitors long-term side effects after the drug enters the market.

1.2 Structure-Based Drug Discovery

The speed of drug discovery campaign can depend on the amount of available knowledge about the system. From the libraries of active compounds to 3D structures of the protein, a new project very often has a solid foundation in the previous research. If the structure of the target protein is known, the rational approach is to apply *Structure-Based Drug Design* (SBDD). Its goal is to use the structural information about the target and possible ligands for rational design and optimization of future compounds. The first protein structures were determined by X-ray crystallography in the 1950s,[9] creating the base for this approach. Since then, the amount of experimental data has grown exponentially. The progress has been made mostly due to

significant technological improvements in X-ray crystallography[10], but also the development of new techniques, e.g. nuclear magnetic resonance (NMR)[11] and transmission electron cryomicroscopy (cryo-EM).[12] The advances in the field allowed determination of structures as complex as human ribosome [13] or as challenging as membrane proteins, including a class of therapeutically relevant G-protein coupled receptors (GPCRs). [14] Currently, the biggest on-line resource gathering structural information about biomolecules is Protein Data Bank (PDB).[15] At the date of writing this thesis, the database contained more than 150.000 entries (Fig.1.2).

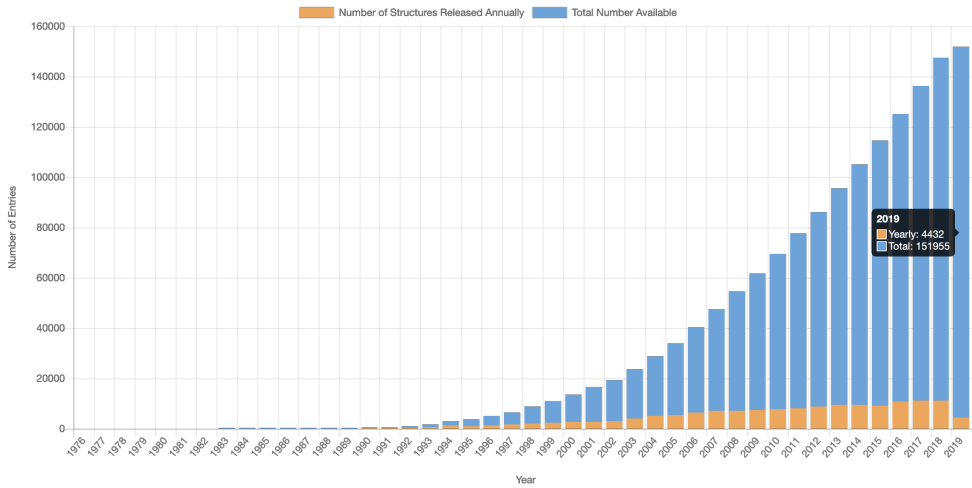

Fig. 1.2 Number of structures deposited in PDB per year. Data sourced from [16]

1.2.1 Molecular Recognition

Molecular recognition refers to a specific pattern of interactions that two molecules make through non-covalent bonds. In the context of biological molecules, patterns formed by proteins and ligands are highly repetitive and understanding how molecules bind gives a predictive power for drug design.

Currently, PDB contains more than 150.000 structures of proteins, and around 75% contains a ligand. With such a vast resource at hand, relevant information on the nature, geometry, and frequency of atomic interactions was described.[17] This knowledge has been used in lead optimization, improvement of docking scoring function in virtual screening, development of protein-ligand interaction fingerprints, and help interpret Structure-Activity Relationship (SAR) data.

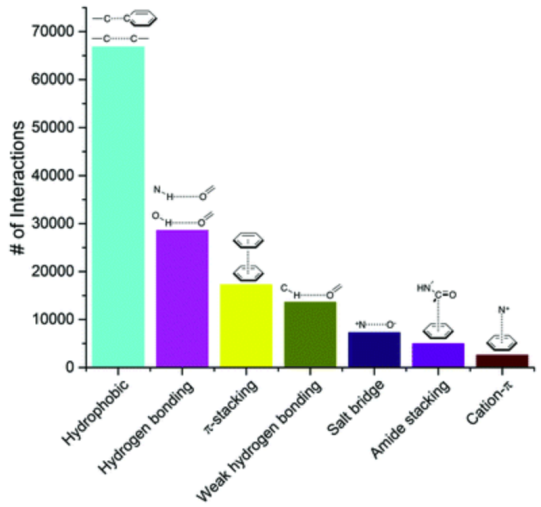

Fig. 1.3 Frequency distribution of the most common non-covalent interactions observed in protein–ligands extracted from the PDB. Graphics sourced from [17]

The most common interactions in protein-ligand complexes are hydrophobic contacts (Fig.1.3), formed by carbon and carbon, halogen or sulfur atom. The contacts between an aliphatic carbon in the receptor and an aromatic carbon in the ligand are the most abundant. [17] This type of interaction is the main contributor of drug-receptor binding. The energetic gain of burying solvent-exposed methyl group into a hydrophobic cavity is about 0.7 kcal mol^{-1} or a 3.2-fold increase in binding constant per methyl group.[18]

The second most common interaction are hydrogen bonds, formed between two electronegative atoms (e.g. nitrogen and oxygen) that share hydrogen. Due to their sharp distance and angular dependencies, hydrogen bonds are providing defined geometry in biological complexes [19, 20] and are contributing to the specificity of molecular recognition.[21] Their contribution to binding free energy can vary between -1.5 to -4.7 kcal mol^{-1}, depending on the molecular context. [18] Usually, a hydrogen bond that is buried in the binding pocket contributes more to the binding free energy, than a similar bond that is solvent-exposed.[22] Forming a new hydrogen bond can also be unfavourable if the desolvation cost is higher than the energetic gain from the new interaction.[23]

Due to the desolvation effect, the transitional penalty of breaking hydrogen bond can be much higher than 5 kcal mol^{-1}.[24] The previous research conducted in the group has shown the existence of water-shielded hydrogen bonds, for which the cost of breaking the interaction is particularly high.[25] In effect, these bonds are acting as kinetic traps.

Other, less frequent interactions include:

- π-stacking - An interaction formed between aromatic rings that can be considered as a subclass of hydrophobic interactions.[26]

- Weak hydrogen bonds - Hydrogen bonds, where a carbon atom is playing the role of hydrogen bond donor. Their contribution to binding energy is minor.[27] However, they take part in protein folding stabilization,[28] enzyme catalysis[29] and in the stabilization of protein-ligand complexes.[30, 31]

- Salt bridges - Contacts formed between a positively charged and negatively charged atoms. Similar to hydrogen bonds, their contribution in binding is highly dependent on the context. In most of the cases, energetic gains are minimal, due to the substantial penalty of desolvating charged groups.[32, 33]

- Amide-π stacking - A bond occurring between an amide group and an aromatic ring.
- Cation-π stacking - An interaction formed by an aromatic ring and a positively charged nitrogen atom. It is known to determine the structure and function of a protein.[34]
- Halogen bonds - A bond occurring between the σ-hole of a halogen atom and a nucleophile. It is not very frequent in protein-ligand complexes. However, it is widely used by medicinal chemists to increase the affinity, the membrane permeability and metabolic stability of compounds.[17]
- Water bridges - A particular type of hydrogen bonds, where a network of structurally stable water molecules mediates the interaction between ligand and protein.
- The last type of interaction are bonds with metals.

Figure 1.4 depicts some of the interactions discussed above.

Molecular recognition is more complicated than just a sum of interactions between protein and ligand. The interactions described above contribute to binding free energy (ΔG) through enthalpy of binding (ΔH), defined as the changes in energy resulting from the formations of non-covalent interactions at the binding interface.[37] This contribution should also include the effect of the solvent and distortion of interactions made in an unbound state. The second component to binding free energy is entropy (ΔS) that measures the distribution of heat energy over the thermodynamic system (Equation 1.1).

$$\Delta G = \Delta H - T\Delta S \tag{1.1}$$

The entropy of binding can be divided into the following terms (Equation 1.2). ΔS_{solv} is the change of the entropy of solvent, associated mainly with the

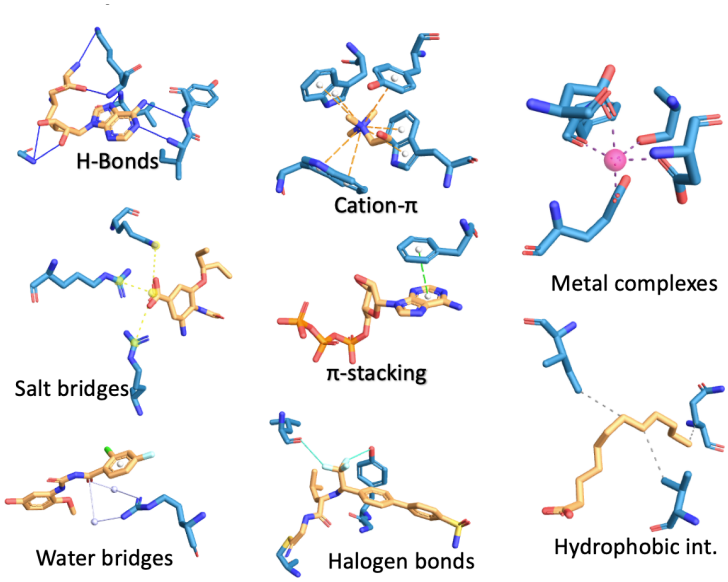

Fig. 1.4 Types of non-covalent interactions in protein-ligand complexes. Graphics created using [35, 36]

release of solvent molecules upon binding, usually contributing favourably to the binding. ΔS_{conf} is the change in conformational entropy that correspond to change in conformational freedom of the protein and the ligand, and it can make a favourable or unfavourable contribution depending on the molecular context.[38, 39] $\Delta S_{r/t}$ is the loss of rotational and translational degrees of freedom upon binding and always contributes unfavourably to the binding. This penalty has to be overcome through either solvent entropy gain (ΔS_{solv}) or large favourable enthalpic gain (molecular interactions).[40]

$$\Delta S = \Delta S_{solv} + \Delta S_{conf} + \Delta S_{r/t} \tag{1.2}$$

The binding, like all chemical processes, is driven by decreases of the binding free energy (ΔG), so its main contributors ΔH and ΔS will play a significant role. For example, a complex that forms multiple favourable non-covalent interactions will have a large negative enthalpy change associated

with binding. However, the restriction of mobility of both protein and ligand will cause a negative entropy change, resulting in a medium-magnitude change in ΔG.[41] On the other hand, an entropy gain is usually associated with an enthalpic penalty because of the energy required for disrupting non-covalent interactions. This delicate balance between these two values is called the enthalpy–entropy compensation. This physical phenomenon has been shown in both experimental[42–44] and theoretical studies.[45, 46] The compensation is influenced by the properties of the solvent, the structure and flexibility of both the ligand and the binding pocket, and changes of forces during binding. [41, 45, 47–50] The effect of enthalpy and entropy is important for rational drug design. The optimization campaigns aim to maximize favourable contributions and minimize penalties.

1.2.2 Structural Stability

In structure-based drug design, binding free energy (ΔG) is the parameter that characterizes binding. Much effort has been made to predict ΔG, in order to guide drug design. Some methods (e.g. docking) approximate the value with a scoring function. However, they often struggle with protein and ligand flexibility and solvation effects, making them imperfect and their performance disappointing [51]. Other methods, like free energy perturbations, perform an extensive simulation with the alchemical transformation of the ligand. They, on the other hand, rely on preexisting data and can be computationally expensive [52].

Blind focus on a single value can be quite dangerous. In SBDD, we are not only interested in the affinity of the compound but also in the way it binds to the target. The structural information is essential to guide the development of a drug candidate. In principle the true binding mode should correspond to the global minimum of binding free energy, making it a useful guideline. However, in practice, a low value of affinity does not mean that the ligand will form a stable binding mode with a protein.

In their recent work, Borgia et al. presented a great example, where a protein-protein complex with picomolar affinity lacks structure.[53] Some efforts have been made to draw attention to from thermodynamics to kinetics, trying to predict k_{off} or residence time [54]. However, the results of some project are criticized as "incomplete and misleading" and the use of residence time as a way to drive a drug discovery program is described as "sub-optimal" [55].

We have postulated that binding can be characterized by structural stability (or structural robustness), which is the ability to form a precise and stable binding mode. This can be translated into active ligands presenting a deep and narrow free energy minimum in the bound state (Fig.1.5). Structural stability can be quantified by introducing small perturbation, usually a displacement of a ligand from its position of equilibrium to a nearby quasi-bound (QB) state where a preselected interaction has just been broken and measuring the energy necessary to perform this action.[56] It is essential to highlight the difference between binding free energy and structural stability. ΔG is simply a difference in energy between bound and unbound state. Structural stability, on the other hand, characterized the steepness of a local minimum. It is quite interesting that the property that is not related to ΔG, based on the quasi-bound state that is thermodynamically irrelevant, works so well in virtual screening.[56]

Structural stability originates from sharp energy barriers that keep atoms in the minimum of energy. The barriers that determine binding kinetics can be caused by intramolecular (i.e., conformational rearrangement), bimolecular (e.g., repulsive transitional configurations) or many-body effects (e.g., desolvation).[58] Hydrogen bonds are perfect candidates to provide structural stability for many reasons. They have very strict distance and angular dependencies [59] and are one of the most frequent interactions in protein-ligand complexes (see section 1.2.1). Due to the desolvation effect, the transitional penalty of breaking hydrogen bond can be quite substantial [24], which is the case for water-shielded HBs, that act as kinetic traps.[25]

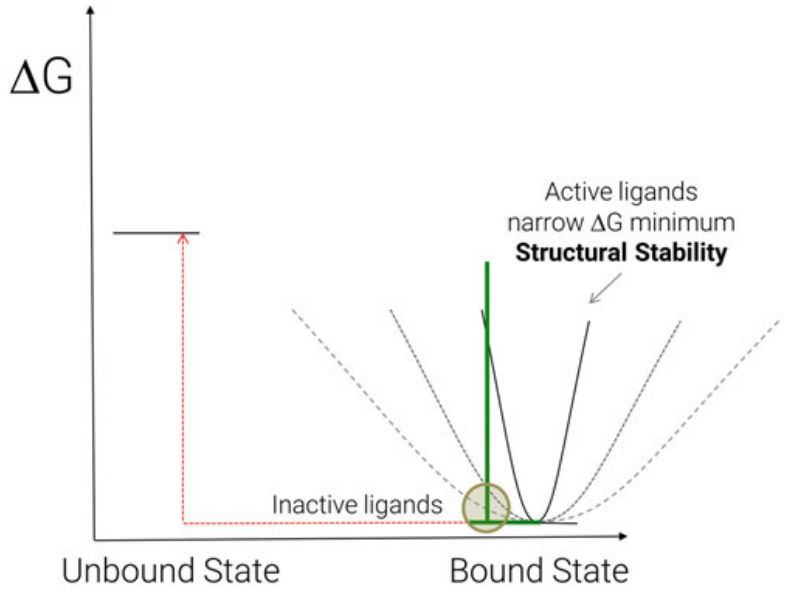

Fig. 1.5 Graphical representation of the quasi-bound state (green lines and circle) in relation to bound and unbound states. Graphics sourced from [57].

Even though structural stability has been proved as a useful property, the real meaning and extent of applicability remain unknown. This thesis will try to expand the concept.

1.3 Computer-Aided Drug Discovery

Computers have been used to accelerate drug discovery for decades. From data acquisition to its analysis, computations find new applications every year. A complete overview of computational methods in drug discovery is a material for a book, so here we will only focus on the methods relevant for the work presented, mainly molecular docking and molecular dynamics. Both of them can be used to rationalize experimental results, but their primary purpose is to make valid predictions about future experiments and reduce the cost of research.

1.3.1 Molecular Docking

Molecular docking is particularly well-known and widely applied due to its high speed and efficiency.[60, 61] It aims to accurately predict ligands conformation and orientation in the binding pocket - a so-called binding mode.[62] A scoring function that aims to approximate the affinity with the target protein through the evaluation of molecular interactions assesses the fit.[61] However, the forces that drive molecular recognition are not easy to understand and even more difficult to simulate by computer.

Many protein-ligand docking programs have been developed and applied in drug discovery projects, including Glide,[63, 64] ICM,[65] rDock,[66] DOCK,[62] GOLD,[67, 68] FlexX[69] and Auto-dock[70]. Most of them work similarly in a multi-step process. The first step is the generation of small molecule's conformation and orientation in the binding pocket, and the second step is evaluation of that pose by a scoring function.

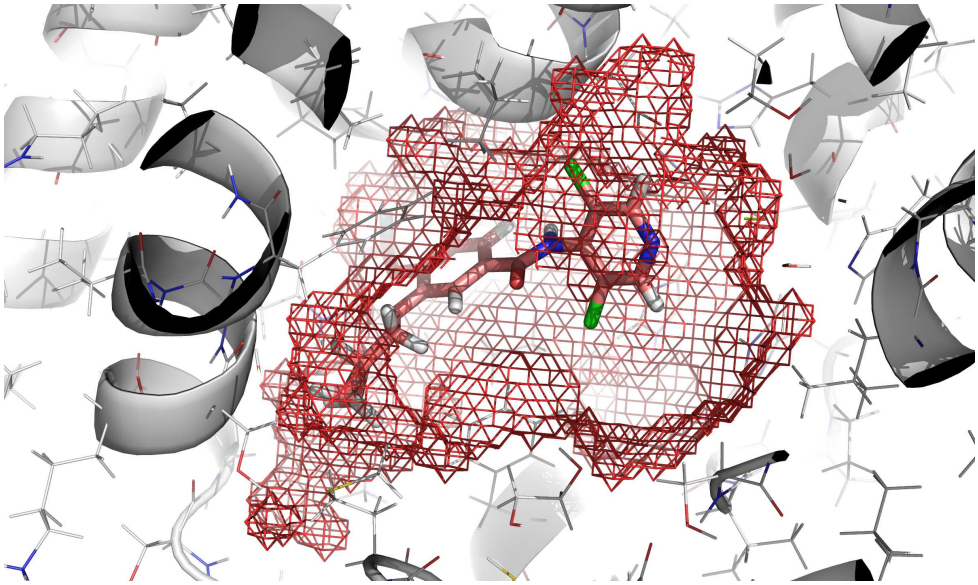

Fig. 1.6 Ligand docked to its binding pocket. Red mesh represents a cavity. Graphics adapted from [71].

The first task, pose generation, can be challenging because even small molecules can have many degrees of freedom that need to be sampled accurately and fast enough to process thousands or millions of compounds. Different programs use different search algorithms that fall into two categories: systematic and stochastic. Systematic approaches aim to sample all degrees of freedom in the molecule. For a molecule with N rotatable bonds, the number of possible conformations N_{conf} is given by equation 1.3 (where θ_i is the size of incremental rotational angle for bond i). Having that in mind, we can see that for bigger molecules, the number of conformations can easily "explode" to non-feasible number. To address that problem ligands are usually incrementally grown into the binding pockets, which can be achieved by defining rigid fragment of the molecule (core), and placing it in the active side. Then the program adds remaining parts of the molecule in a step-wise process, simultaneously exploring possible conformational space of each bond.[72, 69, 73] Other systematic approaches use libraries of pregenerated possible conformations and then performs rigid-body docking.[74] Stochastic algorithms, on the other hand, are making random changes that are later evaluated by a predefined probability function. Popular implementations include Monte Carlo search[75, 76], genetic algorithms[77, 68] and tabu search algorithm.[78, 79]

$$N_{conf} = \prod_{i=1}^{N} \frac{360}{\theta_i} \tag{1.3}$$

In the second step of docking, a scoring function evaluates generated poses. All scoring functions aim to approximate binding free energy with a simplified calculation and can be divided into three classes: force field-based, empirical and knowledge-based. Force field based functions quantify the energy of ligand-receptor interactions and ligand's internal energy. Such scoring functions are based on force field parameters, e.g. AutoDock[70] is based in AMBER force field.[80] More about force fields will be discussed in the section Molecular Dynamics. The main disadvantage of this approach

is that by evaluating interactions in a static image of a complex, we neglect solvation and entropy.

Empirical scoring functions are usually a sum of several parametrized functions that aim to reproduce experimental data, e.g. binding energies.[81] As exemplified with rDock's scoring function (equations 1.4-1.8),[66] many component functions are representing functional terms, e.g. Van der Waals, polar, repulsive, aromatic, solvation and other. The weights of each component are obtained from regression analysis or using modern machine learning approaches.[82, 83] The main advantage is their simplicity and speed, making them ideal for high throughput applications. Additionally, they have terms accounting for non-enthalpic contributions - entropy[84] and solvation.[85, 86] However, the performance of empirical scoring functions is highly dependent on data that was used for training. Therefore, they may not be fully representative of chemical matter.

$$S^{total} = S^{inter} + S^{intra} + S^{site} + S^{restraint} \tag{1.4}$$

$$S^{inter} = W^{inter}_{vdw} S^{inter}_{vdw} + W^{inter}_{polar} S^{inter}_{polar} + W^{inter}_{repul} S^{inter}_{repul} + W^{inter}_{arom} S^{inter}_{arom} + \\ + W_{solv} S_{solv} + W_{rot} N_{rot} + W_{const} \tag{1.5}$$

$$S^{intra} = W^{intra}_{vdw} S^{intra}_{vdw} + W^{intra}_{polar} S^{intra}_{polar} + W^{intra}_{repul} S^{intra}_{repul} + W^{intra}_{dihedral} S^{intra}_{dihedral} \tag{1.6}$$

$$S^{site} = W^{site}_{vdw} S^{site}_{vdw} + W^{site}_{polar} S^{site}_{polar} + W^{site}_{repul} S^{site}_{repul} + W^{site}_{dihedral} S^{site}_{dihedral} \tag{1.7}$$

$$S^{total} = W_{cavity} S_{cavity} + W_{tether} S_{tether} + W_{nmr} S_{nmr} + W_{ph4} S_{ph4} \tag{1.8}$$

Knowledge-based scoring functions are designed to reproduce experimental structures (unlike empirical scoring functions that aim to reproduce binding free energies). They are constructed from atomistic pair potentials that reflect statistics of interactions across experimental structures.[87] Similarly to empirical scoring functions, their advantage is speed and simplicity,

but they fail to evaluate interactions that are underrepresented in limited sets of protein-ligand complex structures.

Following the logic of "wisdom of the crowd", another category of scoring functions exists - consensus scoring. They combine different scoring strategies to balance errors made by each one of them.[88] An example of such scoring function is X-CSCORE that uses GOLD-like, ChemScore, DOCK-like, FlexX and PMF scoring functions.[89] However, given that most of the scoring functions have similar constructions and were trained on similar data, the errors might amplify instead of balance, reducing the popularity of consensus scoring.

Depending on the task, different combinations of the methods presented above are applied. For virtual screening, where the objective is to process millions of compounds, a less accurate sampling algorithm with a simple scoring function can be applied. On the other side of the spectrum, for binding mode prediction, sampling algorithms should account for protein flexibility, and generated poses are evaluated with a full atomistic molecular dynamics.[90]

1.3.2 Molecular Dynamics

Molecular docking usually works with static images of proteins and small molecules. With molecular dynamics simulations, we can put those images into motion and get a more realistic view of biological systems. Ever since the first implementation of this method in 1977 by the Karplus group,[91] many simulation programs have been developed, with most popular being CHARMM,[92] AMBER,[93] GROMACS[94] and OpenMM.[95] They all study interaction and motion of atoms based on Newton's laws of motion. The time-dependent behaviour of the simulated system can be obtained by iterative solving of Newton's second law over small time steps (equation 1.9).

$$f_i(t) = m_i a_i(t) = -\frac{\partial V(x(t))}{\partial x(t)} \tag{1.9}$$

where $f_i(t)$ is the force acting on atom i, m_i is its mass and $a_i(t)$ is acceleration. $x(t)$ is the configuration of the system at given time t represented in $3N$ dimensional space, with N being the number of atoms in the system. Finally, $V(x(t))$ is the potential energy function, usually called a Force Field,[96] and it consists of terms describing both bonded and non-bonded interactions (Equation 1.10).

$$V = \sum_{i}^{bonds} \frac{k_{l,i}}{2}(l_i - l_i^0)^2 + \sum_{i}^{angles} \frac{k_{\alpha,i}}{2}(\alpha_i - \alpha_i^0)^2 + \\ + \sum_{i}^{dihedrals} \{\sum_{k}^{M} \frac{V_{ik}}{2}[1 + cos(n_{ik}\theta_{ik} - \theta_{ik}^0)]\} + \\ + \sum_{i,j}^{pairs} \varepsilon_{ij}[(\frac{r_{ij}^0}{r_{ij}})^1 2 - 2(\frac{r_{ij}^0}{r_{ij}})^6] + \sum_{i,j}^{pairs} \frac{q_i q_j}{4\pi\varepsilon_0 \varepsilon r r_{ij}} \quad (1.10)$$

where each term represents a different type of interactions. The first three describe bonded interactions: stretching of bonds, bending of angles and torsions. The two following non-bonded terms describe: first - Van der Waals interaction, usually represented as Lenard-Jones potential, and second - electrostatic (Coulomb) interactions (Fig.1.7). Modern force fields, e.g. AMBER,[97] CHARMM[98] and OPLS,[99] are well parametrized for proteins and are widely applied in molecular simulations. However, small molecules are much more chemically diverse than proteins, and their parametres in general force fields for organic compounds (GAFF[100] or CGenFF[101]) often fail to describe the molecules accurately. Specific parameters can be supplied by parametrization toolkits, e.g. Antechamber[102] or Parmfit[103]. However, it tends to be very laborious and not feasible for large sets of molecules.

There are many flavours of molecular dynamics. Each method designed to address the issues in drug discovery or to improve classical molecular dynamics. The modifications are meant to accelerate the simulations

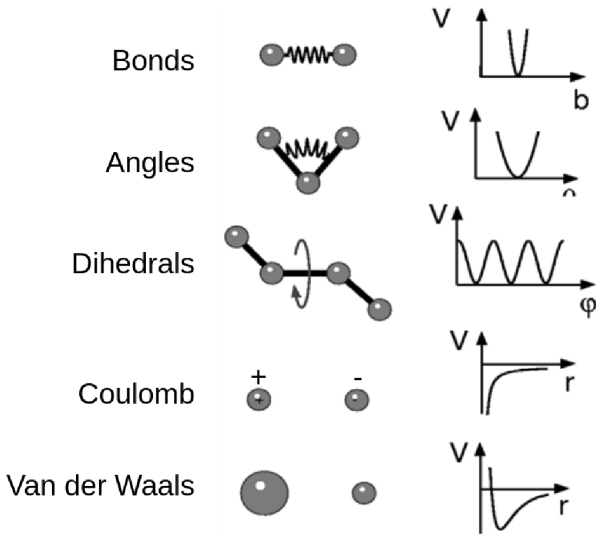

Fig. 1.7 Terms representing different interactions featured in force fields.

(metadynamics[104], coarse-graining approaches [105]), increase the sampling of underrepresented regions of energetic landscape (umbrella sampling[106], replica exchange[107]), bias the system to evolve in the desired direction (steered MD,[108, 109] dynamic docking[110]), or extract physical properties of the system (FEP,[111, 112] MDmix[113]).

Steered molecular dynamics (SMD) deserves additional attention because its variation has been used as the main method in this thesis. In SMD, an additional time-depended harmonic potential is applied to a small molecule to accelerate its binding or unbinding (Fig.1.8). The potential acts like a spring pulling the ligand by the centre of mass or individual atoms on the predefined pathway, a so-called collective variable (CV). The CV can be as simple as increasing the distance between protein and ligand. In practice, however, picking the right CV is a challenging task, especially when the method is used in high throughput on a variety of ligands. Well defined potential allows researchers to calculate the force and the work performed on the system.

Therefore, it characterizes unbinding both qualitatively and quantitatively. The "Jarzynski equality" defines the relationship between irreversible and reversible work,[114] and allows to obtain free energy of the process through a series of pulling simulations.

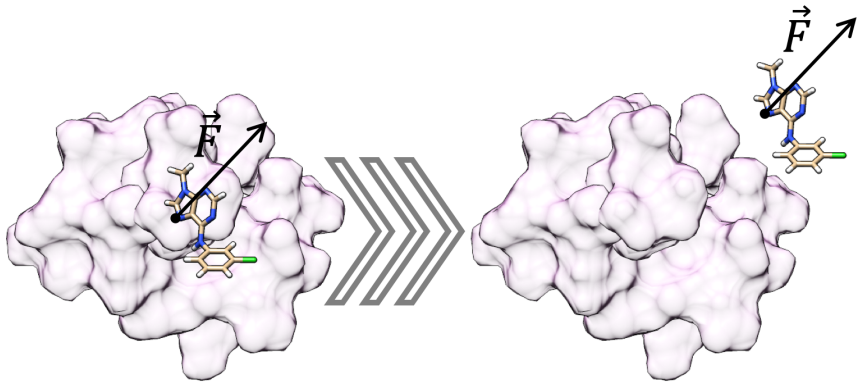

Fig. 1.8 Simplified visual representation of steered molecular dynamics.

1.3.3 Dynamic Undocking

Traditional implementations of molecular docking and molecular dynamic provide a good insight into binding thermodynamics and kinetics. However, they do not address the structural stability of the complex, in the form that is defined in section 1.2.2. In 2017, our research group published an MD-based method to assess structural stability, called Dynamic Undocking (DUck).[115] The method is a type of steered molecular dynamics, where an external potential is applied to rupture a predefined hydrogen bond between the protein and the ligand. Breaking a hydrogen bond does not require a long simulation, so the collective variable is defined to increase the distance between ligand's hydrogen bond donor or acceptor and complementary atom in the protein. During the simulation a force is recorded, and as a result, work against

distance profile is obtained (Fig.1.9b). The state where the work reaches the maximum we define as a quasi-bound state. The work necessary to reach that state (W_{QB}) is an effective factor quantifying structural stability. The steering is run many times in different conditions (two temperatures and different starting points), to increase sampling and explore ligand's flexibility in the binding pocket. Then the lowest individual W_{QB} value is selected as a total stability score. The number of performed SMDs differs depending on the objective of the simulation, from 1-4 runs for virtual screening application to 50-100 whenever we want to get more structural insight about the complex.

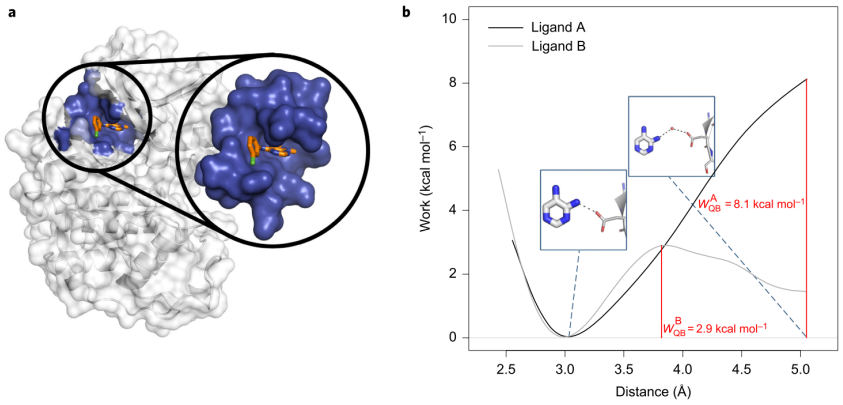

Fig. 1.9 a) An example of a reduced simulation system. b) Work profiles obtained from DUck simulations for a strong (black) and a weak (grey) ligand. Graphics adapted from [115].

There are some simplifications introduced in the method. The protein is reduced only to residues necessary to preserve a local environment of the bond, a so-called chunk (Fig.1.9a). Because of that, additional restraints are applied to all heavy atoms of the chunk to prevent it from falling apart during the simulation. The reduction of the simulation system makes the method much faster than conventional unbinding simulation and allow its application in virtual screening.

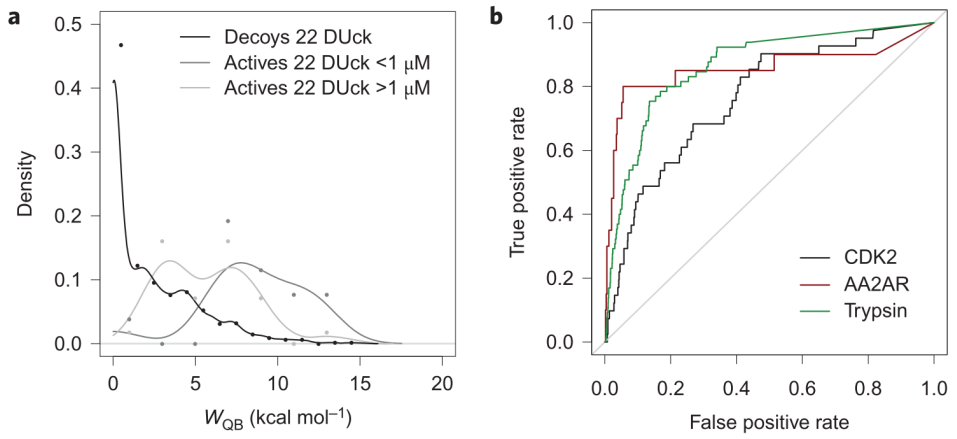

Fig. 1.10 a) Distribution of W_{QB} values of CDK2 ligands. Strong binders are shown in dark grey, weak - light grey and non-binding decoys in black. b) ROC curves for the CDK2 (black), AA2AR (red) and trypsin (green) sets from the directory of useful decoys. Graphics adapted from [115].

The method has been successful at distinguishing actives and form a set of carefully selected decoys for cyclin-dependent kinase 2.[116] The authors observed meaningful differences in the distribution of W_{QB} values for decoys, weak binders (IC50 > 1 μM) and strong binders (IC50 < 1 μM) (Fig.1.10a). The experiment was extended to other targets: adenosine A2A receptor (G protein-coupled receptor) and trypsin (serine protease)(Fig.1.10b). The researchers showed that W_{QB} values do not correlate with results obtained with other popular virtual screening techniques: Glide docking, molecular mechanics Poisson–Boltzmann surface area (MMPBSA) and generalized Born surface area (MMGBSA) rescoring. It showedcthat DUck is not designed to compete with existing methods, but rather complement them. Such strategy was applied in the D3R Grand Challenge 2015, where DUck along with rDock predicted affinity raking of ligands for two interesting targets Hsp90 and MAP4K4.[117] Finally, DUck was prospectively validated as a post-docking filter in virtual screening of fragment database against molecular

chaperone heat shock protein 90 kDa (Hsp90). The hit rate of the screening yielded 38% in comparison to standard 4.4% usually achieved for fragment screening library against this target,[118] and proved its undeniable usefulness in drug discovery.

1.4 Final Remarks

This thesis picks up the work at the end of the last section with an attempt to expand the concept of structural stability. The method has been validated in many ways and carries a useful signal. However, there a few limitations the narrow the extent of its applicability. First of them is a high dependency on the knowledge about the system. The researcher needs to know precisely which hydrogen bond is worth simulating. Very often, the key bond is the most conserved interaction. However, not for all targets we have substantial structural data. Moreover, the researcher needs to select the residues of the protein that are necessary to preserve the local environment of the bond and that will not form a steric clash during the unbinding.

This far, DUck has only been used on four popular systems in virtual screening scenario. There are a few questions we can ask ourselves. How general is structural stability across biologically relevant complexes? How big can be a transitional penalty of breaking a single hydrogen bond and the whole network? How bonds influence each other and affect structural stability? Can structural stability be applied in other areas of drug discovery? These questions and even will be addressed in the following thesis.

It is essential to highlight that this work tries to diverge from a traditional focus on binding free energy (ΔG) and offers a more exotic view on macromolecular complexes. It is fascinating that structural stability carries a signal, even though it does not have any physical meaning and quasi bound state is thermodynamically irrelevant. The method is not meant to replace or even

compete with widely applied molecular docking. It merely offers another tool to get a more complete view of molecular recognition.

Chapter 2

Objectives

The relevance of structural stability in drug design has been shown by the use of DUck in virtual screening campaign, as reported previously.[115] The method provides a fast and easy way to assess hydrogen bond-based structural stability of a complex. However, the cause and consequences of structural stability in molecular recognition remain unknown. DUck still has some limitations and requires previous knowledge about the system to be applied successfully.

General objective

The general objective of this work is to deepen the knowledge of the role and origin of structural stability in molecular recognition and extend its applicability in drug design. We wanted to test DUck on a large and diverse set of protein-ligand complexes and apply it in a more general scenario without detailed knowledge about the simulated system.

Detailed objectives

The specific objectives were the following:

1. Investigate the role of structural stability in biomolecular complexes:
    - Perform a large-scale assessment of hydrogen bond based structural stability on a set of highly trustworthy structures of protein-ligand and protein-fragment complexes.
    - Compare the binding patterns for different classes of proteins
    - Investigate how robust hydrogen bonds are organised in complex's structure.
    - Draw useful conclusions for drug design.
    - Explain the cause of structural stability.

2. Extend the applicability domain of Dynamic Undocking:

    - Combine docking with rDock and post-docking evaluation of poses with DUck into binding mode prediction protocol.
    - Test the protocol on the set of complexes of proteins with drug-like molecules and fragments.

Chapter 3

Publications

This chapter includes two papers that we have published as a result of the PhD project.

In the first paper, entitled "An investigation of structural stability in protein-ligand complexes reveals the balance between order and disorder", we analyse structural stability of a set of diverse complexes. The work introduces a new perspective into the understanding of molecular recognition.

In the second paper, entitled "Structural Stability Predicts the Binding Mode of Protein-Ligand Complexes", we test structural stability in a binding mode prediction protocol. Post-docking reevaluation of poses with DUck improves prediction of fragments and matches the performance of docking software for drug-like molecules.

In the appendix we included a book chapter entitled "Dynamic Undocking: A Novel Method for Structure-Based Drug Discovery" that describes previously published tool - Dynamic Undocking. There we focus in detail on practical aspects of DUck, starting from system preparation and ending with simulation analysis. Additionally, the chapter includes "Notes" section where we share useful tips for beginners that originate from our experience with DUck. The chapter does not contain any new results and is placed there to complement the introduction.

3.1 An investigation of structural stability in protein-ligand complexes reveals the balance between order and disorder

Maciej Majewski[1], Sergio Ruiz-Carmona[1], and Xavier Barril[1,2]

*Communications Chemistry (**2019**), 2(1) pp. 1-8*

1. Institut de Biomedicina de la Universitat de Barcelona (IBUB) and Facultat de Farmacia, Universitat de Barcelona, Av. Joan XXIII 27-31, 08028 Barcelona, Spain.
2. Catalan Institution for Research and Advanced Studies (ICREA), Passeig Lluis Companys 23, 08010 Barcelona, Spain.

COMMUNICATIONS CHEMISTRY

ARTICLE

https://doi.org/10.1038/s42004-019-0205-5 OPEN

An investigation of structural stability in protein-ligand complexes reveals the balance between order and disorder

Maciej Majewski [1], Sergio Ruiz-Carmona [1] & Xavier Barril [1,2]

The predominant view in structure-based drug design is that small-molecule ligands, once bound to their target structures, display a well-defined binding mode. However, structural stability (robustness) is not necessary for thermodynamic stability (binding affinity). In fact, it entails an entropic penalty that counters complex formation. Surprisingly, little is known about the causes, consequences and real degree of robustness of protein-ligand complexes. Since hydrogen bonds have been described as essential for structural stability, here we investigate 469 such interactions across two diverse structure sets, comprising of 79 drug-like and 27 fragment ligands, respectively. Completely constricted protein-ligand complexes are rare and may fulfill a functional role. Most complexes balance order and disorder by combining a single anchoring point with looser regions. 25% do not contain any robust hydrogen bond and may form loose structures. Structural stability analysis reveals a hidden layer of complexity in protein-ligand complexes that should be considered in ligand design.

[1] Institut de Biomedicina de la Universitat de Barcelona (IBUB) and Facultat de Farmacia, Universitat de Barcelona, Av. Joan XXIII 27-31, 08028 Barcelona, Spain. [2] Catalan Institution for Research and Advanced Studies (ICREA), Passeig Lluis Companys 23, 08010 Barcelona, Spain. Correspondence and requests for materials should be addressed to X.B. (email: xbarril@ub.edu)

ARTICLE COMMUNICATIONS CHEMISTRY | https://doi.org/10.1038/s42004-019-0205-5

Biomolecular systems present a large number of degrees of freedom and must find a suitable balance between order and disorder. In the particular case of non-covalent complexes, they can exist in a continuum spectrum of possibilities, ranging from the lock-and-key model to extreme disorder[1,2]. While the importance of target flexibility is well-appreciated in drug discovery[3], the flexibility of small-molecule ligands in their bound state has attracted much less attention. Detailed analyses reveal that ligands often retain residual mobility[4–6]. However, changes in binding mode are more the exception than the norm[7,8] and ligand design based on rigid crystallographic geometries has been remarkably successful[9]. Explicit consideration of multiple binding modes is acknowledged as important for computational studies[10], but invariably leads to more complex formalisms[11,12]. Perhaps for these reasons, little is known about the molecular mechanisms that control structural stability, to what extent do ligands preserve flexibility or what are the energetic and functional consequences of rigidity.

It is important to note that structural stability (robustness) is fundamentally different from thermodynamic stability (i.e., binding free energy; ΔG_{bind}). This is eloquently exemplified in the recent work by Borgia et al., where a protein-protein complex with picomolar affinity is shown to lack structure[2]. While ΔG_{bind} has been the center of attention of scientific research for decades, little attention has been paid to the factors that determine if a complex will be tight or loose. The source of structural robustness must be sought on sharp (and possibly transitory) energetic barriers that keep the atoms in their positions of equilibrium. Such hypothetical barriers, like the ones that determine binding kinetics, could have their origin in intramolecular (i.e., conformational rearrangement), bimolecular (e.g., repulsive transitional configurations) or many-body effects (e.g., desolvation)[13]. But they will only provide structural stability if the barriers are steep and located very close to the position of minimum energy. In that respect, hydrogen bonds (HBs) are ideal candidates because they have strict distance and angular dependencies[14] and are one of the most frequent interaction types in protein-ligand complexes[15]. The contribution of HBs to ΔG_{bind} has been largely debated in the literature[16–20]. The current consensus is that it is highly variable and context dependent, but their contribution to thermodynamic stability is 1.8 kcal mol^{-1} at the most[17]. However, due to desolvation, the transitional penalty of breaking a HB can be much larger[21]. Indeed, we have shown that this is the case for water-shielded HBs, which can even act as kinetic traps[22]. More recently, we have also shown that formation of structurally robust intermolecular HBs at specific positions is a necessary condition for binding, and have developed a method to assess the robustness of individual HBs that is very effective in virtual screening applications[23].

Here, we perform a systematic investigation of the possible role of HBs as structural anchors of protein-ligand complexes. We find that most complexes combine a robust anchoring point with more labile interactions, but cases of completely constricted and very loose complexes also exist. Our findings not only confirm a general role of HBs as source of structural stability, but also offer a new perspective to understand and design ligand-receptor complexes.

Results

Robust hydrogen bonds are common in protein-ligand complexes. Using Dynamic Undocking (DUck), an MD-based computational procedure[23], we have assessed the robustness of every HB in a set of 79 drug-like protein-ligand complexes from the Iridium Data Set[24]. Detailed information about the data set and the selection criteria is presented in Supplementary Methods and Supplementary Table 1. Each HB was pulled to a distance of 5 Å, according to the DUck protocol reported previously[23,25]. In this way, we obtain a work value (W_{QB}) that reflects the cost of breaking each HB. In other words, the W_{QB} value indicates if the interaction under investigation gives rise to a narrow (local) minimum in the free-energy landscape, and estimates its depth. Based on our previous research, we define HBs as robust (i.e., capable of providing structural stability) if $W_{QB} > 6$ kcal mol^{-1}, labile if $W_{QB} < 4$ kcal mol^{-1} and medium otherwise.

The distribution of work values for the entire set of 345 HBs ranges from 0 to 26 kcal mol^{-1}, with a of maximum probability in the 0–6 kcal mol^{-1} region and a gradual decrease thereafter (Fig. 1a). Noteworthy, more than half HBs (57.4%) are robust. In order to provide a critical assessment of these results, we have sought correlation with experimental observables and have also considered if W_{QB} values might be dominated by the interaction energies. Larger W_{QB} values imply a narrower minimum and, thus, restricted mobility, which should translate into a more localized electron density, that is, lower crystallographic B-factors. As B-factors are heavily influenced by the refinement methods used and their absolute values can be meaningless[26,27], we have normalized the B-factor of the ligand atom that makes the hydrogen bond relative to the average B-factor of the whole ligand. Encouragingly, atoms forming HBs with larger W_{QB} values tend to have lower relative B-factors (Supplementary Fig. 4). A second aspect to consider is whether DUck calculations merely reflects short-range protein-ligand interaction, or—as intended—it captures a global effect that considers enthalpic and entropic contributions from both the solute and the solvent. Lack of correlation between interaction energies and W_{QB} confirms that the latter is true (Supplementary Fig. 5). Of particular interest is to assess the effect of charge reinforcement on HBs, as the energetic, entropic and solvation terms of neutral hydrogen bonds and salt bridges are drastically different[28]. We have classified all HBs into neutral, mixed (ionic-neutral) and salt bridges (Fig. 2, Supplementary Data 2). We find that salt bridges are only very slightly skewed towards more robust interactions than neutral HBs. The distributions were compared with two sample Kolmogorov-Smirnov statistical test, yielding p-value of 0.08. Mixed types are completely indistinguishable from neutral ones (p-value = 0.42). Unexpectedly, the maximal values are equal across all three categories. Theoretically, ionic species could provide even larger energetic barriers because their desolvation costs are much larger. We speculate that there may be no biological use for them, as the maximal W_{QB} values observed here already ensure very robust and long-lived structures.

The distribution of robust HBs is rather inhomogeneous across complexes, as they have 2.5 on average, but a quarter of the complexes have none (Fig. 1b). Considering that structural stability is not a requisite for tight binding and that HBs may not the only mechanism capable of providing structural stability, it is striking that 75% of the complexes in this set are anchored through HBs. A further 14% of complexes present medium values and only in 9 cases (11%) all their HBs are labile (Supplementary Fig. 6). Two of those cases are very low affinity complexes. In the remaining cases, structural stability might be provided by other mechanisms or may be lacking (see examples in Supplementary Fig. 6). It is important to note that the level of structural stability reported here may be overestimated due to the composition of the data set, entirely derived from X-ray crystallography, a technique that relies on order to solve structures.

Splitting this analysis by the type of binding site (Fig. 1c–j, Supplementary Table 2) provides strong indication that the behavior is dictated by the nature of the receptor. The proportion of robust complexes increases to 82% in the case of enzyme active sites, which speaks about the need of keeping the substrate in

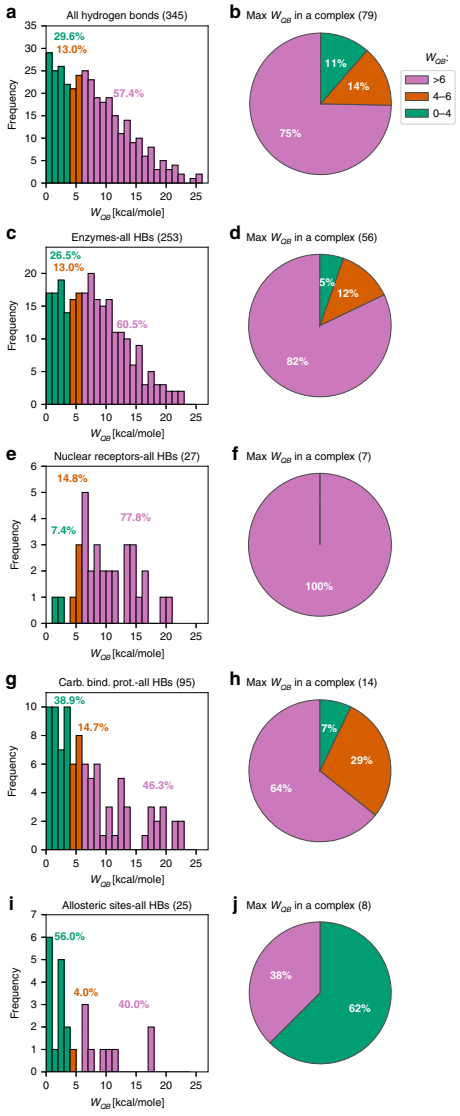

Fig. 1 Frequency of robust HBs in protein-ligand complexes. Histograms of frequency of HBs by W_{QB} value for: **a** all simulated HBs (345), **c** HBs in enzyme active sites (253), **e** HBs in the ligand binding site of nuclear receptors (27), **g** HBs in carbohydrate binding sites (95), **i** HBs in allosteric sites (25). Pie charts showing share of complexes with at least one robust HB (W_{QB} > 6 kcal mol^{-1}, pink), all labile HBs (W_{QB} < 4 kcal mol^{-1}, green) or intermediate situations (red) for: **b** all simulated complexes (79), **d** enzymes (56), **f** nuclear receptors (7), **h** carbohydrate binding site (14), **j** allosteric sites (8)

place for efficient catalysis. Nuclear receptors form fewer HBs with their ligands, but most of them (78%) are robust and all ligands (100%) are well anchored. In this case, forming a rigid structure may be necessary to stabilize the AF2 co-regulatory protein binding surface in an optimal conformation for co-activator binding[29]. Carbohydrate binding sites, on the other hand, form many more HBs with their ligands, but a lower proportion of robust ones (46%). Finally, in the case of allosteric ligands, only 40% of complexes are robust, suggesting that these sites tend to yield looser complexes. As demonstrated in the case of HIV reverse transcriptase inhibitors (Fig. 3c), lack of robust HBs does not preclude tight binding. In fact, a multiplicity of binding modes might be beneficial to preserve binding affinity when the target is mutated, thus averting resistance[30,31]. While the distribution of HB strength between the four types of binding sites that we have defined is quite different (see Supplementary Tables 4 and 5 for statistical tests), individual cases can deviate from the norm (e.g., the allosteric ligand 1YV3 is extremely robust) and more examples will be needed to reach firm conclusion about site-dependence.

Strong hydrogen bonds form fragment-sized structural anchors. To understand whether robust HBs originated from a single or multiple areas on a ligand, all HBs in each complex were clustered, based on their distance in space, into fragment-sized group of atoms (Supplementary Fig. 1). In the majority of complexes (62%) robust HBs were located in a single group, forming a strong structural anchor (Fig. 4, Supplementary Table 6). The concentration of robust interactions on a single site, allowing a some degree of movement to the other parts, minimizes the entropic costs and can be desirable from a binding affinity perspective[6]. Only 23% of ligands form two structural anchors on separate regions, though this is more common in the case of carbohydrate-binding proteins (Supplementary Table 7). Three exceptional ligands manage to form 3 distinct stable anchors. Interestingly, they have completely unrelated functions, chemical structures and physical properties but—at least in two of those cases—there is a possible functional explanation for the extreme robustness (Fig. 5).

The distribution of W_{QB} per number of HBs in a local group (Fig. 4f) is suggestive of cooperative behavior. HBs in isolation usually do not form robust interactions (mean and median values: (4.7 ± 4.1) and 3.7 kcal mol^{-1}, respectively), although in exceptional cases they can reach values above 10 kcal mol^{-1}. By contrast, when three or more HBs cluster together, formation of robust complexes is the most common outcome (mean and median values: (9.4 ± 5.8) and 9.0 kcal mol^{-1}, respectively). The HBs within these clusters present relatively similar W_{QB} values (Supplementary Fig. 7), suggesting that they often behave in a concerted-like manner. This synergic and mutually dependent behavior not only ensures higher barriers to dissociation, but is also well-suited to provide selectivity, as small changes in the composition or geometry of one of the partners may result in large changes in magnitude of W_{QB} (see example in Supplementary Fig. 8).

Protein-fragment complexes are more static than protein-ligand complexes. The observation that most drug-like ligands combine tightly bound regions with looser ones makes us wonder about fragment-sized ligands. Do they balance order and disorder in some other way (e.g., using fewer attachment points)? Or, perhaps, depending on the site they bind to, they are either dynamic or fully constrained? In order to answer these questions, we have extended our analysis with a set of 27 fragment-protein complexes (126 individual HBs) from the SERAPhiC dataset[32].

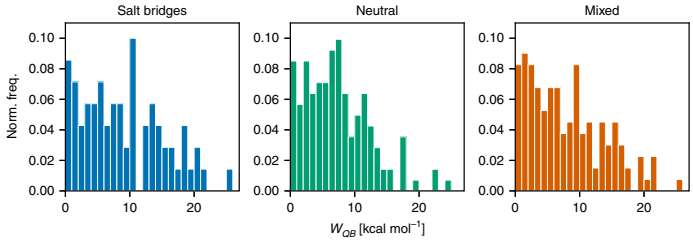

Fig. 2 Distribution of robustness of HBs by bond's charge. Histograms presenting distribution of W_{QB} values in the set of HBs from Iridium DS, divided into salt bridges, neutral and mixed (ion-neutral) interactions

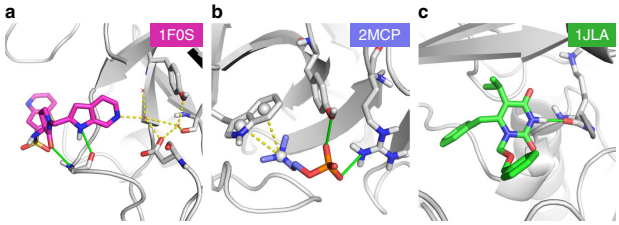

Fig. 3 Structures of protein-ligand complexes that form potentially labile structures. Weak hydrogen bonds ($W_{QB} < 4$ kcal mol^{-1}) marked in green. **a** Complex of FXa with inhibitor RPR208707 (PDB id 1F0S; $K_i = 18$ nM) forms two direct, but labile, HBs with the protein. An additional water-mediated HB with the catalytic residues (yellow dotted lines) might provide structural stability. **b** An antibody that recognizes phosphocholine (PDB id 2MCP) forms two charge-reinforced but labile HBs. A cation-pi interaction (yellow dotted lines) might provide structural stability. **c** Reverse transcriptase inhibitor (PDB id 1JLA; $IC_{50} = 6$ nM) forms a single but labile HB with the protein. No other source of structural stability is apparent

Strikingly, we find that fragments have an almost identical behavior to standard ligands, with 49% of robust HBs (2.3 per ligand) and 73% of ligands presenting at least one robust interaction. The distribution and maximal W_{QB} values are also very similar (Fig. 6). This indicates that, proportionally, fragments are more static than standard ligands. This agrees with the observations that fragments have a more enthalpic binding[33] and that they have a higher proportion of buried HBs[34]. It also justifies that, in spite of their low binding affinity, most fragments already have a well-defined binding mode that serves as a foundation from which to spread and catch additional interactions. However, not all fragments form robust interactions and we propose that these are less suitable as starting points because their binding mode can change, confounding structure-activity interpretation and rendering optimization more difficult. Indeed, fragments are known to change their binding mode when evolved into larger molecules[7,35–39]. These may be attempts at building on what is assumed to be a solid foundation but turns out to be unstable ground, a possibility that we shall investigate in the future. It should also be noted that the fraction of well-anchored fragments may be different for fragments hits that fail to crystallize. The overlap between X-ray crystallography and other biophysical screening methods can be rather low[40] and progressing fragments that fail to crystallize is deemed difficult but worthwhile[41].

Structural stability is a consequence of binding free energy and desolvation. Finally, we want to consider what is the origin of the free energy barrier that causes structural stability. Knowing that a HB has a large W_{QB} value can be likened to knowing the k_{off} of a compound without knowing the k_{on} nor ΔG_{bind}: larger values may indicate that it has a higher transition state (if ΔG_{bind} remains the same; Fig. 7a), that the complex is thermodynamically more stable (if k_{on} remains the same; Fig.7b), or a combination thereof. In this data set, we find that anchoring sites often correspond to binding hot spots. This is indeed the case for all kinases and proteases, which have a well-known binding hot spot (Supplementary Table 2, Supplementary Fig. 1), as well as for most fragments. In such cases, ΔG_{bind} must be a component of W_{QB}, but there is no correlation between both magnitudes (Supplementary Fig. 9), as already noted[23]. Thus, we conclude that W_{QB} must be largely dominated by a transitory dissociation penalty. The origin of this penalty can be explained by a physical decoupling between HB rupture and resolvation, as described for water-shielded hydrogen bonds[22]. In support of this view, several studies of the reverse event have identified desolvation of the binding pocket as the rate-limiting step in ligand association[21,42,43]. Indeed, solvent exposed HBs invariably lead to low W_{QB} values (but note that they can be thermodynamically stable)[44], whereas water-shielding is a necessary but not sufficient condition of robust HBs (Supplementary Fig. 10).

Discussion

Taken together, our results show that structural stability is a common property of protein-ligand complexes, but not an universal one. Cases of loose complexes, while relatively rare (10-20%), can be found even in a dataset originating exclusively from X-ray crystallography, a technique that requires structural homogeneity of the sample. The proportion could be larger

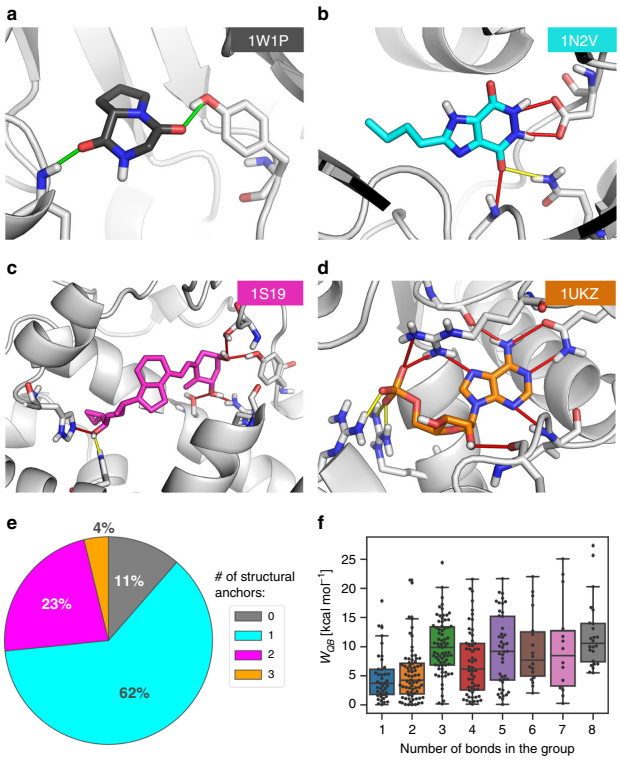

Fig. 4 Distribution of complexes based on the number of structural anchors. Representative of each group is presented in the following image: **a** 0 anchors: Chitinase B with inhibitor (PDB id 1W1P; $IC_{50} = 5$ mM); **b** 1 anchor: Queuine tRNA-ribosyltransferase with inhibitor (PDB id 1N2V; $K_i = 83$ μM), **c** 2 anchors: Vitamin D3 receptor with calcipotriol (PDB id 1S19; $K_d = 0.31$ nM) and **d** 3 anchors: Uridylate kinase-AMP (PDB id 1UKZ). Weak hydrogen bonds ($W_{QB} < 4$ kcal mol^{-1}) marked in green, medium ($4 \leq W_{QB} < 6$ kcal mol^{-1}) in yellow and strong ($W_{QB} \geq 6$ kcal mol^{-1}) in red. **e** Pie chart presenting distribution of number of anchors across the data set. **f** Distribution of strength of HBs (W_{QB}) versus the number of HBs per group of atoms. The box shows the quartiles and the whiskers show the rest of distribution excluding outliers. The swarmplot showing all data points is placed in top of the boxplot

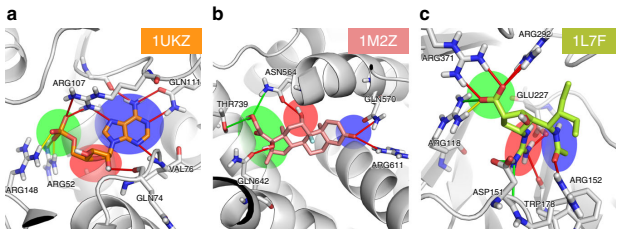

Fig. 5 Structures of completely constricted complexes hint at potential functional role. Cases in the dataset where the ligand presents three structural anchors are: **a** Uridilate kinase with AMP (PDB id 1UKZ) where the base, ribose and phosphate of the nucleotide are forming three distinctive centers of interactions. Structural stability may be necessary for efficient catalysis. **b** Glucocorticoid receptor ligand-binding domain bound to dexamethasone (PDB id 1M2Z; $K_d = 19$ nM). The ligand has three regions that form robust interaction, well separated in space but located on the steroid core, thus behaving as a single rigid block. Structural stability may be necessary for agonistic response. **c** Influenza virus neuraminidase with inhibitor BCX-1812 (PDB id 1L7F; K_i single digit nM for various virus strains). Three different functional groups branching out of the pentane scaffold form robust interactions in this extremely polar and solvent exposed binding site. Weak hydrogen bonds ($W_{QB} < 4$ kcal mol^{-1}) marked in green, medium ($4 \leq W_{QB} < 6$ kcal mol^{-1}) in yellow and strong ($W_{QB} \geq 6$ kcal mol^{-1}) in red. Structural anchors are marked with shaded areas: green, red, and blue

amongst ligands that fail to crystallize. The level of residual mobility is also larger and more common than the static X-ray structures lead to think, as also concluded by a recent independent study[4]. In fact, most complexes balance order and disorder by combining a firm anchor with more relaxed peripheral interactions. Depending on the nature of the ligand and the binding site, each complex adopts a particular degree of robustness, that ranges from the very tight (e.g., nuclear receptor agonists) to the very loose (e.g., HIV-RT allosteric inhibitors). Each one of these solutions entails important consequences that have, so far, been neglected in drug design. First of all, a firm anchor provides a framework from which to grow and capture additional interactions, and the preservation of a common binding mode helps interpreting structure-activity relationships. This is particularly important for fragments as starting points for lead discovery. Secondly, structural robustness can have functional implications, particularly in the case of receptors, where flexibility has been linked to the agonist/antagonist response[29,45]. Thirdly, structural stability implies an entropic penalty and must be balanced to avoid loss of potency[6,46]. Finally, the deep and narrow energetic minima that cause rigidity also imply large penalties for small recognition defects, thus increasing the fidelity of the recognition event. This has been shown for protease-substrate pairs[47] and HIV-protease inhibitors[48]. In conclusion, this work opens up the possibility of understanding and designing structural robustness in ligand-receptor complexes. We suggest that robustness analysis, which can help understand and control the level of

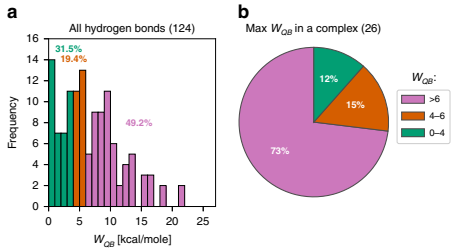

Fig. 6 Frequency of robust HBs in protein-fragment complexes. **a** Histogram of frequency of HBs by W_{QB} value for all simulated HBs (124) in SERAPhiC dataset. **b** Pie chart showing share of complexes with at least one robust HB ($W_{QB} > 6$ kcal mol^{-1}, pink), all labile HBs ($W_{QB} < 4$ kcal mol^{-1}, green) or intermediate situations (red) for all protein-fragment complexes (26)

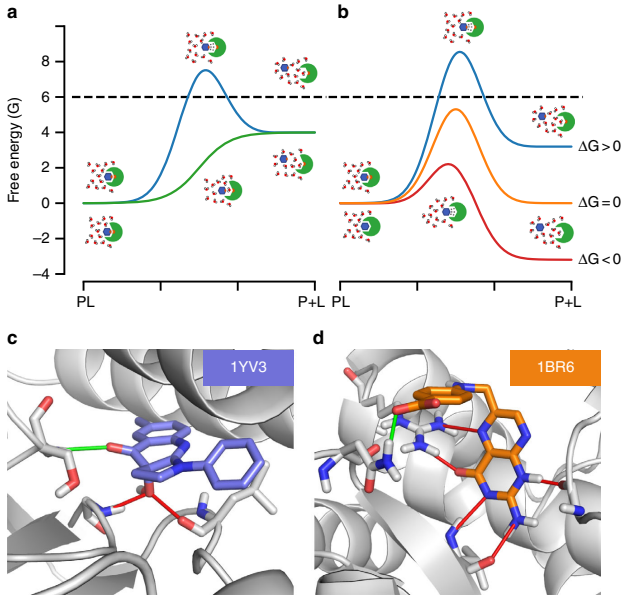

Fig. 7 Ways of achieving structural robustness. **a** Idealized representation of two dissociation pathways for complexes with the same ΔG_{bind} and different desolvation costs. The images above the blue curve shows the state of the system in bound, transition and unbound state of complex with well shielded, stable hydrogen bond. The images below the green curve show analogous images for the complex with solvent exposed hydrogen bond. **b** Likewise for three complexes with the same desolvation cost but different ΔG_{bind}. The images represent complexes with excellent shape complementarity that form (above the blue curve) or don't form (below the red curve) favorable hydrogen-bonding pairs. The black dashed line marks the energy cutoff that classifies bond as structurally stable. **c** Example of a complex with high dissociation cost due to extreme water-shielding. **d** Example of a complex with high dissociation cost due to a tight network of multiple HBs. Weak hydrogen bonds ($W_{QB} < 4$ kcal mol^{-1}) marked in green and strong ($W_{QB} \geq 6$ kcal mol^{-1}) in red

mobility, should be an essential part of ligand design, not least because rigid parts demand more precise complementarity than flexible ones. Qualitatively, a visual inspection can reveal water-shielded HBs (Fig. 7c) and HB clusters (Fig. 7d), which are tell-tale signs of robustness. Quantitatively, DUck simulations offer an inexpensive and automated protocol to calculate W_{QB}. While HBs appear to be the most common means of achieving structural robustness, other interaction types (e.g., cation-pi, water-mediated HBs, halogen bonds) should be considered in the future.

Methods

Datasets information. See Supplementary Methods and Supplementary Tables 1–3.

Systems preparation and dynamic undocking. See Supplementary Methods, Supplementary Figs 1–3 and Supplementary Data 1 and 2.

Results analysis. See Supplementary Figs 4–10 and Supplementary Tables 4–7.

Data availability

All data generated during the current study are available as a part of the Supplementary Information in the form of sdf and mol2 files.

Received: 26 October 2018 Accepted: 8 August 2019
Published online: 17 September 2019

References

1. Tompa, P. & Fuxreiter, M. Fuzzy complexes: polymorphism and structural disorder in protein-protein interactions. *Trends Biochem. Sci.* **33**, 2–8 (2008).
2. Borgia, A. et al. Extreme disorder in an ultrahigh-affinity protein complex. *Nature* **555**, 61–66 (2018).
3. Cozzini, P. et al. Target flexibility: an emerging considertaion in drug discovery. *J. Med. Chem.* **51**, 6237–6255 (2008).
4. Van Zundert, G. C. P. et al. QFit-ligand reveals widespread conformational heterogeneity of drug-like molecules in X-ray electron density maps. *J. Med. Chem.* **61**, 11183–11198 (2018).
5. Klebe, G. Applying thermodynamic profiling in lead finding and optimization. *Nat. Rev. Drug Discov.* **14**, 95–110 (2015).
6. Glas, A., Wamhoff, E.-C., Kruger, D. M., Rademacher, C. & Grossmann, T. N. Increased conformational flexibility of a macrocycle–receptor complex contributes to reduced dissociation rates. *Chem. Eur. J.* **23**, 16157–16161 (2017).
7. Malhotra, S. & Karanicolas, J. When does chemical elaboration induce a ligand to change its binding mode? *J. Med. Chem.* **60**, 128–145 (2017).
8. Kuhnert, M. et al. Tracing binding modes in hit-to-lead optimization: chameleon-like poses of aspartic protease inhibitors. *Angew. Chem. Int. Ed.* **54**, 2849–2853 (2015).
9. Sliwoski, G., Kothiwale, S., Meiler, J. & Lowe, E. W. Computational methods in drug discovery. *Pharmacol. Rev.* **66**, 334–395 (2014).
10. Mobley, D. L. & Dill, K. A. Binding of small-molecule ligands to proteins: 'what you see' is not always 'what you get'. *Structure* **17**, 489–498 (2009).
11. Kaus, J. W. et al. How to deal with multiple binding poses in alchemical relative protein-ligand binding free energy calculations. *J. Chem. Theory Comput.* **11**, 2670–2679 (2015).
12. Gill, S. C. et al. Binding modes of ligands using enhanced sampling (BLUES): rapid decorrelation of ligand binding modes via nonequilibrium candidate Monte Carlo. *J. Phys. Chem. B* **122**, 5579–5598 (2018).
13. Pan, A. C., Borhani, D. W., Dror, R. O. & Shaw, D. E. Molecular determinants of drug–receptor binding kinetics. *Drug Discov. Today* **18**, 667 (2013).
14. Bissantz, C., Kuhn, B. & Stahl, M. A medicinal chemist's guide to molecular interactions. *J. Med. Chem.* **53**, 5061–5084 (2010).
15. Ferreira de Freitas, R. & Schapira, M. A systematic analysis of atomic protein–ligand interactions in the PDB. *Med. Chem. Commun.* **8**, 1970–1981 (2017).
16. Fersht, A. R. The hydrogen bond in molecular recognition. *Trends Biochem. Sci.* **12**, 301–304 (1987).
17. Pace, C. N. Energetics of protein hydrogen bonds. *Nat. Struct. Mol. Biol.* **16**, 681–682 (2009).
18. Pace, C. N. et al. Contribution of hydrogen bonds to protein stability. *Protein Sci.* **23**, 652–661 (2014).
19. Gao, J., Bosco, D. A., Powers, E. T. & Kelly, J. W. Localized thermodynamic coupling between hydrogen bonding and microenvironment polarity substantially stabilizes proteins. *Nat. Struct. Mol. Biol.* **16**, 684–690 (2009).
20. Nick Pace, C., Martin Scholtz, J. & Grimsley, G. R. Forces stabilizing proteins. *FEBS Lett.* **588**, 2177–2184 (2014).
21. Mondal, J., Friesner, R. A. & Berne, B. J. Role of desolvation in thermodynamics and kinetics of ligand binding to a kinase. *J. Chem. Theory Comput.* **10**, 5696–5705 (2014).
22. Schmidtke, P., Javier Luque, F., Murray, J. B. & Barril, X. Shielded hydrogen bonds as structural determinants of binding kinetics: application in drug design. *J. Am. Chem. Soc.* **133**, 18903–18910 (2011).
23. Ruiz-carmona, S. et al. Dynamic undocking and the quasi-bound state as tools for drug discovery. *Nat. Chem.* **9**, 201–206 (2017).
24. Warren, G. L., Do, T. D., Kelley, B. P., Nicholls, A. & Warren, S. D. Essential considerations for using protein-ligand structures in drug discovery. *Drug Discov. Today* **17**, 1270–1281 (2012).
25. Majewski, M., Ruiz-Carmona, S. & Barril, X. in *Rational Drug Design: Methods and Protocols* (eds. Mavromoustakos, T. & Kellici, T. F.) 195–215 (Springer, New York, 2018).
26. Kleywegt, G. J. & Jones, T. A. in *Methods in Enzymology* 208–230 (Elsevier, 1997).
27. Parthasarathy, S. & Murthy, M. R. N. On the correlation between the main-chain and side-chain atomic displacement parameters (B values) in high-resolution protein structures. *Acta Crystallogr. Sect. D. Biol. Crystallogr.* **55**, 173–180 (1999).
28. Barril, X., Aleman, C., Orozco, M. & Luque, F. J. Salt bridge interactions: stability of the ionic and neutral complexes in the gas phase, in solution, and in proteins. *Proteins Struct. Funct. Bioinforma.* **32**, 67–79 (1998).
29. Mayer-Wrangowski, S. C. & Rauh, D. Monitoring ligand-induced conformational changes for the identification of estrogen receptor agonists and antagonists. *Angew. Chem. Int. Ed.* **54**, 4379–4382 (2015).
30. Das, K. et al. Roles of conformational and positional adaptability in structure-based design of TMC125-R165335 (Etravirine) and related non-nucleoside reverse transcriptase inhibitors that are highly potent and effective against wild-type and drug-resistant HIV-1 variants. *J. Med. Chem.* **47**, 2550–2560 (2004).
31. Lee, W. G., Chan, A. H., Spasov, K. A., Anderson, K. S. & Jorgensen, W. L. Design, conformation, and crystallography of 2-naphthyl phenyl ethers as potent anti-HIV agents. *ACS Med. Chem. Lett.* **7**, 1156–1160 (2016).
32. Favia, A. D., Bottegoni, G., Nobeli, I., Bisignano, P. & Cavalli, A. SERAPhiC: a benchmark for in silico fragment-based drug design. *J. Chem. Inf. Model.* **51**, 2882–2896 (2011).
33. Ferenczy, G. G. & Keseru, G. M. Thermodynamics of fragment binding. *J. Chem. Inf. Model.* **52**, 1039–1045 (2012).
34. Giordanetto, F., Jin, C., Willmore, L., Feher, M. & Shaw, D. E. Fragment hits: what do they look like and how do they bind? *J. Med. Chem.* **62**, 3381–3394 (2019).
35. Drwal, M. N. et al. Structural insights on fragment binding mode conservation. *J. Med. Chem.* **61**, 5963–5973 (2018).
36. Mpamhanga, C. P. et al. One scaffold, three binding modes: novel and selective pteridine reductase 1 inhibitors derived from fragment hits discovered by virtual screening. *J. Med. Chem.* **52**, 4454–4465 (2009).
37. Casale, E. et al. Fragment-based hit discovery and structure-based optimization of aminotriazoloquinazolines as novel Hsp90 inhibitors. *Bioorg. Med. Chem.* **22**, 4135–4150 (2014).
38. Han, X. et al. Discovery of potent and selective CDK8 inhibitors through FBDD approach. *Bioorg. Med. Chem. Lett.* **27**, 4488–4492 (2017).
39. Forster, A. B. et al. The identification of a novel lead class for phosphodiesterase 2 inhibition by fragment-based drug design. *Bioorg. Med. Chem. Lett.* **27**, 5167–5171 (2017).
40. Schiebel, J. et al. Six biophysical screening methods miss a large proportion of crystallographically discovered fragment hits: a case study. *ACS Chem. Biol.* **11**, 1693–1701 (2016).
41. Erlanson, D. A., Davis, B. J., Jahnke, W. & Box, G. Perspective fragment-based drug discovery: advancing fragments in the absence of crystal structures. *Cell Chem. Biol.* **26**, 9–15 (2019).
42. Dror, R. O. et al. Pathway and mechanism of drug binding to G-protein-coupled receptors. *Proc. Natl Acad. Sci. USA* **108**, 13118–13123 (2011).
43. Schuetz, D. A. et al. Ligand desolvation steers on-rate and impacts drug residence time of heat shock protein 90 (Hsp90) Inhibitors. *J. Med. Chem.* **61**, 4397–4411 (2018).

44. Ciulli, A., Williams, G., Smith, A. G., Blundell, T. L. & Abell, C. Probing hot spots at protein-ligand binding sites: a fragment-based approach using biophysical methods. *J. Med. Chem.* **49**, 4992–5000 (2006).
45. Ghanouni, P. et al. Functionally different agonists induce distinct conformations in the G protein coupling domain of the β2Adrenergic receptor. *J. Biol. Chem.* **276**, 24433–24436 (2001).
46. Brandt, T. et al. Congeneric but still distinct: how closely related trypsin ligands exhibit different thermodynamic and structural properties. *J. Mol. Biol.* **405**, 1170–1187 (2011).
47. Fuchs, J. E. et al. Cleavage entropy as quantitative measure of protease specificity. *PLoS Comput. Biol.* **9**, e1003007 (2013).
48. Shen, Y., Radhakrishnan, M. L. & Tidor, B. Molecular mechanisms and design principles for promiscuous inhibitors to avoid drug resistance: lessons learned from HIV-1 protease inhibition. *Proteins Struct. Funct. Bioinforma.* **83**, 351–372 (2015).

Acknowledgements

We thank C. Galdeano and F. J. Luque for helpful discussions and paper revision. The research was funded under the EU Horizon 2020 program, Marie Skłodowska-Curie grant agreement No. 675899 (FRAGNET). Spanish Ministerio de Economia (SAF2015-68749-R). Catalan government (2014 SGR 1189). Barcelona Supercomputing Center (computational resources).

Author contributions

X.B. designed the project; M.M. performed calculations; S.R.C. contributed new analytic tools; M.M. and X.B. analyzed data and wrote the paper.

Additional information

Supplementary information accompanies this paper at https://doi.org/10.1038/s42004-019-0205-5.

Competing interests: The authors declare no competing interests.

Reprints and permission information is available online at http://npg.nature.com/reprintsandpermissions/

Publisher's note Springer Nature remains neutral with regard to jurisdictional claims in published maps and institutional affiliations.

Supplementary Methods

Data Sets

As an object of calculations we selected a set of 120 high-trustworthy structures of protein-ligand complexes collected in Iridium Data set.[1] Refined protein structures and binding modes of ligands with assigned protonation and tautomeric states were provided by developers of the set. Due to limitations of used methods, some cases were excluded from calculations. First excluded group were complexes that did not possess any intermolecular hydrogen bonds (3 cases in Iridium). Coordination complexes with metal ions (28 cases) were also excluded. They are known to be stable structures, however they are not faithfully represented by the molecular mechanics force-field. Cases of multiple ligands in a binding pocket (5 cases) were also excluded, due to complexity of analysis, as well as ligands that were deemed non-drug like (6 cases). In case of 1hgh ligand was present in two binding pockets, differing in affinity.[2] In this case we simulated and analyzed both of the pockets separately. After the reduction of the set we were left with 78 complexes and 79 binding pockets. Classification of the structures is presented in Supplementary Table 1.

Supplementary Table 1 Classification of complexes from Iridium DS. Structures classified based on sutabilility for simulation.

Simulated structures	1a28, 1ai5, 1b9v, 1br6, 1c1b, 1cvu, 1dds, 1exa, 1ezq, 1f0s, 1f0t, 1f0u, 1fcx, 1fcz, 1fh8, 1fh9, 1fhd, 1fm6, 1fvt, 1g9v, 1gm6, 1h1p, 1h1s, 1hgh-1, 1hgh-2, 1hgi, 1hgj, 1hwi, 1ivb, 1ivd, 1ive, 1ivf, 1jla, 1k1j, 1k3u, 1ke5, 1l2s, 1l7f, 1lpz, 1lqd, 1m2z, 1ml1, 1mq6, 1mts, 1n2j, 1n2v, 1n46, 1of1, 1owe, 1oyt, 1pmn, 1q1g, 1q41, 1qhi, 1rob, 1s19, 1tow, 1tt1, 1u4d, 1ukz, 1ulb, 1unl, 1uou, 1v0p, 1w1p, 1w2g, 1x8x, 1ydr, 1yds, 1ydt, 1yv3, 1yvf, 1ywr, 2ack, 2br1, 2mcp, 2pcp, 3ptb, 4ts1
No HB	1ctr, 1fl3, 1p2y
Not drug like	1fjs, 1fm9, 1fq5, 1gwx, 1hgg, 1pso
Metal ion	1azm, 1cx2, 1dd7, 1eoc, 1frp, 1hdy, 1hq2, 1hww, 1iy7, 1jd0, 1lrh, 1mbi, 1mmv, 1mzc, 1n1m, 1oq5, 1p62, 1r58, 1r9o, 1uml, 1xm6, 1xoq, 1yqy, 2ctc, 2tmn, 4aah, 4cox, 1hp0
Additional ligand	1d3h, 1hnn, 1hvy, 1pbd, 1sq5

Supplementary Table 2 Classification of structures in Iridium DS based on function.

Category	PDB codes
Enzymes	1ai5, 1b9v, 1cvu, 1dds, 1ezq, 1f0s, 1f0t, 1f0u, 1fh8, 1fh9, 1fhd, 1fvt, 1gm8, 1h1p, 1h1s, 1hwi, 1ivb, 1ivd, 1ive, 1ivf, 1k1j, 1ke5, 1l2s, 1l7f, 1lpz, 1lqd, 1ml1, 1mq6, 1mts, 1n2j, 1n2v, 1of1, 1owe, 1oyt, 1pmn, 1q1g, 1q41, 1qhi, 1rob, 1u4d, 1ukz, 1ulb, 1unl, 1uou, 1v0p, 1w1p, 1w2g, 1x8x, 1ydr, 1yds, 1ydt, 1ywr, 2ack, 2br1, 3ptb, 4ts1
Kinases	1fvt, 1h1p, 1h1s, 1ke5, 1of1, 1pmn, 1q41, 1qhi, 1u4d, 1ukz, 1w2g, 1ydr, 1yds, 1ydt, 1ywr, 2br1
Proteases	1ezq, 1f0s, 1f0t, 1f0u, 1k1j, 1lpz, 1lqd, 1mq6, 1mts, 3ptb
Receptors	Nuclear receptors: 1a28, 1exa, 1fcx, 1fcz, 1fm6, 1m2z, 1n46, 1s19 Glutamate receptor: 1tt1
Carbohydrate binding prot.	1b9v, 1br6, 1fh8, 1fh9, 1fhd, 1hgh_1, 1hgi, 1hgj, 1ivb, 1ivd, 1ive, 1ivf, 1l7f, 1w1p
Allosteric sites	1c1b, 1g9v, 1hgh_2, 1jla, 1k3u, 1m2z, 1yv3, 1yvf

Second validation consisted of 53 high-quality X-ray models of fragment-protein complexes gathered in SERAPhiC dataset.[3] Protonation states of both protein structures and ligands were provided by developers of the data set. The same as in case of Iridium, some systems were excluded from the simulations: no hydrogen bonds (7 cases), additional ligands (5 cases) and metal ions (17 cases). After the reduction, 26 binding pockets were left in 24 different PDB structures. Three structures (1e2i, 1ofz, 2hdq) possess two ligands per protein indicated by “a” and “b” next to PDBid. Both pockets in entries 1ofz and 2hdq were treated as separate cavities in simulation and analysis stage. Complex 1e2i possesses 2 enantiomers in the same binding pocket. Both isomers were simulated separately, but in the analysis both of them were treated as a single pocket. Classification of the structures is presented in Supplementary Table 3.

Supplementary Table 3 Classification of complexes from SERAPhiC data set. Classification of complexes from Iridium DS. Structures classified based on sutabilility for simulation.

Simulated structures	1e2i_a, 1e2i_b, 1f5f, 1f8e, 1h46, 1k0e, 1mlw, 1ofz_a, 1ofz_b, 1r5y, 1sd1, 1tku, 1w1a, 1ynh, 2bkx, 2brt, 2f6x, 2fgq, 2hdq_a, 2hdq_b, 2i5x, 2iba, 2j5s, 2p1o, 2q6m, 2uy5, 3eko
No HB	1sqn, 1ui0, 1uwc, 2cix, 2qwx, 3c0z, 3dsx
Metal ion	1m2x, 1m3u, 1s5n, 1t0l, 1wog, 1x07, 1xfg, 1y2k, 1yv5, 2aie, 2fdv, 2ff2, 2gg7, 2gvv, 2rdr, 2v77, 2zvj
Additional ligand	1fsg, 1pwm, 1yki, 2b0m, 2bl9

Systems preparation

Structures of protein ligand complexes were provided by Iridium Data set's developers. The ligands had preassigned protonation and tautomeric states, which were then verified to reassure the right ligand parametrization. The protein structures were initially prepared by protonation at pH = 7 with MOE.[4] The protonation states were then inspected visually and questionable cases were verified with publication associated with PDB code.

Hydrogen bonds in complexes were identified using Chimera FindHBond function.[5] Then each bond was treated as a core for the individual simulation system. In order to perform Dynamic Undocking only a part of the protein was selected for the MD simulation. So-called chunk consists of residues necessary to preserve ligand's key interaction. First, crystal water molecules, additional molecules and ions were removed from protein structure. Then all residues with at least one atom within 7 Å of the key interaction were selected. Additional residues were included in order to prevent formation of artificial solvent channels. The residues that were not selected, were removed from the structure, forming the base chunk. In order to remove artificial charges, truncated chains were then acetylated or N-methylated, as needed. Reducing the system minimizes the influence of peripheral interactions and simplifies dissociation pathway. Additionally, it reduces time of calculation.

Dynamic Undocking

469 (345 for Iridium and 124 for SERAPhiC) individual hydrogen bonds were identified for 105 binding pockets for each bond individual system was created containing ligand and chunk of a protein. Then each system was prepared according to Dynamic Undocking protocol,[6,7] using parameters:

- Equilibration length: 1 ns
- MD chunk length: 0.5 ns
- SMD length: 0.5 ns
- SMD displacement: 2.5 Å
- Force constant: 50 kcal mol^{-1} $Å^{-2}$

- W_{QB} threshold: 0.4 kcal mol^{-1} (to avoid early termination of the protocol)
- Maximum DUck SMD runs: 19

Preparation of the simulations was run by previously developed Molecular Operating Environment[4] Scientific Vector Language script available online. The script performs the following actions:

- Calculates AM1-BCC charges for the ligand.[8]
- Assigns atom types and non-bonded parameters to the ligand, using parm@Frosst force field.[9]
- Identifies the pair of atoms making the key interaction.
- Writes the files necessary to carry out the MD simulations with AMBER 12.[10] (AMBER99 force field is used to parametrize protein).
- Generates valid topology and coordinate files for each system using AMBER's tLeap.

With those parameters each bond was subjected to 40 steered molecular dynamics (SMD) trajectories at 300 K and 325 K (20 trajectories in each temperature). In case of low energy bonds, the simulations were terminated after reaching the value below 0.4 kcal mol^{-1}. Setting the early termination threshold allows avoiding simulation of low stability systems. In this project, the value is very low and does not influence many systems. Here, only 4 systems in Iridium and 2 in SERAPhiC were terminated before reaching full 40 SMDs. All the simulations were performed with AMBER14 adapted for running in graphics processing unit (GPUs) and executed at the Barcelona Supercomputing Centre using NVIDIA Tesla M2090 GPUs. The work necessary to reach quasi-bound state (W_{QB}) in which the hydrogen bond has just been broken, was calculated for each individual trajectory.[6] The lowest value out of the set was then selected as a final stability score, because in that trajectory the ligand followed dissociation pathway that allowed it to escape the pocket. The final W_{QB} value reflects bond's resistance to deviate from the optimal geometry. All the bonds are classified with their location, stability (W_{QB}), character (salt bridge, charged or neutral) in the Supplementary Data 1 and 2.

It is worth noticing that individual W_{QB} values do not have an associated error value. To assess the convergence of simulation, 40 SMDs per hydrogen bond were randomly split into 4 equal parts of 10 SMDs. For each part the lowest W_{QB} value was identified and then 4 selected values

were averaged into a new value, called "Mean-W_{QB}" with calculated standard deviation (STD). Both of values are included in Supplementary Data 1 and 2 The conventionally calculated W_{QB} and Mean-W_{QB} are very similar (Supplementary Fig. 3), with correlation equal to 0.99.

Supplementary Figure 1 Depicted ligands from Iridium DS, with corresponding PDB codes. Atoms that make hydrogen bonds with the protein were highlighted and the W_{QB} value associated with that bond is written below the atom (multiple values in cases when the atom is making more than one hydrogen bond). The colour of highlight symbolizes fragment-sized group of atoms. Atom were grouped based on the distance with the cut-off of 4 Å and a few classifications were corrected based on visual inspection.

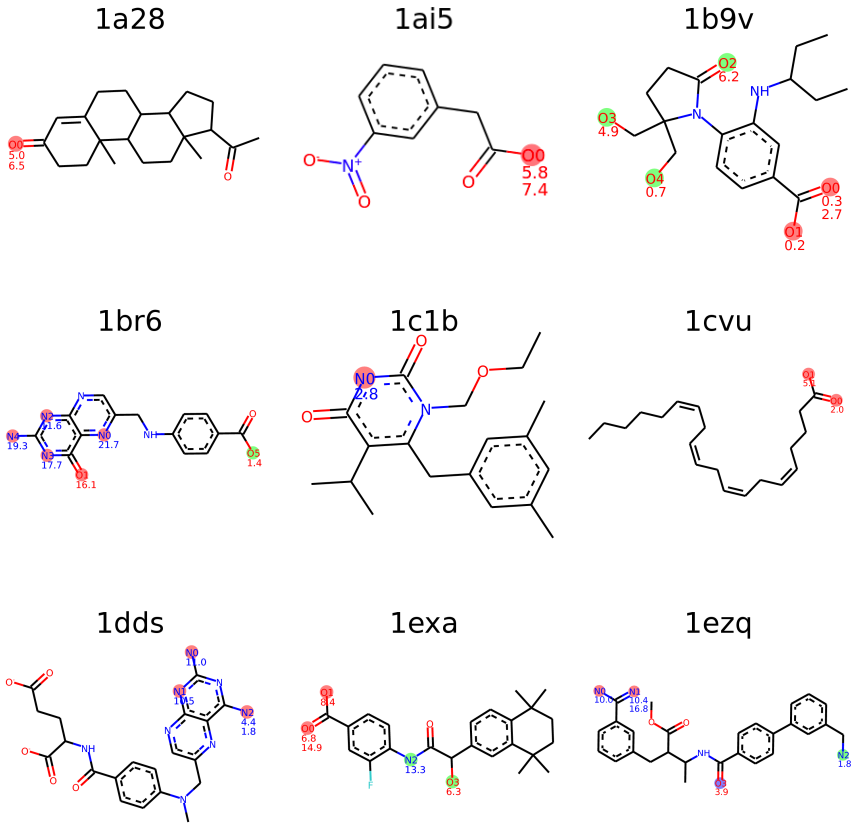

1f0s

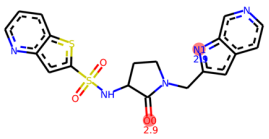

1f0t

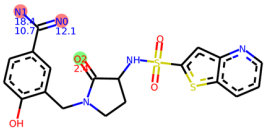

1f0u

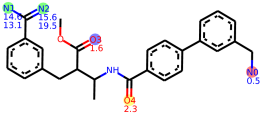

1fcx

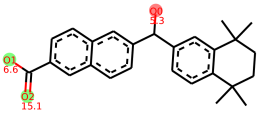

1fcz

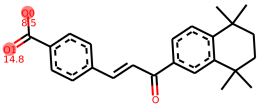

1fh8

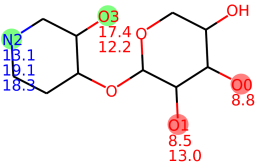

1fh9

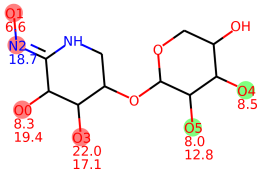

1fhd

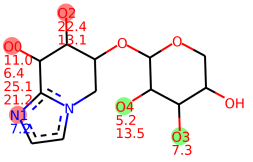

1fm6

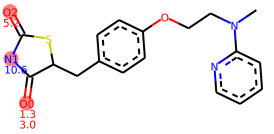

1fvt

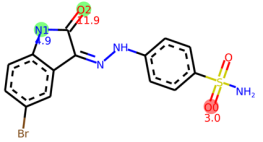

1g9v

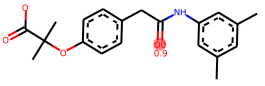

1gm8

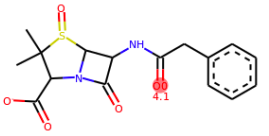

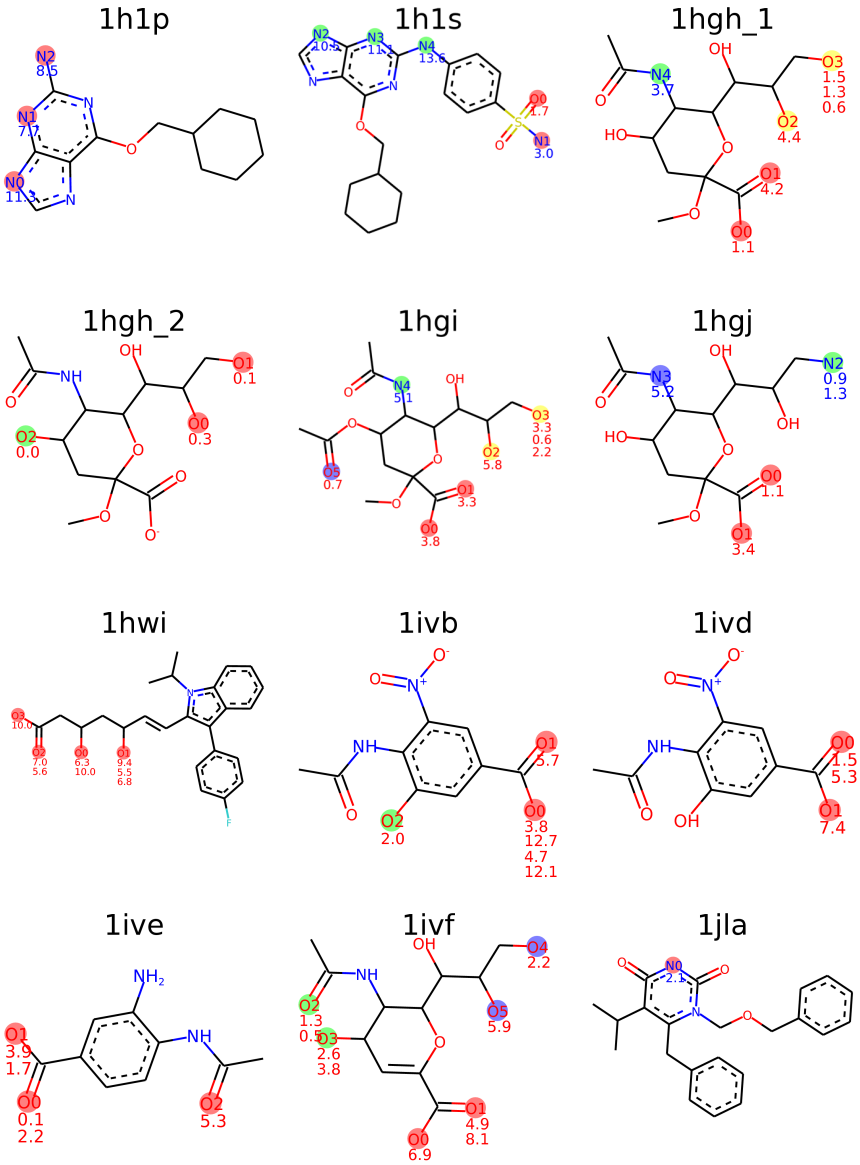
1h1p
1h1s
1hgh_1
1hgh_2
1hgi
1hgj
1hwi
1ivb
1ivd
1ive
1ivf
1jla

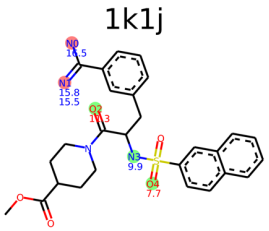
1k1j

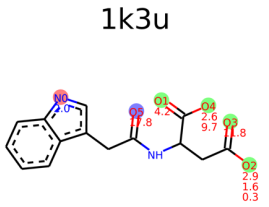
1k3u

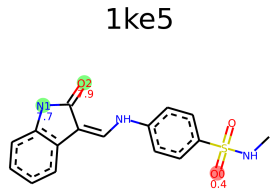
1ke5

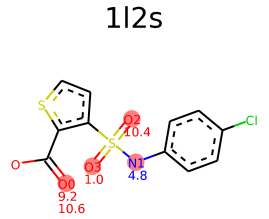
1l2s

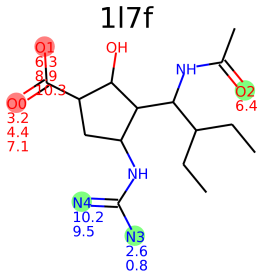
1l7f

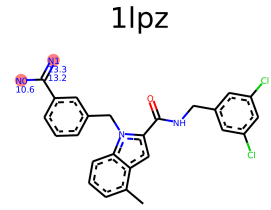
1lpz

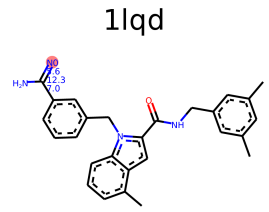
1lqd

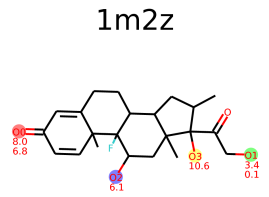
1m2z

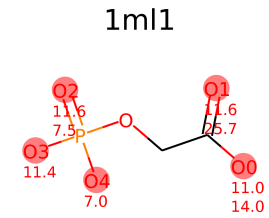
1ml1

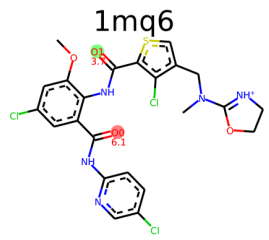
1mq6

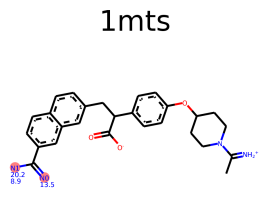
1mts

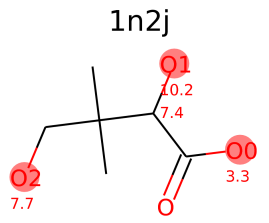
1n2j

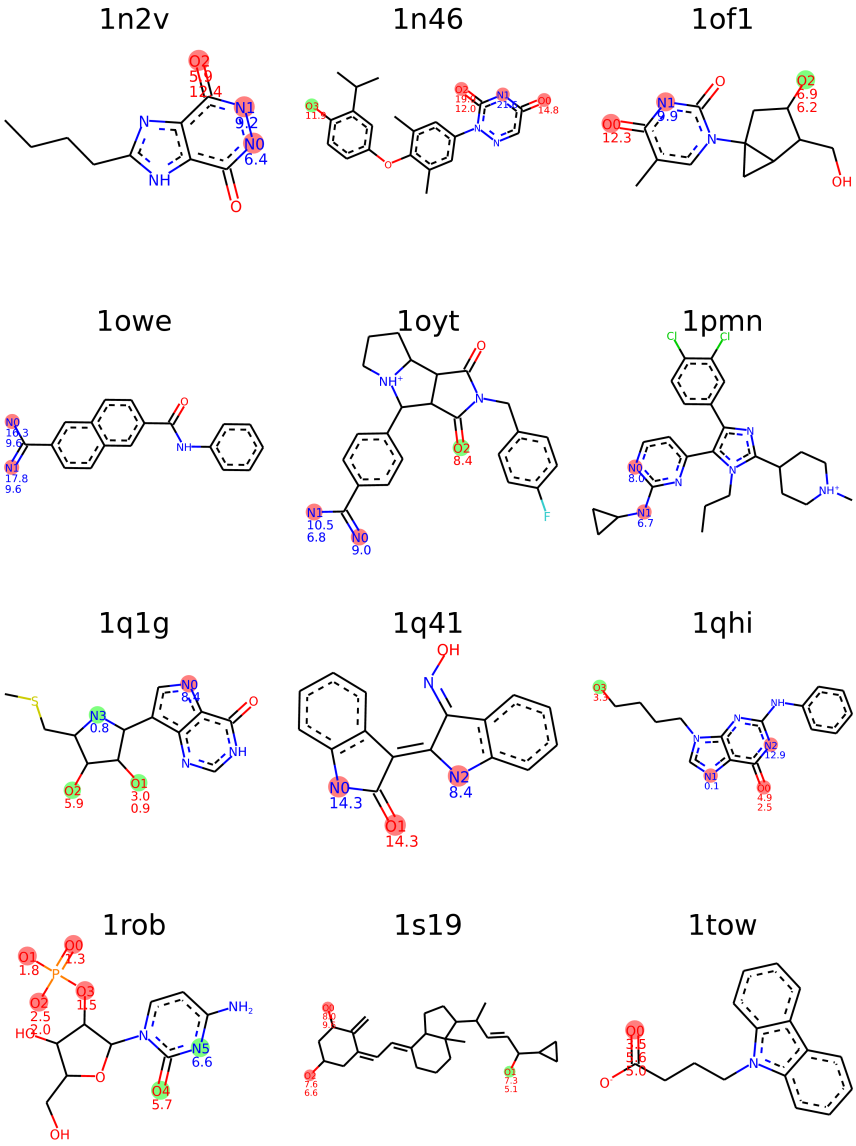
1n2v
1n46
1of1
1owe
1oyt
1pmn
1q1g
1q41
1qhi
1rob
1s19
1tow

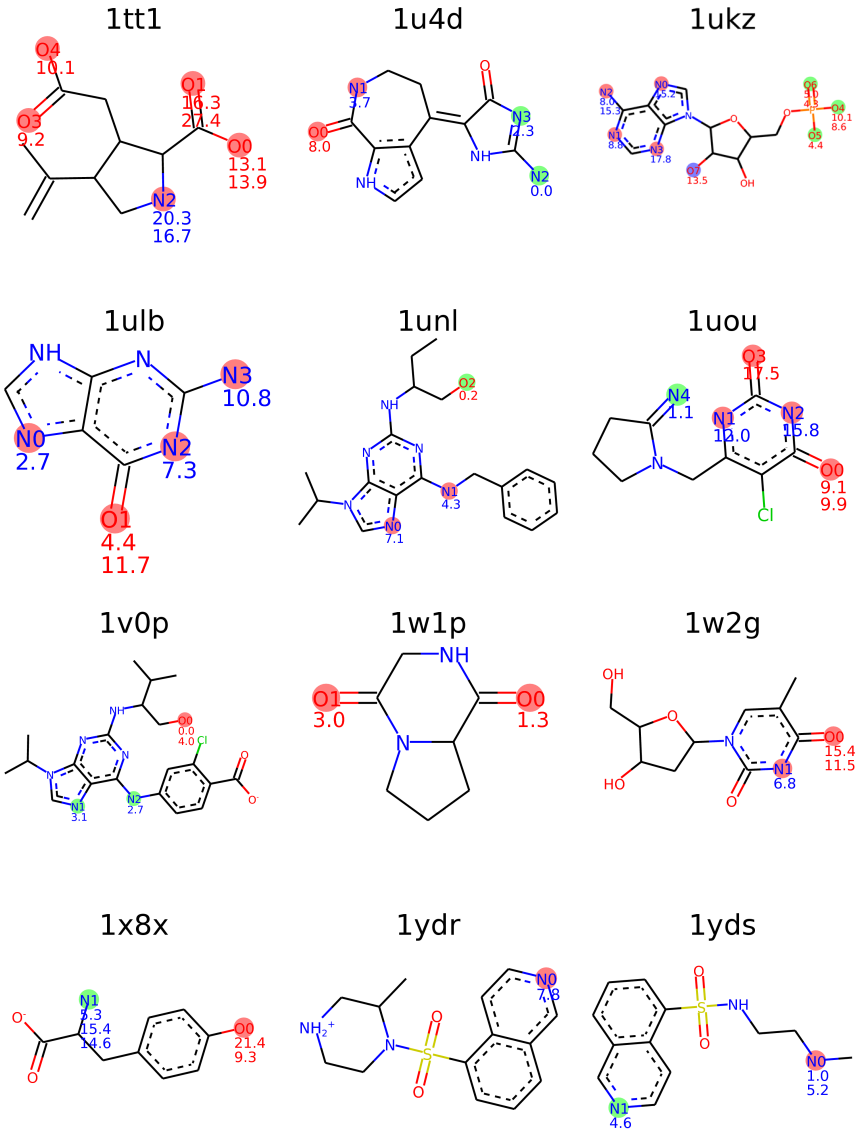
1tt1
1u4d
1ukz
1ulb
1unl
1uou
1v0p
1w1p
1w2g
1x8x
1ydr
1yds

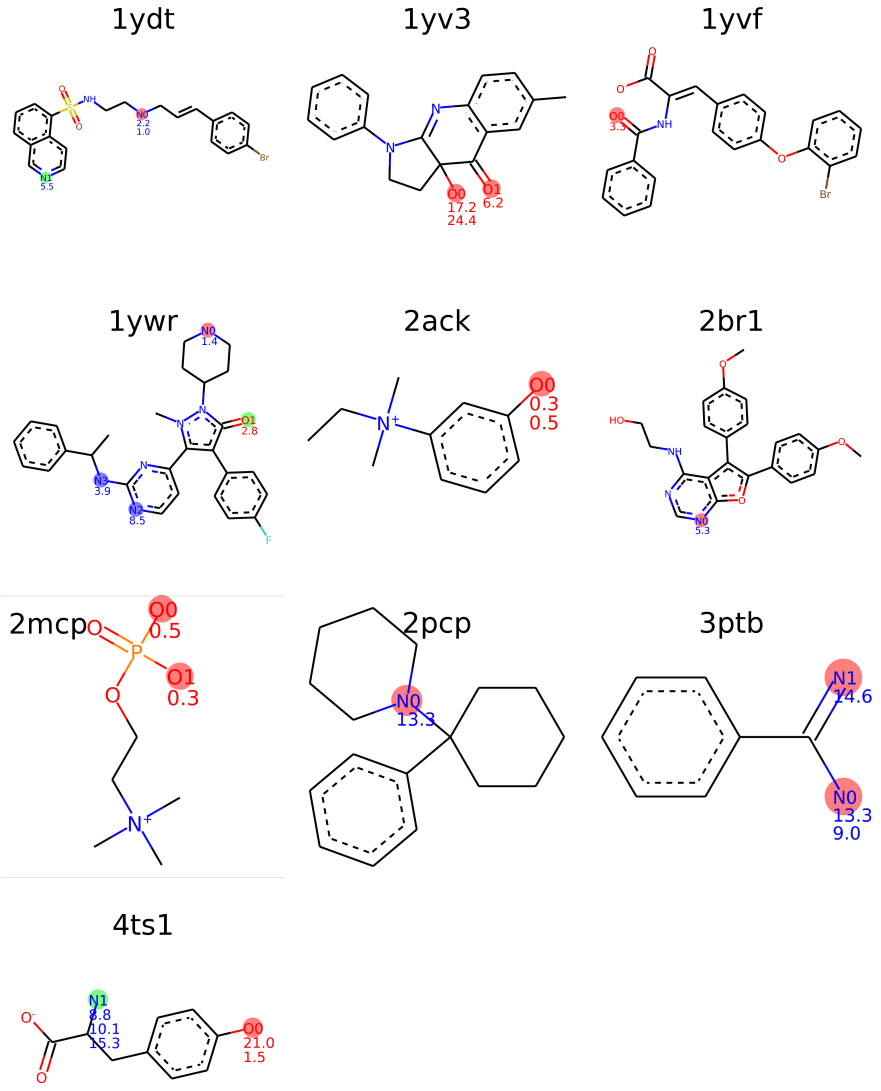
1ydt
1yv3
1yvf
1ywr
2ack
2br1
2mcp
2pcp
3ptb
4ts1

Supplementary Figure 2 Depicted ligands from SERAPhiC DS, with corresponding PDB codes. Atoms that make hydrogen bonds with the protein were highlighted and the W_{QB} value associated with that bond is written below the atom (multiple values in cases when the atom is making more than one hydrogen bond).

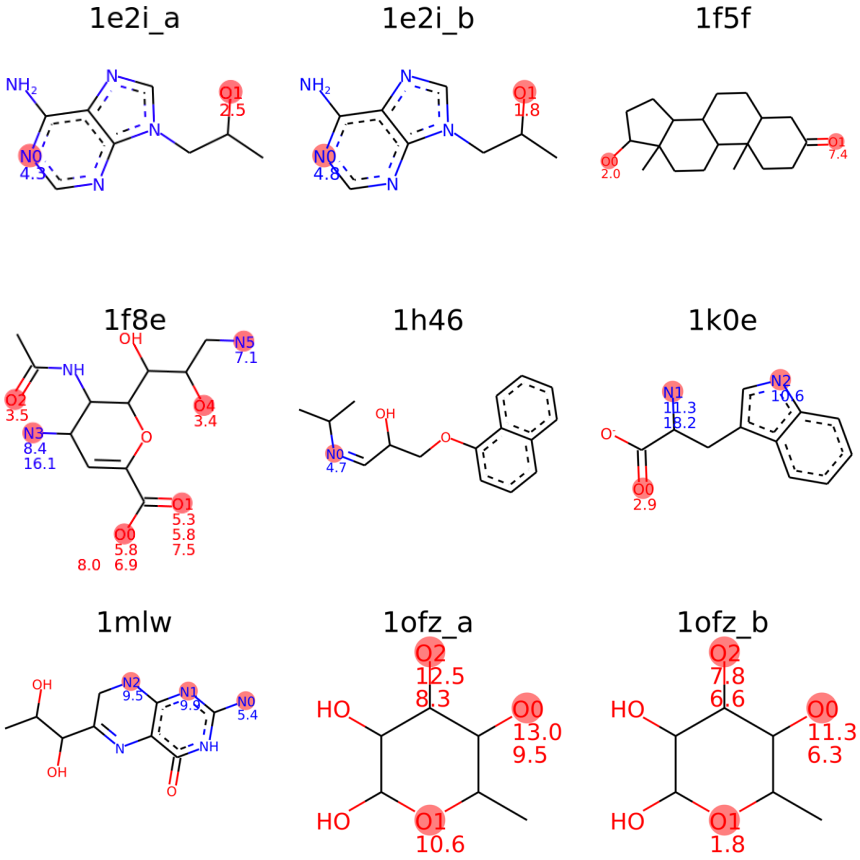

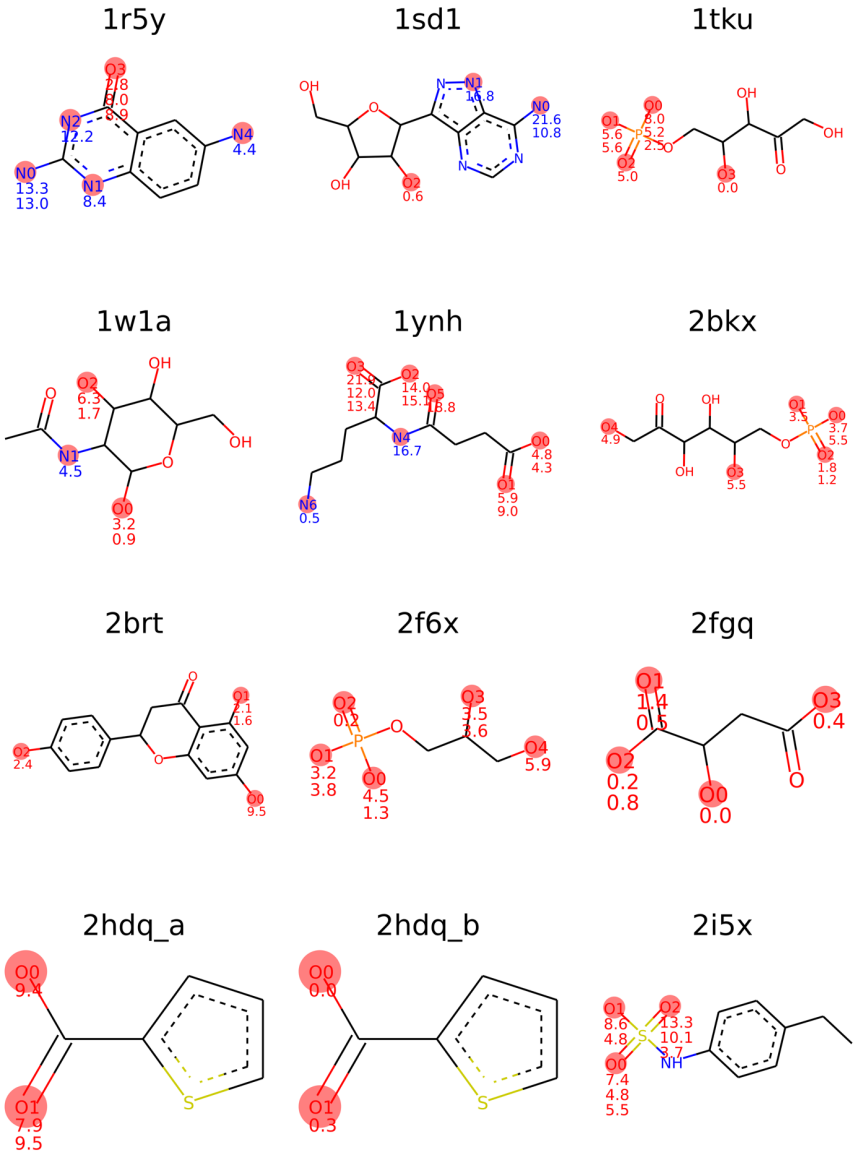
1r5y
1sd1
1tku
1w1a
1ynh
2bkx
2brt
2f6x
2fgq
2hdq_a
2hdq_b
2i5x

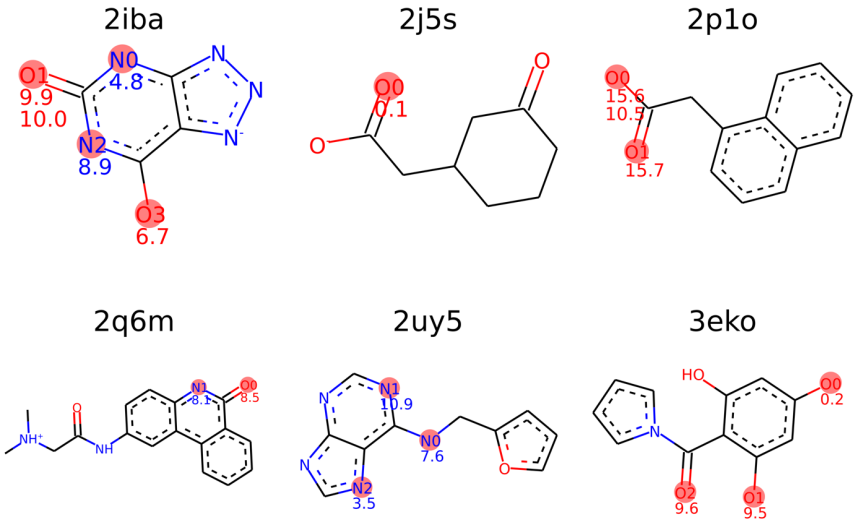

Supplementary Figure 3 Mean-W_{QB} value with standard deviation plotted against W_{QB} value. Error bars show standard deviation of "Mean W_{QB}". W_{QB} value does not have the error associated with it.

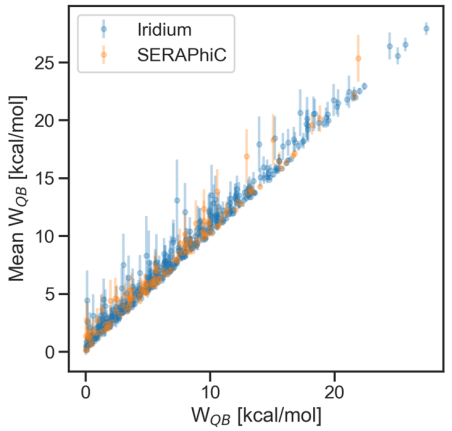

Results analysis

Supplementary Figure 4 Normalized β-factor of atom that makes the hydrogen bond in function of calculated W_{QB}. β-factor has been normalized against β-factors of other atoms of the ligand in PDB structure. Liable hydrogen bonds are depicted in blue and strong hydrogen bonds are depicted in green. The atoms with β-factor below the average are marked in magenta and the ones with β-factor above the average are marked in red. The side panels show the distribution of selected points as a kde-plots.

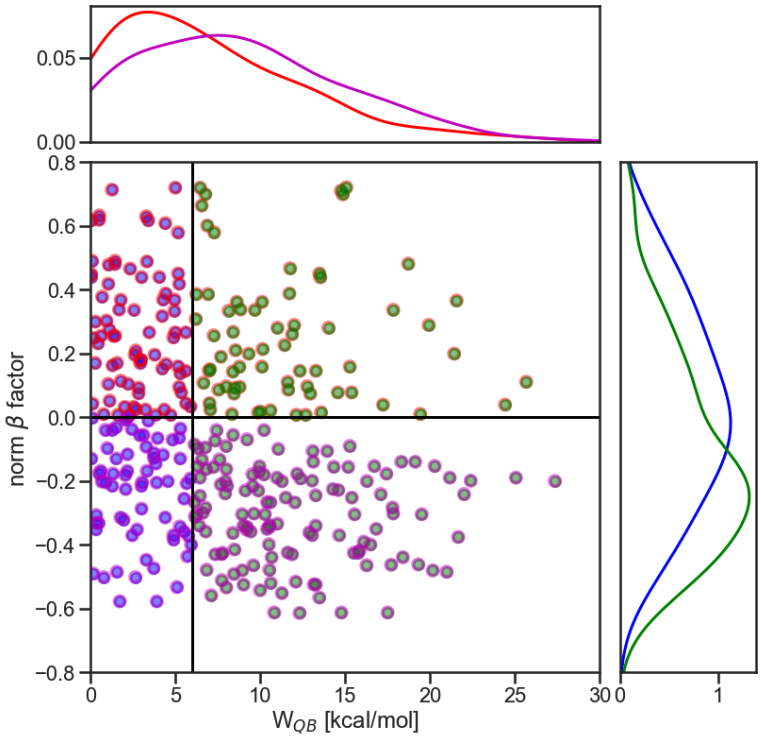

Supplementary Figure 5 A series of plots comparing W_{QB} value with potential energy calculations for hydrogen bonds from Iridium DS. The energy was computed as electrostatic potential energy (plots in the middle), and sum of electrostatic and Van der Waals potential energy (right plots). The energies were plotted for: a) interaction between atoms that form hydrogen bond, b) interaction of atom from ligand that form hydrogen bond with all atoms from chunk, c) interaction of atom form chunk that from hydrogen bond with all atoms from ligand, and d) Interaction of atoms that form hydrogen bond with the rest of the structure.

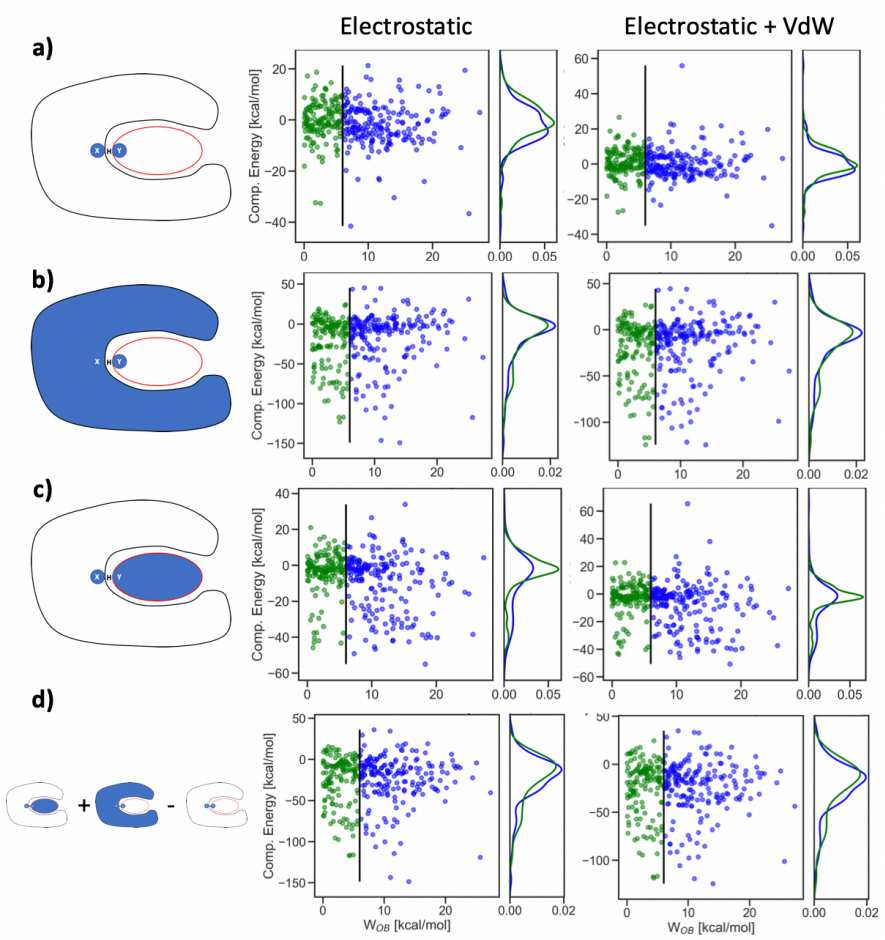

Supplementary Figure 6 Structures of protein-ligand complexes that do not poses any robust hydrogen bond. Weak hydrogen bonds (W_{QB} < 4 kcal/mol) marked in green. The first group (green, PDB codes: 1JLA and 1C1B) represents complexes of reverse transcriptase. Activity data of molecules: IC50 = 6 nM for 1JLA[11] and EC50 = 0.6 nM for 1C1B[12]. The second group (orange, PDB codes: 1HGH_2 and 1W1P) represent ligands with low activity. 1W1P has IC50 value of 5 mM[13]. 1HGH_2 is a ligand bound in the secondary binding side of hemagglutinin with considerably lower affinity that the primary binding site.[2] Third group (violet, PDB codes: 2ACK and 2MCP) represents complexes stabilized by cation-pi interaction, making hydrogen bonds weak. The interaction between cation and the centroid of tryptophan was marked in yellow. The last group (magenta, PDB codes: 1F0S, 1G9V and 1YVF) represents complexes stabilized by water mediated hydrogen bonds. The water network is marked as red '+' and the water mediated interactions are marked as yellow. Activity data of molecules K_i = 18 nM for 1F0S[14] and IC50 = 100 nM for 1YVF.[15]

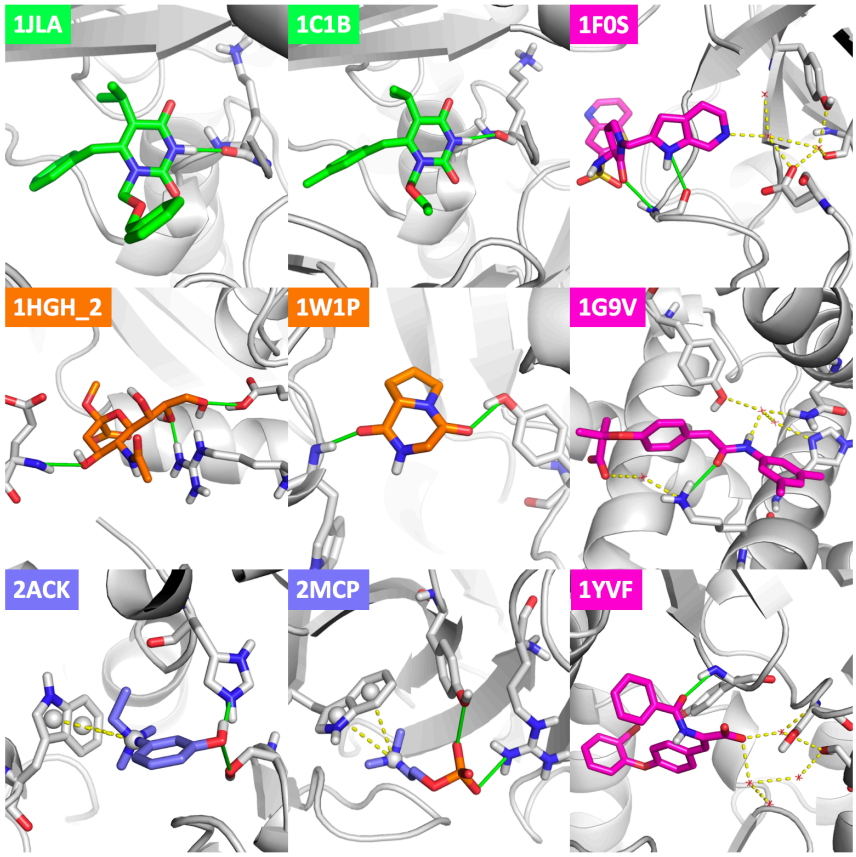

Supplementary Table 4 Two sample Kolmogorov-Smirnov statistical test of distribution of W_{QB} values across the four types of binding sites defined in Figure 1.

p-values	Enzymes	Nuclear receptors	Carbohydrate binding prot.	Allosteric sites
Enzymes				
Nuclear receptors	0.071			
Carbohydrate binding prot.	0.055	3.3e-3		
Allosteric sites	0.011	8.2e-4	0.24	

Supplementary Table 5 The average number of total and robust hydrogen bonds for the four types of binding sites defined in Figure 1.

Avg. HBs	Total	Robust
Enzymes	4.52	2.73
Nuclear receptors	3.86	3
Carbohydrate binding prot.	6.79	3.14
Allosteric sites	3.13	1.25

Supplementary Table 6 Simulated structures classified by the number of structural anchors.

Number of structural anchors	PDB codes
0	1c1b, 1f0s, 1g9v, 1hgh-2, 1jla, 1w1p, 1yvf, 2ack, 2mcp
1	1a28, 1ai5, 1b9v, 1br6, 1cvu, 1dds, 1ezq, 1f0t, 1f0u, 1fcz, 1fm6, 1fvt, 1gm8, 1h1p, 1h1s, 1hgj, 1hwi, 1ivb, 1ivd, 1ive, 1ke5, 1l2s, 1lpz, 1lqd, 1ml1, 1mq6, 1mts, 1n2j, 1n2v, 1owe, 1pmn, 1q41, 1qhi, 1rob, 1tow, 1tt1, 1u4d, 1ulb, 1unl, 1uou, 1v0p, 1w2g, 1ydr, 1ydt, 1yv3, 1ywr, 2br1, 2pcp, 3ptb
2	1exa, 1fcx, 1fh8, 1fh9, 1fhd, 1hgh-1, 1hgi, 1ivf, 1k1j, 1k3u, 1n46, 1of1, 1oyt, 1q1g, 1s19, 1x8x, 1yds, 4ts1
3	1l7f, 1m2z, 1ukz

Supplementary Table 7 Distribution of carbohydrate binding proteins based on the number of anchoring points.

No. anchoring points	No. complexes	%
0	1	7.1
1	6	42.9
2	6	42.9
3	1	7.1

Supplementary Figure 7 Standard deviation of W_{QB} values within each cluster of hydrogen bonds selected based on Supplementary Figure 1 (marked in blue). Standard deviation of collected individual values separated by the number of hydrogen bonds in the group (marked in red).

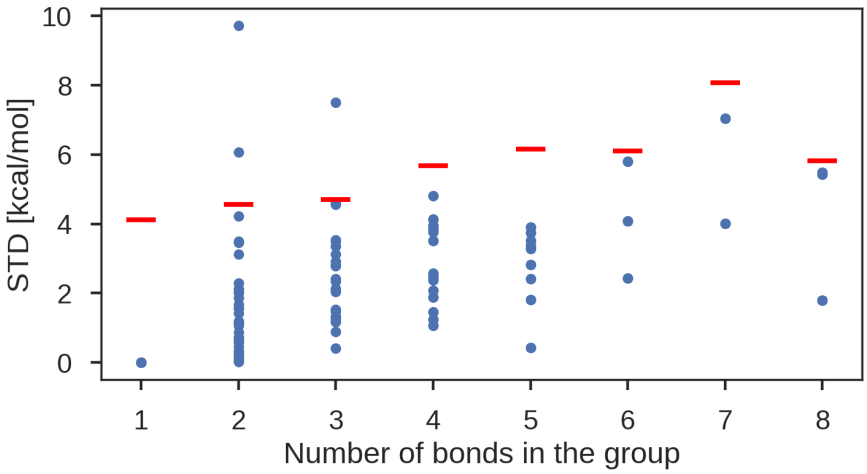

Supplementary Figure 8 Depicted structures of ligand with PDB code 1n46 in the correct protonation state (left figure) in protonated form (middle figure). Atoms making hydrogen bonds are highlighted and the value listed below the atom correspond to W_{QB} value of a bond made by this atom. Miscalculated protonation state not only is responsible for not forming an important interaction (W_{QB}=21.6 kcal/mol) but also significantly decreases the strength of 3 HBs in the local environment (from W_{QB}=19.9, 14.8 and 12.0 kcal/mol to W_{QB}=11.8, 11.9 and 9.4 kcal/mol, respectively). Both protonation states are predicted to exist at pH 7 (www.chemicalize.org). The right figure shows hydrogen bond network of considered scaffold.

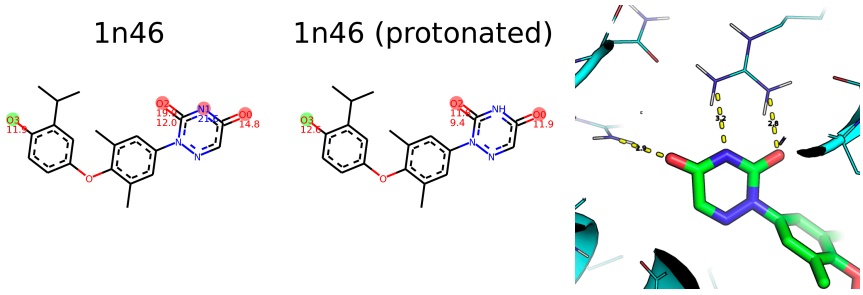

Supplementary Figure 9 Binding free energy versus maximal W_{QB} value. Plot is based on a set of complexes with publicly available activity data. Binding energy was calculated based on: ΔG (blue), IC50 (green), K_D (red) or K_i (purple) measurements.

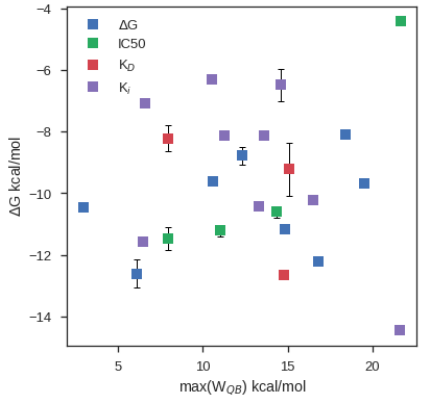

Supplementary Figure 10 Relation between structural stability and solvent exposure. The plot shows W_{QB} value in function of Solvent Accessible Surface Area (SASA) of the atom in the protein that makes the main hydrogen bond with ligand. All DUck-simulation data for Iridium DS (345 data points) are plotted.

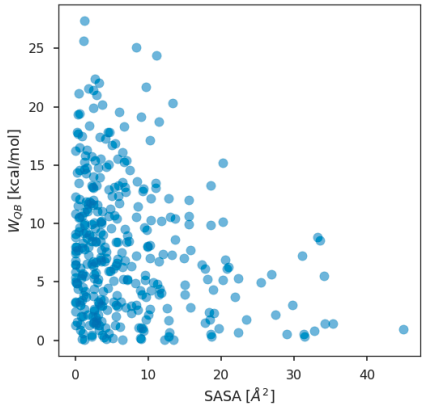

Supplementary References

1. Warren, G. L., Do, T. D., Kelley, B. P., Nicholls, A. & Warren, S. D. Essential considerations for using protein-ligand structures in drug discovery. *Drug Discov. Today* **17,** 1270–1281 (2012).
2. Sauter, N. K. *et al.* Binding of Influenza Virus Hemagglutinin to Analogs of Its Cell-Surface Receptor , Sialic Acid : Analysis by Proton Nuclear Magnetic Resonance Spectroscopy and. *Biochemistry* **31,** 9609–9621 (1992).
3. Favia, A. D., Bottegoni, G., Nobeli, I., Bisignano, P. & Cavalli, A. SERAPhiC : A Benchmark for in Silico Fragment-Based Drug Design. *J. Chem. Inf. Model.* **51,** 2882–2896 (2011).
4. Molecular Operating Environment (MOE). (2018).
5. Pettersen, E. F. *et al.* UCSF Chimera - A visualization system for exploratory research and analysis. *J. Comput. Chem.* **25,** 1605–1612 (2004).
6. Ruiz-carmona, S. *et al.* Dynamic undocking and the quasi-bound state as tools for drug discovery. *Nat. Chem.* **9,** 201–206 (2017).
7. Majewski, M., Ruiz-Carmona, S. & Barril, X. in *Rational Drug Design. Methods in Molecular Biology* (eds. Mavromoustakos, T. & Kellici, T. F.) 195–215 (Humana Press, 2018). doi:https://doi.org/10.1007/978-1-4939-8630-9_11
8. Jakalian, A., Jack, D. B. & Bayly, C. I. Fast, efficient generation of high-quality atomic charges. AM1-BCC model: II. Parameterization and validation. *J. Comput. Chem.* **23,** 1623–1641 (2002).
9. Bayly, C. I., McKay, D. & Truchon, J. F. An Informal AMBER Small Molecule Force Field: parm@Frosst. *Computational Chemistry Ltd* (2011).
10. Case, D. A. *et al.* AMBER 12. (2012).
11. Hopkins, A. L. *et al.* Complexes of HIV-1 Reverse Transcriptase with Inhibitors of the HEPT Series Reveal Conformational Changes Relevant to the Design of Potent Non-Nucleoside Inhibitors. 1589–1600 (1996). doi:10.1021/jm960056x
12. Kireev, D. B., Chre, J. R., Grierson, D. S. & Monneret, C. A 3D QSAR Study of a Series of HEPT Analogues : The Influence of Conformational Mobility on HIV-1 Reverse Transcriptase Inhibition. **2623,** 4257–4264 (1997).
13. Houston, D. R. *et al.* Structure-Based Exploration of Cyclic Dipeptide Chitinase Inhibitors. 5713–5720 (2004). doi:10.1021/jm049940a
14. Pinto, D. J. P., Smallheer, J. M., Cheney, D. L., Knabb, R. M. & Wexler, R. R. Factor Xa Inhibitors : Next-Generation Antithrombotic Agents. 6243–6274 (2010). doi:10.1021/jm100146h
15. Pfefferkorn, J. A. *et al.* Inhibitors of HCV NS5B polymerase . Part 1 : Evaluation of the southern region of (2Z) -2- (benzoylamino) -3- (5-phenyl-2- furyl) acrylic acid. **15,** 2481–2486 (2005).

3.2 Structural Stability Predicts the Binding Mode of Protein-Ligand Complexes

Maciej Majewski[1], and Xavier Barril[1,2]

*Journal of Chemical Information and Modeling (**2020**)*

1. Institut de Biomedicina de la Universitat de Barcelona (IBUB) and Facultat de Farmacia, Universitat de Barcelona, Av. Joan XXIII 27-31, 08028 Barcelona, Spain.
2. Catalan Institution for Research and Advanced Studies (ICREA), Passeig Lluis Companys 23, 08010 Barcelona, Spain.

JCIM JOURNAL OF CHEMICAL INFORMATION AND MODELING

pubs.acs.org/jcim Article

Structural Stability Predicts the Binding Mode of Protein−Ligand Complexes

Maciej Majewski and Xavier Barril*

Cite This: https://dx.doi.org/10.1021/acs.jcim.9b01062 Read Online

ACCESS | Metrics & More | Article Recommendations | Supporting Information

ABSTRACT: The prediction of a ligand's binding mode into its macromolecular target is essential in structure-based drug discovery. Even though tremendous effort has been made to address this problem, most of the developed tools work similarly, trying to predict the binding free energy associated with each particular binding mode. In this study, we decided to abandon this criterion, following structural stability instead. This view, implemented in a novel computational workflow, quantifies the steepness of the local energy minimum associated with each potential binding mode. Surprisingly, the protocol outperforms docking scoring functions in case of fragments (ligands with MW < 300 Da) and is as good as docking for drug-like molecules. It also identifies substructures that act as structural anchors, predicting their binding mode with particular accuracy. The results open a new physical perspective for binding mode prediction, which can be combined with existing thermodynamic-based approaches.

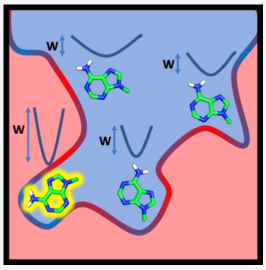

INTRODUCTION

Drug discovery is an expensive process, consuming both time and resources. Computational methods can be applied at various stages of this process to increase overall efficiency.[1] Molecular docking is particularly well known and widely applied in this context. Primarily, it is used to predict the binding mode of a (potential or actual) ligand into the binding site of its protein target.[2−4] The fit is assessed by a scoring function that, through the evaluation of molecular interactions, approximates the free energy of binding (ΔG_{BIND}) with the protein.[3] Many protein−ligand docking programs have been developed and applied in drug discovery projects, including Glide,[5,6] ICM,[7] rDock,[8] DOCK,[4] GOLD,[9,10] FlexX,[11] and Auto-dock.[12] However, the methods remain imperfect, and their performance can be disappointing.[13,14] Incorrect predictions can be caused by inaccuracies in scoring function[3,15] that very often neglect solvation effects and entropy[16−19] as well as difficulties quantifying some interactions, such as water-mediated contacts.[20] Moreover, many methods are based on a static representation of biomolecules forced by X-ray structures, and the influence of protein flexibility on binding cannot be underestimated.[21,22] Alternative approaches to improve binding mode prediction have been described in the literature. Some apply methods with a better theoretical background to rescore a subset of poses.[23−28] Others carry out molecular dynamics (MD) simulations of the complex to confirm that the predicted binding mode is stable[29−31] or to explore drug−target binding event fully.[32,33] Significant improvements in accuracy and reliability of predictions have been made by coupling induced-fit docking with stability assessment of the pose by metadynamics.[34] However, there is still room for improvement, and orthogonal methods that could complement the existing ones would be particularly useful.

Recently, we have proposed that protein−ligand complexes are not only thermodynamically stable but also structurally robust, and that true ligands present a larger resistance to the rupture of key interactions than decoys. This represents an alternative to standard thermodynamic approaches (Figure 1) and, as both perspectives are uncorrelated, they can be combined very effectively in virtual screening for drug discovery.[35,36] In practice, structural stability is measured as the work necessary to displace a ligand from its position of equilibrium to a nearby quasi-bound (QB) state where a preselected interaction has just been broken (W_{QB}). Intriguingly, this property should work because W_{QB} only informs the depth of a local minimum and the QB state is irrelevant from a thermodynamic perspective. An extensive investigation of protein−ligand complexes provided a possible explanation to this apparent paradox: while robustness is not a prerequisite for binding, cases of labile protein−ligand complexes are rare, and the vast majority present strong resistance to even minor structural perturbations.[37] This may obey a functional need or simply reflect the intrinsic properties of proteins. Encouraged by these results, here, we apply the concept of structural

Received: November 14, 2019
Published: February 13, 2020

https://dx.doi.org/10.1021/acs.jcim.9b01062
J. Chem. Inf. Model. XXXX, XXX, XXX−XXX

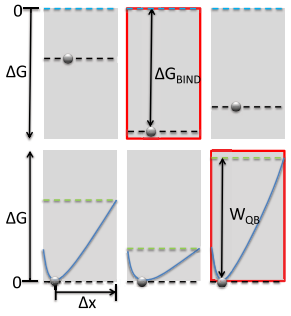

Figure 1. Standard thermodynamics-based methods (top) aim at predicting the free energy difference between the unbound (blue dashed line) and bound states (black dashed line). The bound state with the most negative ΔG_{BIND} (middle box in this example) is considered as the correct solution. Structural stability methods (bottom) introduce a structural perturbation to the bound state ($\Delta x \approx 2$ Å). The binding mode that opposes the most resistance to such perturbation is considered as the correct solution (rightmost box in this case). The work needed to take the ligand into a quasi-bound state (W_{QB}) reflects the depth of the free energy minimum (green dashed lines) but provides no reference to the unbound state. The circle represents ligand in its bound state.

robustness (W_{QB}) to the problem of binding mode prediction. To do so, we have extended the Dynamic Undocking (DUck) method to consider global structural stability rather than the stability provided by a single predefined interaction, as was done before.[37] Surprisingly, the method performs better than standard (thermodynamics-based) methods. This has important practical implications for drug design but also raises the question as to why a local property (steepness of free energy minima around the binding mode) percolates to a global property (absolute free energy of the binding mode) and can, therefore, be used to identify the correct binding mode of a ligand.

METHODS

To assess the applicability of DUck in binding mode prediction, we designed a multistep protocol. First, rDock, a docking program that performs exhaustive sampling of the protein−ligand configurational space,[8,38] is used to generate potential binding modes (poses). The top 5 unique scoring poses are then considered in the next step, where all protein−ligand hydrogen bonds are automatically detected and their W_{QB} values evaluated using DUck.

Data Sets. We selected SERAPhiC data set[39] to evaluate the performance of our approach. It contains 53 high-quality X-ray models of fragment−protein complexes. The curators provided a set of complexes with verified binding modes as well as assigned protonation and tautomeric states for both ligands and receptors. Some of the complexes were not suitable for simulation or analysis, and thus were excluded from the calculation. These include 7 cases that did not possess any intermolecular hydrogen bonds (at present DUck only assesses the stability of hydrogen bonds), 16 complexes with metal ions because molecular mechanics force fields do not faithfully represent organometallic complexes, and 5 complexes with multiple ligands in the binding pocket because of complexity of analysis. Simulation of one of the complexes (1xfg) did not complete successfully due to an unresolved error of the molecular dynamics software in the restraint definition. This resulted in 27 remaining binding pockets from 24 different PDB structures. Three structures possess two ligands per protein indicated by "a" and "b" next to the PDBid (Table S1). The structure with PDBid 1e2i possesses two possible enantiomers of 9-hydroxypropyladenine in the binding pocket.[40] The electron density did not allow a clear stereochemistry assignment, and both *R* and *S* enantiomers of fragment showed a reasonable fit (0.82 and 0.91, respectively).[39] For this target, docking and DUck simulations were conducted separately for each enantiomer; however, to avoid redundancy of data in the analysis, both forms were treated as one cavity. Entry 1ofz is a complex of lectin with two anomers of fucose.[41] The β anomer of the sugar is included in the data set, and it was found bound to two distinct binding sides. In the last case of entry 2hdq, carboxythiophene molecules were bound in multiple spots.[42] The authors included two poses most likely to be pharmaceutically relevant. Both pockets in entries 1ofz and 2hdq were treated as separate cavities in the simulation and analysis stage.

A second data set used in the project is a collection of complexes with drug-like molecules, Iridium data set.[43] The set consists of 120 diverse and highly trustworthy protein−ligand complexes. The curators of this data set provided a collection of refined protein structures and verified binding modes. Again, not all of the complexes were suitable for DUck simulation: 3 cases that did not possess any intermolecular hydrogen bonds; 28 complexes with metal ions; 5 complexes with multiple ligands in the binding pocket; and 6 cases where the ligand was classified as not drug-like. One complex (1hgh) possesses two distinctive binding pockets that differ in affinity[44] (Figure S1). For this case, simulation and analysis were conducted for each pocket independently. The simulation of two complexes did not complete successfully due to the error mentioned before. These cases were also discarded from the analysis. The final set consisted of 76 complexes and 77 binding pockets. Table S1 features the full classification of structures.

Ligand and Protein Preparation. Fragment data set, SERAPhiC, contained a fully protonated collection of ligands and proteins.[39] However, a few cases were corrected after manual inspection. Iridium data set contained a set of ligands with assigned protonation and tautomeric states. Molecules were then manually inspected and corrected if needed. Protonation states of residues of corresponding protein structures were assigned using Molecular Operating Environment (MOE)[45] at pH 7.0. Then, structures were manually inspected, and questionable cases were corrected, consulting the publication of origin whenever needed. The prepared protein structures were then saved in MOL2 format and used as input for rDock. The full set of proteins and corresponding ligands for both data sets is shared as a part of the Supporting Information.

Molecular Docking. Molecular docking was run with rDock,[8] a reliable open-source program, developed in the group. rDock has been reported to provide excellent sampling,[46] which makes it ideal for generating a diverse collection of putative binding modes. As an input, we provided MOL2 files with receptors and SDF files with ligands. The cavity was defined using the reference ligand method with the crystallized ligand found in the PDB structure as a reference and a distance of 6 Å to define the maximal extent of the cavity around the ligand. Docking was performed with default rDock

https://dx.doi.org/10.1021/acs.jcim.9b01062
J. Chem. Inf. Model. XXXX, XXX, XXX−XXX

Journal of Chemical Information and Modeling pubs.acs.org/jcim Article

parameters,[8] with 100 individual runs per ligand, which is considered very exhaustive sampling. Four cases of multiple binding modes per complexes of 1hgh, 1e2i, 1ofz, and 2hdq were treated as separate cavities. In the case of 1hgh, 1ofz, and 2hdq, the cavities were not overlapping. Entry 1e2i had slightly different cavities depending on the enantiomer (Figure S1).

For each binding pocket, 100 generated poses were sorted based on the total docking score and a set of unique top-scoring poses was selected based on root-mean-square deviation (RMSD). The top-scoring pose was chosen initially, then the remaining poses were iterated, and the ones that differed more than the RMSD cutoff value from any of the previously selected poses were included in the new selection. For fragments (SERAPhiC), an RMSD cutoff of 1.5 Å is appropriate to define a new pose as distinct, and for drug-like molecules (Iridium) the cutoff is 2.0 Å.[47] For six systems, none of the poses generated by rDock had an RMSD lower than 2 Å relative to the crystallographic pose (Table 1). For four of these systems (1dds, 1ezq, 1f0u, and 1lqd), we considered the lowest RMSD pose as the correct one because the RMSD value was below 3 Å. The two remaining cases, 1g9v and 1ydt, did not obey the criterion with the lowest RMSD pose being 3.09 for 1g9v and 3.24 for 1ydt.

Due to limitations in computational power, only the five best-scoring unique poses were selected for further simulation. Additionally, in the case of three structures (1cvu, 1g9v, 1n2j), a pose with the lowest RMSD compared to the crystallographic structure was included as the sixth pose in selection because it was not a part of the top five poses. In the case of 1n2j, the added pose ended up being selected by DUck; however, for the remaining cases, additional pose had no influence on the final result.

Dynamic Undocking. To evaluate the poses selected in the previous step, we used DUck.[35] It is a method based on Steered Molecular Dynamics (SMD) that assesses the robustness of hydrogen bonds. In the SMD, an intermolecular HB is pulled from 2.5 to 5.0 Å, measuring the work necessary to cause this displacement. In a posterior analysis, we retrieve the work needed to take the HB from its equilibrium distance (usually 3 Å) to the breaking point (where the work profile reaches a maximum and starts to decrease), or 5.0 Å, whatever occurs first. We refer to this point of rupture as the quasi-bound (QB) state and the work needed to reach it is denoted W_{QB}. Large W_{QB} values indicate that the HB is located in a deep and narrow minimum on the free energy surface and shows that (regardless of its contribution to ΔG_{BIND}) the HB provides structural stability to the protein−ligand complex. From previous research, we deduced that robust bonds possess W_{QB} higher than 6 kcal/mol and labile ones less than 4 kcal/mol.[37]

Previously, the method was tested only as a virtual screening application and was relying on a single preselected "key interaction" with the protein. This approach makes DUck highly dependent on the previous knowledge of the system, meaning that the user has to be confident in the bond selection. Here, we aim to use the method as a blind tool, simulating all possible hydrogen bonds in the complex and then evaluating each pose based on the W_{QB} values of individual HB. This approach makes the method more applicable in binding mode prediction. For 375 selected poses in Iridium and 136 in SERAPhiC, 1203 and 538 hydrogen bonds were identified using Chimera FindHBond function, respectively.[48]

As an input, DUck requires ligand and a subset (chunk) of protein that will preserve the local environment of the bond (Figure S2). Using the chunk instead of the full protein saves on computational cost but also creates a simple dissociation pathway for the ligand, thus ensuring that W_{QB} reflects only the intrinsic robustness of the HB and its immediate surroundings. The chunk was created for each HB separately. Usually, chunks are selected manually, however, to deal with such a big number of HBs we automated the process. The script first selects residues within 7 Å from the atoms forming the main interactions and then includes additional residues that cross the surface span on heavy atoms of initial selection. Next, the chains are capped with *N*-methyl or acetyl group. The scripts can be obtained from the authors upon request.

Every individual hydrogen bond, corresponding to a particular ligand pose−protein chunk pair, was then simulated with DUck according to previously published protocol with default parameters.[36] The length of the molecular dynamics step simulated between SMD steps was 0.5 ns. To ensure extensive sampling, 40 SMD were run for each simulated interaction (20 sequential runs, each with two parallel simulations at 300 and 325 K). This number of runs provides a trustworthy evaluation of the bond while still keeping the simulation cost affordable for such a big data set. The W_{QB} threshold (a variable that causes early termination of the protocol) was set to 0.1 kcal/mol, thus ensuring exhaustive sampling for all HBs except those that break spontaneously. Preparation of the selected systems was executed with a MOE[45] Scientific Vector Language script available online.[49] The script calculates AM1-BCC charges for the ligand[50] and assigns atom types and nonbonded parameters to the ligand from the parm@Frosst force field.[51] It also identifies the atoms forming the hydrogen bond, produces the files necessary to perform the MD simulations with AMBER 14[52] (AMBER99S-Bildn force field is used to parametrize protein), and calls the AMBER tLeap program to generate valid topology and coordinate files. All of the simulations were run at the Barcelona Supercomputing Center using NVIDIA Tesla M2090 GPUs.

To compare results for generated poses with crystallographic data, true binding modes extracted from crystal structures were also simulated with DUck according to the protocol described above.

Individual W_{QB} values are combined into a single molecule-wide score in various manners. The formulas are listed as follows

$$\text{DUck\_max} = \max(\{W_{QB_1}, ..., W_{QB_n}\}) \quad (1)$$

$$\text{DUck\_min} = \min(\{W_{QB_1}, ..., W_{QB_n}\}) \quad (2)$$

$$\text{DUck\_ave} = \frac{\sum_{i=1}^{n} W_{QB_i}}{n} \quad (3)$$

$$\text{DUck\_sum} = \sum_{i=1}^{n} W_{QB_i} \quad (4)$$

$$\text{DUck\_group} = \sum_{i=1}^{k} \text{Gr}_i \quad (5)$$

$$\text{DUck\_group\_max} = \max(\{\text{Gr}_1, ..., \text{Gr}_k\}) \quad (6)$$

https://dx.doi.org/10.1021/acs.jcim.9b01062
J. Chem. Inf. Model. XXXX, XXX, XXX−XXX

where n is the number of individual W_{QB} values for a given pose, k is the number of groups for that pose, and Gr is a value assigned to a group. Atoms making hydrogen bonds were grouped based on the distance in space. Gr can be defined by one of the following equations

$$\text{Gr\_max} = \max(\{W_{QB_1}, ..., W_{QB_m}\}) \quad (7)$$

$$\text{Gr\_ave} = \frac{\sum_{i=1}^{m} W_{QB_i}}{m} \quad (8)$$

$$\text{Gr\_sum} = \sum_{i=1}^{m} W_{QB_i} \quad (9)$$

$$\text{Gr\_max x HB} = \text{Gr\_max} \cdot m \quad (10)$$

$$\text{Gr\_min x HB} = \min(\{W_{QB_1}, ..., W_{QB_m}\}) \cdot m \quad (11)$$

where m is the number of individual W_{QB} values for a given group.

Performance Assessment. To assess the quality of the predictions, the RMSD between predicted binding mode and the X-ray pose was calculated using the *sdrmsd* tool implemented in rDock.[8]

The performance was assessed by calculating the percentage of complexes for which the RMSD between X-ray and selected pose is below a set cutoff. The cutoff is usually 2 Å for drug-like molecules and 1.5 Å for fragments.[47] To extract more information, the success rate was measured as a function of the threshold and presented as a plot (Figures 2 and 3).

To compare DUck's performance with baseline, we assessed the success of rDock and random selection. For rDock, the pose with the lowest total score (highest predicted affinity) was selected. For random selection, we randomly selected a pose out of the poses simulated by DUck. The plots corresponding to random selection, presented in Figures 2 and 3, were created by averaging 10 000 individual selections.

RESULTS AND DISCUSSION

DUck Outperforms Docking in Fragment Binding Mode Prediction. To use structural stability for binding mode prediction, the W_{QB} values corresponding to individual HBs have to be combined into a single "stability score". Previous DUck applications focused on a single, preselected, hydrogen bond that was considered essential for the complex. This works well in virtual screening,[35] but we wanted to overcome this limitation and expand the analysis to all detected hydrogen bonds without any knowledge-based bias. As there are many potential ways of combining individual W_{QB} values into a collective score and the internal degrees of freedom of the ligand can complicate any analysis, we initially focused our attention on the so-called fragments. These are the simplest possible type of ligands, with a molecular weight in a range of 78−300 Da, at least one ring, and very few rotatable bonds.[39] We have tested four simple ways of translating individual W_{QB} values into an aggregated score, each corresponding to a different assumption. The first assumption is that the strongest link defines the complex, and thus we take the maximum of all W_{QB} values (DUck_max) and select the binding mode capable of making the single most robust interaction as the correct one. In the opposite assumption, once the weakest link is broken, the rest of the interactions fall spontaneously, and thus we take the minimum of all W_{QB} values (DUck_min) and select the binding mode with the largest DUck_min value as the correct one. Midway between the two former hypotheses, we may assume that the work needed to break the complex corresponds to the average W_{QB} (DUck_ave). Alternatively, we can hypothesize that each hydrogen bond acts independently and that their contributions are additive (DUck_sum), and thus binding modes forming more hydrogen bonds are more likely to be selected.

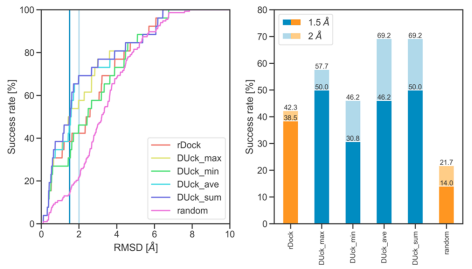

Figure 2. On the left, the plot representing success rate as a function of the RMSD cutoff between generated binding mode and the reference for SERAPhiC data set. On the right, barplot representing success rate at 1.5 and 2 Å, based on the plot on the left. Estimated errors are included in Table S2.

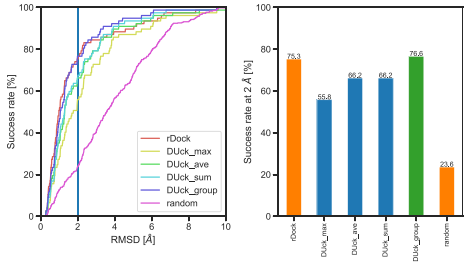

Figure 3. On the left, the success rate as a function of the RMSD cutoff between generated binding mode and the reference for the Iridium data set. On the right, the barplot representing success rate at 2 Å, based on the plot on the left. Estimated errors are included in Table S2.

Docking fragments is more challenging than bigger (e.g., drug-like) molecules because their small size allows them to fit into the binding site in multiple orientations and different

Table 1. Classification of Failed Prediction Cases[a]

category	PDBid
rDock failed to generate pose with RMSD lower than 2 Å from the reference pose	1dds, 1ezq, 1f0u, **1g9v**, 1lqd, **1ydt**
rDock failed to predict the binding mode	1f0s, 1f0t, 1f0u, 1ive, 1l2s, 1lqd, 1n2j, 1n2v, 1owe, 1pmn, 1q1g, 1s19, 1tow, 1ukz, 2ack
DUck failed to predict the binding mode	1c1b, 1dds, 1ezq, 1f0t, 1fcx, 1fcz, 1fm6, 1h1p, 1hgh_2, 1k1j, 1k3u, 1mq6, 1yvf, 2ack

[a]Cases with the lowest RMSD pose higher than 3 Å are bolded.

https://dx.doi.org/10.1021/acs.jcim.9b01062
J. Chem. Inf. Model. XXXX, XXX, XXX−XXX

Journal of Chemical Information and Modeling pubs.acs.org/jcim Article

subpockets. As the difference in free energy between the various possible solutions is generally small, inaccuracies in the scoring functions can be amplified.[47] Typically, a predicted binding mode is considered correct if its RMSD with the experimental structure is below 2.0 Å but, owing to their small size, an RMSD cutoff of 1.5 Å may be more appropriate for fragments.[47] Thus, we report both metrics (Figure 2). For docking with rDock, the success rate is 38.5% at 1.5 Å and 42.3% at 2.0 Å, which is in line with the values reported for other docking programs.[39] Two W_{QB} combinations clearly outperform docking, with success rates of 46.2% (1.5 Å) and 69.2% (2.0 Å) for DUck_ave and 50% (1.5 Å) and 69.2% (2.0 Å) for DUck_sum. This demonstrates the usefulness of structural stability to solve the docking problem and highlights the surprising fact that W_{QB}, a parameter-free value extracted from molecular simulations in near-equilibrium conditions, outperforms the parametric scoring functions tailored to this specific application. The DUck_min combination, on the other hand, performs worse than docking, with success rates of 30.8% (1.5 Å) and 46.2% (2.0 Å). This allows us to discard the "weakest link" hypothesis, which will not be considered any further.

DUck Is As Good As Docking for Drug-Like Ligands. Next, we evaluated the method on a diverse set of drug-like ligands. In this case, the ligands have up to 37 heavy atoms and are generally formed by several rigid units connected with rotatable bonds (five per molecule, on average).[43] In this data set, the DUck scores yield success rates with 2 Å cutoff of 55.8% for DUck_max, 66.2% for DUck_ave, and 66.2% for DUck_sum (Figure 3). This performance is similar to the fragments and much better than random selection (23.6%), but as docking bigger ligands represents an easier problem, now the structural stability score underperforms compared to standard docking scoring functions. The docking program rDock, used here as a reference, yields a success rate of 75.3% at the RMSD threshold of 2 Å (Figure 3), comparable to other docking programs such as Vina (63%) or Vinardo (72%) for the whole Iridium data set.[53] The docking program also outperforms DUck for other RMSD thresholds.

An explanation for the relative loss of performance of structural stability for larger ligands is that individual W_{QB} values should be combined differently. In previous work, we analyzed the stability of experimental binding modes, finding that structural stability is generally provided by a subset of atoms that act as structural anchors rather than by the whole ligand. Other parts of the ligand lack structural stability, which would be favorable from an entropic perspective, or they may act as secondary anchors.[37] Hence, we sought a combination of W_{QB} values that could identify the predicted pose with the best-anchored substructure. To realize this idea, the hydrogen bonds were grouped based on the distance from each other, classifying them in the same group if the distance between atoms in the ligand that made the bonds of interest was below a set cutoff. To obtain a stability score per group, we considered the same simple combinations as before: maximal of all values (Gr_max), average (Gr_ave) and sum (Gr_sum). In the previous work, we saw that the stability of anchors is often provided by a tight network of hydrogen bonds that may act cooperatively.[37] To transfer that knowledge and favor groups with more HBs, we added two additional combinations, namely maximal value multiplied by the number of bonds in the group (Gr_max x HB) and minimal value multiplied by the number of bonds in the group (Gr_min x HB). The last metric has the same reasoning as DUck_min for fragments but also accounts for the multiple bond effect. Then, the combined stability score for a complex was set as the sum of values for individual groups. The maximal value of all groups DUck_group_max (i.e., assuming that only the best-anchored group matters) was tested as an alternative, however, it performs significantly worse than the sum of all groups (Figure S3). This is in agreement with the observation that approximately one in four complexes present more than one anchoring site.[37]

First, we analyze the success rate as a function of the distance cutoff, which is the only adjustable parameter (Figure 4). Three scoring metrics (Gr_ave, Gr_max, and Gr_min x HB) perform significantly better than the whole-molecule scores. Worthy of note, in all of the cases, the optimal cutoff is in the 3−4 Å range, which corresponds to a local (group-based) analysis of structural stability. Shorter cutoff values provide an atom-based analysis, while longer values converge toward the whole-molecule score. This observation confirms that structural stability is essential at the local level, i.e., ligands require an anchoring point but can have untethered regions. Quite surprisingly for a method that only evaluates hydrogen bonds and has a single fitted parameter (the cutoff distance), DUck with optimal group scoring (DUck_group) has a success rate (76.6%) that is as good as docking, which has multiple adjustable parameters optimized for this task (Figure 3). Noteworthily, the best-performing option (Gr_ave) represents a straightforward scoring scheme where all W_{QB} values are weighted equally. With similar performance, Gr_max and Gr_MinxHB give all of the weight to a single HB per group (the one with maximum and minimal W_{QB} values). This indicates that more sophisticated combinations of W_{QB} values have the potential to yield even better results.

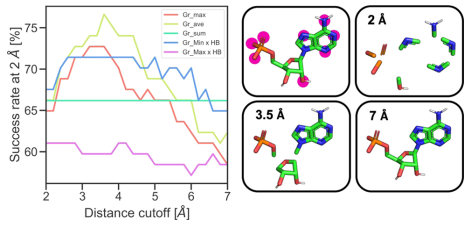

Figure 4. On the left, the success rate at 2 Å as a function of distance cutoff used for different grouping approaches. On the right, fragmentation of the ligand (PDBid: 1UKZ) for distance cutoff of 2, 3.5, and 7 Å. Atoms making hydrogen bonds are highlighted in magenta.

DUck and Docking Are Naturally Complementary. In the next step, we identified the cases in which scoring approaches had failed to select the correct pose. Both rDock and DUck_group had a similar number of failed predictions, with 14 for DUck and 15 for rDock (Table 1). By selecting poses with DUck, we improved the prediction for 13 of rDock's failed predictions (Figure S4). Only two failures are common for both methods, which highlights that DUck is complementary rather than competitive to rDock. We reviewed manually all of the cases where DUck was not successful. Four of the systems were previously identified as complexes without stable hydrogen bonds in their true binding

https://dx.doi.org/10.1021/acs.jcim.9b01062
J. Chem. Inf. Model. XXXX, XXX, XXX−XXX

mode: 1c1b, a reverse transcriptase allosteric ligand; 1hgh_2, an hemagglutinin ligand binding to a secondary binding pocket; and 1yvf and 2ack, two complexes where HBs do not provide structural stability but other interaction types might (water-mediated HBs and cation−π interactions, respectively).[37] It is not surprising that the protocol, which is based on structural stability, fails in binding mode prediction of exceptionally labile complexes. Pleasingly, we noticed that for half of DUck's failed cases (1dds, 1ezq, 1f0t, 1fcx, 1fcz, 1fm6, 1k1j) the prediction was correct for a part of the molecule (Figures 5 and S4). The matching part corresponds to the structural anchor (i.e., the part of ligand that provides structural stability), identified in the previous work[37] and represents the more ordered region of the ligand, based on experimental temperature factors (Figure S6). A high overall RMSD of a pose is caused by the remaining, more labile, part of the ligand, which adopts an incorrect orientation. It is quite striking that the method can predict the binding mode of structural anchor in 66 cases, increasing the success rate to 87.6% in comparison to 81.8% for rDock. This shows the predictive power of DUck and indicates that it can be very useful as a rescoring method, complementary to docking.

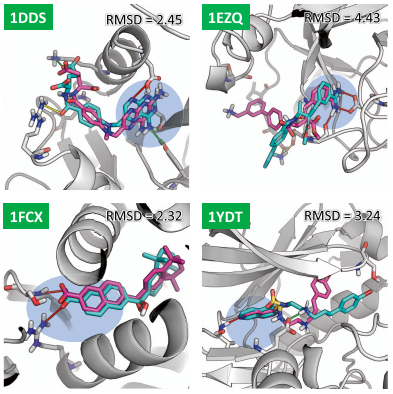

Figure 5. Examples of complexes for which prediction with DUck was apparently unsuccessful (RMSD > 2.0 Å) but the substructure that acts as the anchor was correctly predicted. The protein is depicted in gray, the predicted pose selected by DUck in cyan, and the reference pose in magenta. The structural anchor is marked with a blue circle. DUck predicts the binding mode of the structural anchor in 88% of cases vs 82% for docking.

CONCLUSIONS

We investigated whether hydrogen bond-based structural stability can be used to distinguish the true binding mode of a ligand from a set of binding poses generated by a docking program. Initially, we focused on a set of protein−fragment complexes, where a selection based on stability turned out to be much more effective than a docking score. Next, DUck was applied to a set of bigger drug-like ligands. Owing to their internal degrees of freedom, in this case, a global structural stability score must partition the ligands into separate units, with distinct rigidity behavior: some parts (anchors) attach firmly to the protein, while other regions may be freer to move.[37] With this strategy, DUck score performs as well as standard (thermodynamics-based) docking methods, with the added benefit that, even for failed cases, it can predict if the ligand has a structural anchor and how this part of the molecule binds. Noteworthily, the method has a single adjustable parameter (the distance used to cluster atoms into anchors) and has not been optimized for this task, while docking software has reached a much higher level of maturity. Future developments looking at more complex scoring schemes may bring about further improvements.

The method is just in its infancy and not without limitations. It fails for complexes that do not form any robust interaction. The proportion of such cases is relatively low (ca. 10%). The exact number is still unknown, as there may be complexes that utilize mechanisms other than hydrogen bonds to achieve structural stability.[37] For this reason, one of the priorities will be to extend the method to other interaction types, such as water-mediated hydrogen bonds, cation−π interactions, or halogen bonds. The same problem occurs at the substructure level: our approach can predict very well the binding mode of the anchor but is clueless about other parts of the ligand. Better integration with existing docking software should ensure that DUck is applied judiciously, taking the best from each method. As an MD-based method, its computational cost is substantial and it cannot compete with much faster and simpler docking scoring functions but (i) our current protocol can be optimized to reduce the computational cost by several-fold (e.g., longer integration steps with atom-mass repartitioning, shorter simulations, next-generation hardware) and (ii) empirical scoring functions (e.g., based on machine learning) could be developed to predict W_{QB}.

Fundamentally, our study opens an alternative view of protein−ligand complexes. The binding mode of a ligand corresponds to its global minimum in the free energy landscape. In good logic, all existing methods are designed to benchmark the binding poses against the unbound state. Instead, we measure the depth of the free energy well in a narrow window around the binding pose. Surprisingly, this local property can identify the correct binding mode even better than standard methods. This implies that, in most cases, the correct binding mode corresponds to the minimum with the steepest slope (Figure 1). At present, it is unclear if this is a unique property of protein−ligand complexes or whether it will also be found in other types of supramolecular systems, such as host−guest complexes.

ASSOCIATED CONTENT

Supporting Information

The Supporting Information is available free of charge at https://pubs.acs.org/doi/10.1021/acs.jcim.9b01062.

Set of SDF files with reference ligands and predicted poses, and MOL2 files with protein structures. Iridium (ZIP).

SERAPhiC (ZIP)

Classification of complexes from Iridium and SERAPhiC datasets; binding cavities with generated grid of the complexes that possess two binding pockets (1hgh, 1ofz, 2hdg) or with two enantiomers in the same binding pocket; example of chunk created for PDBid: 1eqz and based on the hydrogen bond formed by ligand and residue D188; plot representing success rate at 2 Å as a function of distance cutoff used for the group definition

https://dx.doi.org/10.1021/acs.jcim.9b01062
J. Chem. Inf. Model. XXXX, XXX, XXX−XXX

for iridium data set; predicted binding modes (BM) of ligands listed in Table 1; time performance of the simulation with a graph representing each step; crystal structures of complexes depicted in Figure 5; error estimation of success rates extracted from Figures 2 and 3 (PDF)

AUTHOR INFORMATION

Corresponding Author

Xavier Barril − *Institut de Biomedicina de la Universitat de Barcelona (IBUB) and Facultat de Farmacia, Universitat de Barcelona, Barcelona, Spain; Catalan Institution for Research and Advanced Studies (ICREA), Barcelona 08010, Spain;* orcid.org/0000-0002-0281-1347; Email: xbarril@ub.edu

Author

Maciej Majewski − *Institut de Biomedicina de la Universitat de Barcelona (IBUB) and Facultat de Farmacia, Universitat de Barcelona, Barcelona, Spain;* orcid.org/0000-0003-2605-8166

Complete contact information is available at: https://pubs.acs.org/10.1021/acs.jcim.9b01062

Notes

The authors declare no competing financial interest.

ACKNOWLEDGMENTS

The research was funded under the EU Horizon 2020 program, Marie Skłodowska-Curie grant agreement No. 675899 (FRAGNET), Spanish Ministerio de Economia (SAF2015-68749-R), Catalan government (2014 SGR 1189), and Barcelona Supercomputing Center (computational resources).

REFERENCES

(1) Jorgensen, W. L. The Many Roles of Computation in Drug Discovery. *Science* **2004**, *303*, 1813−1818.

(2) Bajorath, J. Integration of Virtual and High-Throughput Screening. *Nat. Rev. Drug Discovery* **2002**, *1*, 882−894.

(3) Kitchen, D. B.; Decornez, H.; Furr, J. R.; Bajorath, J. Docking and Scoring in Virtual Screening for Drug Discovery: Methods and Applications. *Nat. Rev. Drug Discovery* **2004**, *3*, 935−949.

(4) Kuntz, I. D.; Blaney, J. M.; Oatley, S. J.; Langridge, R.; Ferrin, T. E. A Geometric Approach to Macromolecule-Ligand Interactions. *J. Mol. Biol.* **1982**, *161*, 269−288.

(5) Friesner, R. A.; Murphy, R. B.; Repasky, M. P.; Frye, L. L.; Greenwood, J. R.; Halgren, T. A.; Sanschagrin, P. C.; Mainz, D. T. Extra Precision Glide: Docking and Scoring Incorporating a Model of Hydrophobic Enclosure for Protein−Ligand Complexes. *J. Med. Chem.* **2006**, *49*, 6177−6196.

(6) Friesner, R. A.; Banks, J. L.; Murphy, R. B.; Halgren, T. A.; Klicic, J. J.; Mainz, D. T.; Repasky, M. P.; Knoll, E. H.; Shelley, M.; Perry, J. K.; Shaw, D. E.; Francis, P.; Shenkin, P. S. Glide: A New Approach for Rapid, Accurate Docking and Scoring. 1. Method and Assessment of Docking Accuracy. *J. Med. Chem.* **2004**, *47*, 1739−1749.

(7) Abagyan, R.; Totrov, M.; Kuznetsov, D. ICM—a New Method for Protein Modeling and Design: Applications to Docking and Structure Prediction from the Distorted Native Conformation. *J. Comput. Chem.* **1994**, *15*, 488−506.

(8) Ruiz-Carmona, S.; Alvarez-Garcia, D.; Foloppe, N.; Garmendia-Doval, A. B.; Juhos, S.; Schmidtke, P.; Barril, X.; Hubbard, R. E.; Morley, S. D. RDock: A Fast, Versatile and Open Source Program for Docking Ligands to Proteins and Nucleic Acids. *PLoS Comput. Biol.* **2014**, *10*, 1−7.

(9) Jones, G.; Willett, P.; Glen, R. C. Molecular Recognition of Receptor Sites Using a Genetic Algorithm with a Description of Desolvation. *J. Mol. Biol.* **1995**, *245*, 43−53.

(10) Jones, G.; Willett, P.; Glen, R. C.; Leach, A. R.; Taylor, R. Development and Validation of a Genetic Algorithm for Flexible Docking Gareth. *J. Mol. Biol.* **1997**, *267*, 727−748.

(11) Rarey, M.; Kramer, B.; Lengauer, T.; Klebe, G. A Fast Flexible Docking Method Using an Incremental Construction Algorithm. *J. Mol. Biol.* **1996**, *261*, 470−489.

(12) Goodsell, D. S.; Olson, A. J. Automated Docking of Substrates to Proteins by Simulated Annealing. *Proteins: Struct., Funct., Bioinf.* **1990**, *8*, 195−202.

(13) Bolcato, G.; Cuzzolin, A.; Bissaro, M.; Moro, S.; Sturlese, M. Can We Still Trust Docking Results? An Extension of the Applicability of DockBench on PDBbind Database. *Int. J. Mol. Sci.* **2019**, *20*, No. 3558.

(14) Chen, Y.-C. Beware of Docking! *Trends Pharmacol. Sci.* **2015**, *36*, 78−95.

(15) Warren, G. L.; Andrews, C. W.; Capelli, A. M.; Clarke, B.; LaLonde, J.; Lambert, M. H.; Lindvall, M.; Nevins, N.; Semus, S. F.; Senger, S.; Tedesco, G.; Wall, I. D.; Woolven, J. M.; Peishoff, C. E.; Head, M. S. A Critical Assessment of Docking Programs and Scoring Functions. *J. Med. Chem.* **2006**, *49*, 5912−5931.

(16) Korb, O.; Ten Brink, T.; Raj, F. R. D. V. P.; Keil, M.; Exner, T. E. Are Predefined Decoy Sets of Ligand Poses Able to Quantify Scoring Function Accuracy? *J. Comput.-Aided Mol. Des.* **2012**, *26*, 185−197.

(17) Sousa, S. F.; Fernandes, P. A.; Ramos, M. J. Protein−Ligand Docking: Current Status and Future Challenges. *Proteins: Struct., Funct., Bioinf.* **2006**, *65*, 15−26.

(18) Mysinger, M. M.; Shoichet, B. K. Supporting Information Rapid Context-Dependent Ligand Desolvation in Molecular Docking. *J. Chem. Inf. Model.* **2010**, *50*, 1561−1573.

(19) Hsieh, J.-H.; Yin, S.; Wang, X. S.; Liu, S.; Dokholyan, N. V.; Tropsha, A. Cheminformatics Meets Molecular Mechanics: A Combined Application of Knowledge-Based Pose Scoring and Physical Force Field-Based Hit Scoring Functions Improves the Accuracy of Structure-Based Virtual Screening. *J. Chem. Inf. Model.* **2012**, *52*, 16−28.

(20) Verdonk, M. L.; Cole, J. C.; Hartshorn, M. J.; Murray, C. W.; Taylor, R. D. Improved Protein−Ligand Docking Using GOLD. *Proteins: Struct., Funct., Bioinf.* **2003**, *52*, 609−623.

(21) Amaral, M.; Kokh, D. B.; Bomke, J.; Wegener, A.; Buchstaller, H. P.; Eggenweiler, H. M.; Matias, P.; Sirrenberg, C.; Wade, R. C.; Frech, M. Protein Conformational Flexibility Modulates Kinetics and Thermodynamics of Drug Binding. *Nat. Commun.* **2017**, *8*, No. 2276.

(22) Wang, Y.; Martins, J. M.; Lindorff-Larse, K. Biomolecular Conformational Changes and Ligand Binding: From Kinetics to Thermodynamics. *Chem. Sci.* **2017**, *8*, 6466−6473.

(23) Rastelli, G.; Degliesposti, G.; Del Rio, A.; Sgobba, M. Binding Estimation after Refinement, a New Automated Procedure for the Refinement and Rescoring of Docked Ligands in Virtual Screening. *Chem. Biol. Drug Des.* **2009**, *73*, 283−286.

(24) Graves, A. P.; Shivakumar, D. M.; Boyce, S. E.; Jacobson, M. P.; Case, D. A.; Shoichet, B. K. Rescoring Docking Hit Lists for Model Cavity Sites: Predictions and Experimental Testing. *J. Mol. Biol.* **2008**, *377*, 914−934.

(25) Guimarães, C. R. W.; Cardozo, M. ChemInform Abstract: MM-GB/SA Rescoring of Docking Poses in Structure-Based Lead Optimization. *J. Chem. Inf. Model.* **2008**, *48*, 958−970.

(26) Lyne, P. D.; Lamb, M. L.; Saeh, J. C. Accurate Prediction of the Relative Potencies of Members of a Series of Kinase Inhibitors Using Molecular Docking and MM-GBSA Scoring. *J. Med. Chem.* **2006**, *49*, 4805−4808.

(27) Thompson, D. C.; Humblet, C.; Joseph-McCarthy, D. Investigation of MM-PBSA Rescoring of Docking Poses. *J. Chem. Inf. Model.* **2008**, *48*, 1081−1091.

(28) Chaves, E. J. F.; Padilha, I. Q. M.; Arau′jo, D. A. M.; Rocha, G. B. Determining the Relative Binding A Ffi Nity of Ricin Toxin A

https://dx.doi.org/10.1021/acs.jcim.9b01062
J. Chem. Inf. Model. XXXX, XXX, XXX−XXX

Inhibitors by Using Molecular Docking and Nonequilibrium Work. *J. Chem. Inf. Model.* **2018**, *58*, 1205−1213.
(29) Kuhn, B.; Gerber, P.; Schulz-Gasch, T.; Stahl, M. Validation and Use of the MM-PBSA Approach for Drug Discovery. *J. Med. Chem.* **2005**, *48*, 4040−4048.
(30) Okimoto, N.; Futatsugi, N.; Fuji, H.; Suenaga, A.; Morimoto, G.; Yanai, R.; Ohno, Y.; Narumi, T.; Taiji, M. High-Performance Drug Discovery: Computational Screening by Combining Docking and Molecular Dynamics Simulations. *PLoS Comput. Biol.* **2009**, *5*, No. e1000528.
(31) Hou, T.; Wang, J.; Li, Y.; Wang, W. Assessing the Performance of the MM/PBSA An1. Hou, T., J. Wang, Y. Li, and W. Wang. 2011. Assessing the Performance of the MM/PBSA and MM/GBSA Methods. 1. The Accuracy of Binding Free Energy Calculations Based on Molecular Dynamics Simulations. J. Chem. I. *J. Chem. Inf. Model.* **2011**, *51*, 69−82.
(32) Gioia, D.; Bertazzo, M.; Recanatini, M.; Masetti, M.; Cavalli, A. Dynamic Docking: A Paradigm Shift in Computational Drug Discovery. *Molecules* **2017**, *22*, 2029.
(33) Decherchi, S.; Berteotti, A.; Bottegoni, G.; Rocchia, W.; Cavalli, A. The Ligand Binding Mechanism to Purine Nucleoside Phosphorylase Elucidated via Molecular Dynamics and Machine Learning. *Nat. Commun.* **2015**, *6*, No. 6155.
(34) Clark, A. J.; Tiwary, P.; Borrelli, K.; Feng, S.; Miller, E. B.; Abel, R.; Friesner, R. A.; Berne, B. J. Prediction of Protein-Ligand Binding Poses via a Combination of Induced Fit Docking and Metadynamics Simulations. *J. Chem. Theory Comput.* **2016**, *12*, 2990−2998.
(35) Ruiz-carmona, S.; Schmidtke, P.; Luque, F. J.; Baker, L.; Matassova, N.; Davis, B.; Roughley, S.; Murray, J.; Hubbard, R.; Barril, X. Dynamic Undocking and the Quasi-Bound State as Tools for Drug Discovery. *Nat. Chem.* **2017**, *9*, 201−206.
(36) Majewski, M.; Ruiz-Carmona, S.; Barril, X. Dynamic Undocking: A Novel Method for Structure-Based Drug Discovery. In *Rational Drug Design. Methods in Molecular Biology*; Mavromoustakos, T.; Kellici, T. F., Eds.; Humana Press: New York, NY, 2018; pp 195−215.
(37) Majewski, M.; Ruiz-carmona, S.; Barril, X. An Investigation of Structural Stability in Protein-Ligand Complexes Reveals the Balance between Order and Disorder. *Commun. Chem.* **2019**, *2*, 1−8.
(38) Soler, D.; Westermaier, Y.; Soliva, R. Extensive Benchmark of RDock as a Peptide - Protein Docking Tool. *J. Comput. Aided. Mol. Des.* **2019**, *33*, 613−626.
(39) Favia, A. D.; Bottegoni, G.; Nobeli, I.; Bisignano, P.; Cavalli, A. SERAPhiC: A Benchmark for in Silico Fragment-Based Drug Design. *J. Chem. Inf. Model.* **2011**, *51*, 2882−2896.
(40) Vogt, J.; Perozzo, R.; Pautsch, A.; Prota, A.; Schelling, P.; Pilger, B.; Folkers, G.; Scapozza, L.; Schulz, G. E. Nucleoside Binding Site of Herpes Simplex Type 1 Thymidine Kinase Analyzed by X-Ray Crystallography. *Proteins: Struct., Funct., Genet.* **2000**, *41*, 545−553.
(41) Wimmerova, M.; Mitchell, E.; Sanchez, J.-F.; Gautier, C.; Imberty, A. Crystal Structure of Fungal Lectin Six-Bladed β-Propeller Fold and Novel Fucose Recognition Mode for Aleuria Aurantia Lectin. *J. Biol. Chem.* **2003**, *278*, 27059−27067.
(42) Babaoglu, K.; Shoichet, B. K. Deconstructing Fragment-Based Inhibitor Discovery. *Nat. Chem. Biol.* **2006**, *2*, 720−723.
(43) Warren, G. L.; Do, T. D.; Kelley, B. P.; Nicholls, A.; Warren, S. D. Essential Considerations for Using Protein-Ligand Structures in Drug Discovery. *Drug Discovery Today* **2012**, *17*, 1270−1281.
(44) Sauter, N. K.; Hanson, H. J. E.; Glick, G. D.; Brown, J. H.; Crowther, R. L.; Park, S.; Skehel, J. J.; Wiley, D. C. Binding of Influenza Virus Hemagglutinin to Analogs of Its Cell-Surface Receptor, Sialic Acid: Analysis by Proton Nuclear Magnetic Resonance Spectroscopy And. *Biochemistry* **1992**, *31*, 9609−9621.
(45) Molecular Operating Environment (MOE), Chemical Computing Group ULC: 1010 Sherbooke St. West, Suite #910, Montreal, QC, Canada, H3A 2R7, 2018.
(46) Wang, Z.; Sun, H.; Yao, X.; Li, D.; Xu, L.; Li, Y.; Tian, S.; Hou, T. Comprehensive Evaluation of Ten Docking Programs on a Diverse Set of Protein-Ligand Complexes: The Prediction Accuracy of Sampling Power and Scoring Power. *Phys. Chem. Chem. Phys.* **2016**, *18*, 12964−12975.
(47) Verdonk, M. L.; Giangreco, I.; Hall, R. J.; Korb, O.; Mortenson, P. N.; Murray, C. W. Docking Performance of Fragments and Druglike Compounds. *J. Med. Chem.* **2011**, *54*, 5422−5431.
(48) Pettersen, E. F.; Goddard, T. D.; Huang, C. C.; Couch, G. S.; Greenblatt, D. M.; Meng, E. C.; Ferrin, T. E. UCSF Chimera - A Visualization System for Exploratory Research and Analysis. *J. Comput. Chem.* **2004**, *25*, 1605−1612.
(49) Dynamic Undocking github page. https://github.com/CBDD/duck.
(50) Jakalian, A.; Jack, D. B.; Bayly, C. I. Fast, Efficient Generation of High-Quality Atomic Charges. AM1-BCC Model: II. Parameterization and Validation. *J. Comput. Chem.* **2002**, *23*, 1623−1641.
(51) Bayly, C. I.; McKay, D.; Truchon, J. F. *An Informal AMBER Small Molecule Force Field: Parm@Frosst*; Computational Chemistry Ltd., 2011.
(52) Case, D. A.; Babin, V.; Berryman, J.; Betz, R.; Cai, Q.; Cerutti, D.; Cheatham Iii, T.; Darden, T.; Duke, R.; Gohlke, H.; Goetz, A. W.; Gusarov, S.; Homeyer, N.; Janowski, P.; Kaus, J.; Kolossváry, I.; Kovalenko, A.; Lee, T. S.; LeGrand, S.; Luchko, T.; Luo, R.; Madej, B.; Merz, K. M.; Paesani, F.; Roe, D. R.; Roitberg, A.; Sagui, C.; Salomon-Ferrer, R.; Seabra, G.; Simmerling, C. L.; Smith, W.; Swails, J.; Walker, R. C.; Wang, J.; Wolf, R. M.; Wu, X.; Kollman, P. A. *Amber 14*; University of California, 2014.
(53) Quiroga, R.; Villarreal, M. A. Vinardo: A Scoring Function Based on Autodock Vina Improves Scoring, Docking, and Virtual Screening. *PLoS One* **2016**, *11*, No. e0155183.

https://dx.doi.org/10.1021/acs.jcim.9b01062
J. Chem. Inf. Model. XXXX, XXX, XXX−XXX

Structural stability predicts the binding mode of protein-ligand complexes

Maciej Majewski,† and Xavier Barril*,†‡

† Institut de Biomedicina de la Universitat de Barcelona (IBUB) and Facultat de Farmacia, Universitat de Barcelona, Av. Joan XXIII 27-31, 08028 Barcelona, Spain

‡ Catalan Institution for Research and Advanced Studies (ICREA), Passeig Lluis Companys 23, 08010 Barcelona, Spain

*E-mail: xbarril@ub.edu

Supplementary Information – Structural stability predicts the binding mode of protein-ligand complexes

Table S1. Classification of complexes from Iridium and SERAPhiC datasets.

Category	PDBid	
	Iridium DS	SERAPhiC DS
Simulated structures	1a28, 1b9v, 1br6, 1c1b, 1cvu, 1dds, 1exa, 1ezq, 1f0s, 1f0t, 1f0u, 1fcx, 1fcz, 1fh8, 1fh9, 1fhd, 1fm6, 1fvt, 1g9v, 1h1p, 1h1s, 1hgh-1, 1hgh-2, 1hgi, 1hgj, 1hwi, 1ivb, 1ivd, 1ive, 1ivf, 1jla, 1k1j, 1k3u, 1ke5, 1l2s, 1l7f, 1lpz, 1lqd, 1m2z, 1ml1, 1mq6, 1mts, 1n2j, 1n2v, 1n46, 1of1, 1owe, 1oyt, 1pmn, 1q1g, 1q41, 1qhi, 1rob, 1s19, 1tow, 1tt1, 1u4d, 1ukz, 1ulb, 1unl, 1uou, 1v0p, 1w1p, 1w2g, 1x8x, 1ydr, 1yds, 1ydt, 1yv3, 1yvf, 1ywr, 2ack, 2br1, 2mcp, 2pcp, 3ptb, 4ts1	1e2i_a, 1e2i_b, 1f5f, 1f8e, 1h46, 1k0e, 1mlw, 1ofz_a, 1ofz_b, 1r5y, 1sd1, 1tku, 1w1a, 1ynh, 2bkx, 2brt, 2f6x, 2fgq, 2hdq_a, 2hdq_b, 2i5x, 2iba, 2j5s, 2p1o, 2q6m, 2uy5, 3eko
Simulation failure	1ai5, 1gm8	1xfg
No hydrogen bond	1ctr, 1fl3, 1p2y	1sqn, 1ui0, 1uwc, 2cix, 2qwx, 3c0z, 3dsx
Not drug like	1fjs, 1fm9, 1fq5, 1gwx, 1hgg, 1pso	-
Metal ion	1azm, 1cx2, 1dd7, 1eoc, 1frp, 1hdy, 1hq2, 1hww, 1iy7, 1jd0, 1lrh, 1mbi, 1mmv, 1mzc, 1n1m, 1oq5, 1p62, 1r58, 1r9o, 1uml, 1xm6, 1xoq, 1yqy, 2ctc, 2tmn, 4aah, 4cox, 1hp0	1m2x, 1m3u, 1s5n, 1t0l, 1wog, 1x07, 1y2k, 1yv5, 2aie, 2fdv, 2ff2, 2gg7, 2gvv, 2rdr, 2v77, 2zvj
Additional ligand	1d3h, 1hnn, 1hvy, 1pbd, 1sq5	1fsg, 1pwm, 1yki, 2b0m, 2bl9

Supplementary Information – Structural stability predicts the binding mode of protein-ligand complexes

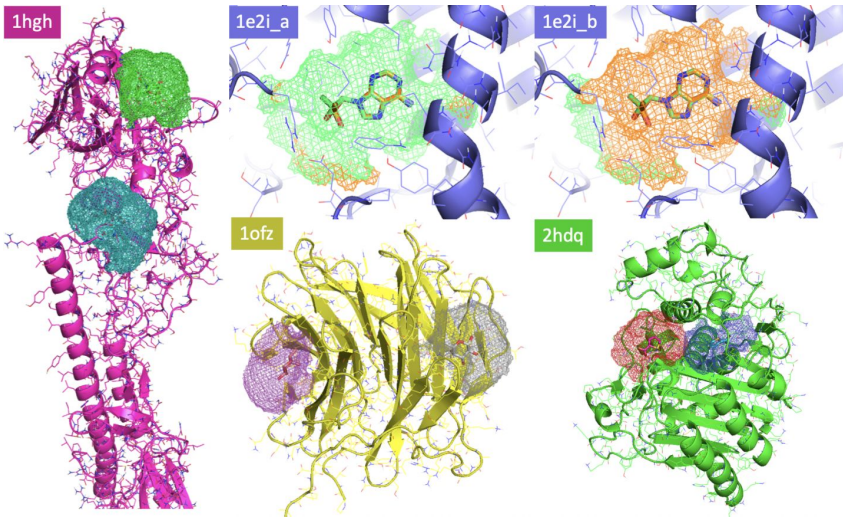

Figure S1. Binding cavities with generated grid of the complexes that possess two binding pockets (1hgh, 1ofz, 2hdg) or with two enantiomers in the same binding pocket (1e2i).

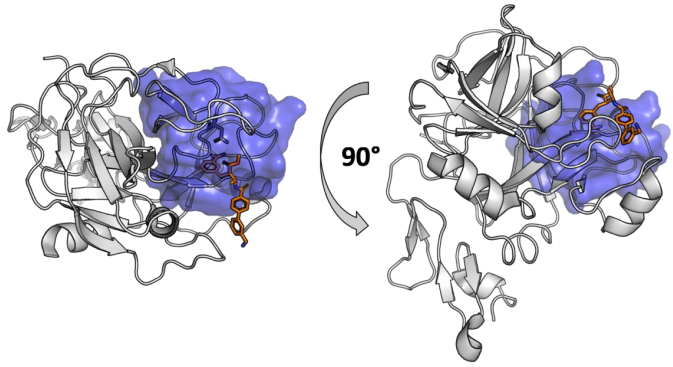

Figure S2. An example of chunk (blue surface) created for PDBid: 1eqz and based on the hydrogen bond (black dashed line) formed by ligand (orange sticks) and residue D188 (grey sticks).

Supplementary Information – Structural stability predicts the binding mode of protein-ligand complexes

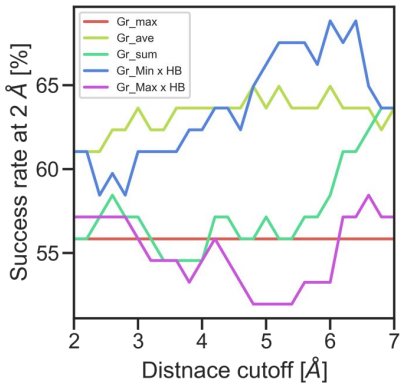

Figure S3. The plot representing success rate at 2 Å in function of distance cutoff used for the group definition for Iridium dataset. The stability score of a group is selected based on definition presented in Methods, and the final score for the molecule is calculated as a maximum of group values.

Supplementary Information – Structural stability predicts the binding mode of protein-ligand complexes

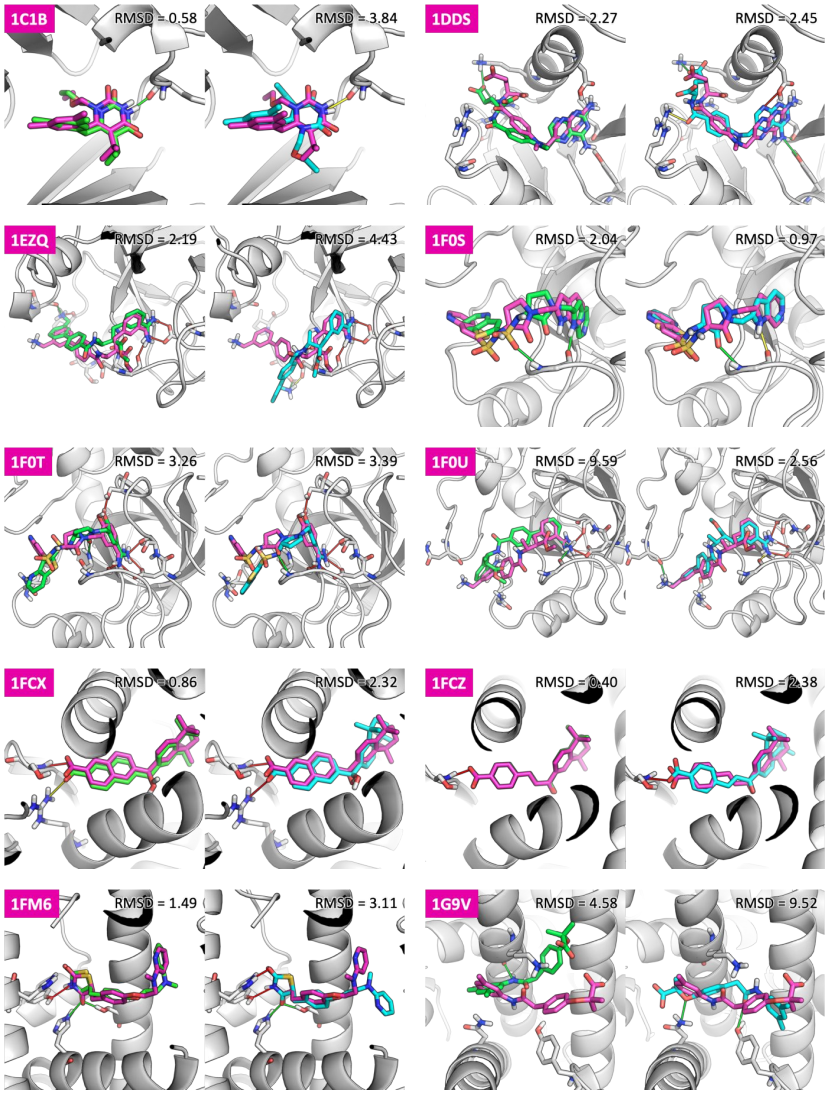

Supplementary Information – Structural stability predicts the binding mode of protein-ligand complexes

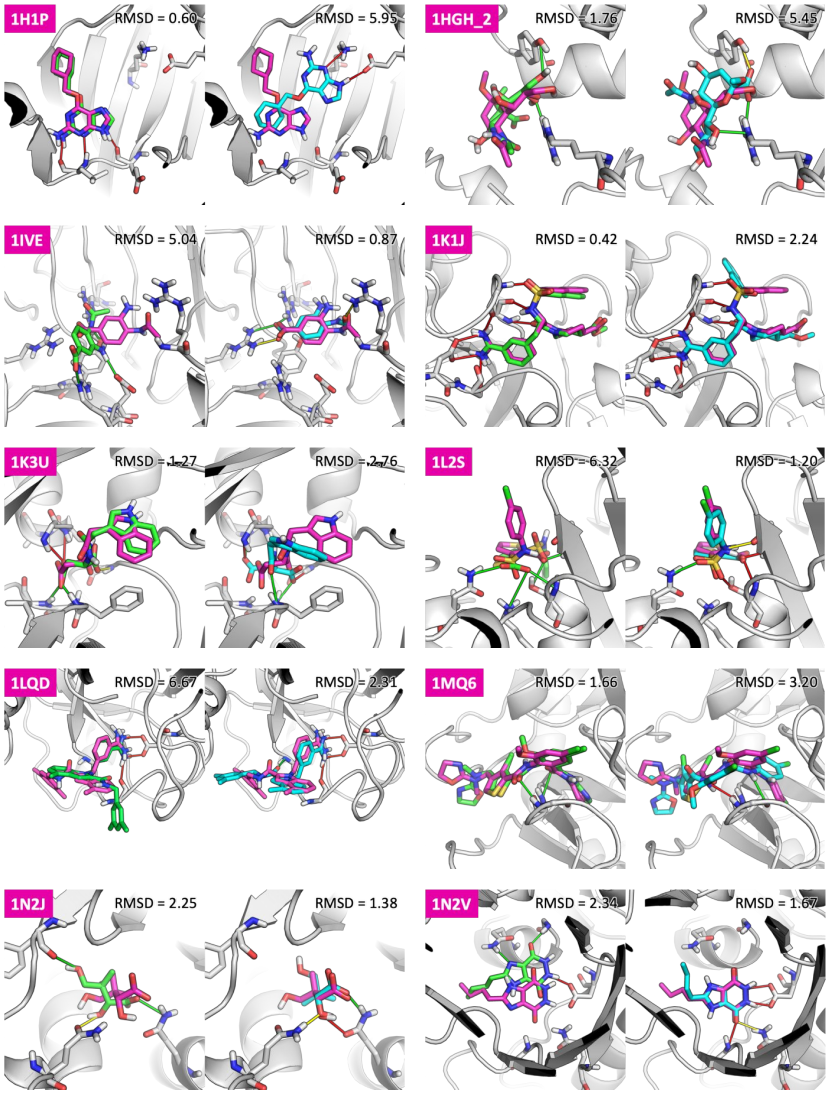

Supplementary Information – Structural stability predicts the binding mode of protein-ligand complexes

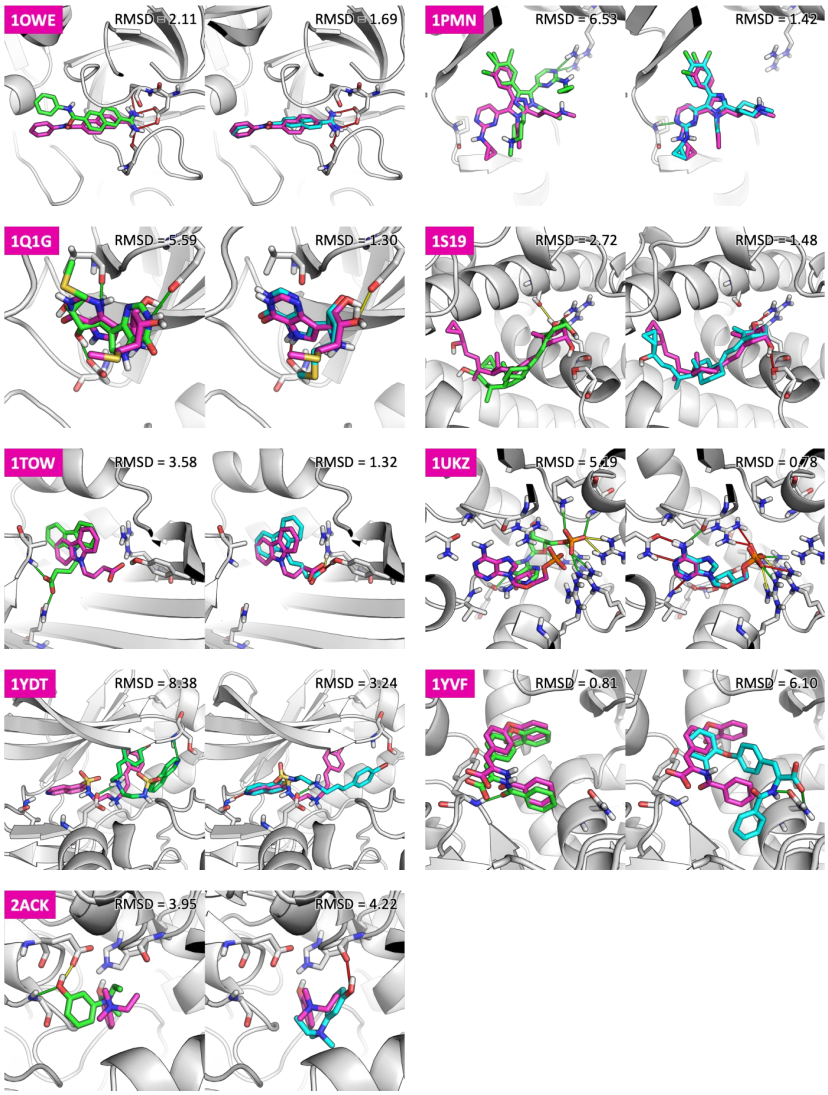

Figure S4. Predicted binding modes (BM) of ligands listed in Table 1. On the left side of each panel BM selected by rDock depicted in green, and on the right side BM selected by DUck depicted in cyan. True binding modes are depicted in magenta.

Supplementary Information – Structural stability predicts the binding mode of protein-ligand complexes

Sim. Time [ns]	1.4	0.5 x 2	0.5	0.5 x 2
Wall clock time [min]	48	19 x 2	15	19 x 2

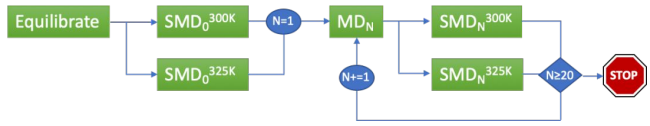

Figure S5. Time performance of the simulation with a graph representing each step. "Wall clock time" was calculated for the average system of 25 000 atoms (chunk, ligand and solvent, all including hydrogens) simulated on NVIDIA Tesla M2090 GPUs. For a single hydrogen bond, the complete simulation of such system takes 18.2 GPU hours. Depending on the size of the system, the simulation time can vary by about 20%. A pose makes on the average 4 hydrogen bonds, and we simulated 5 poses per ligand. The total estimate of the time necessary to simulate 1 ligand is 364 GPU hours (72.8 h per pose). The computational performance can be further optimized by changing simulation length, number of replicas, type of enhanced sampling method, number of particles, integration time-step using atomic mass repartitioning, better parallelization, next generation GPUs, etc.

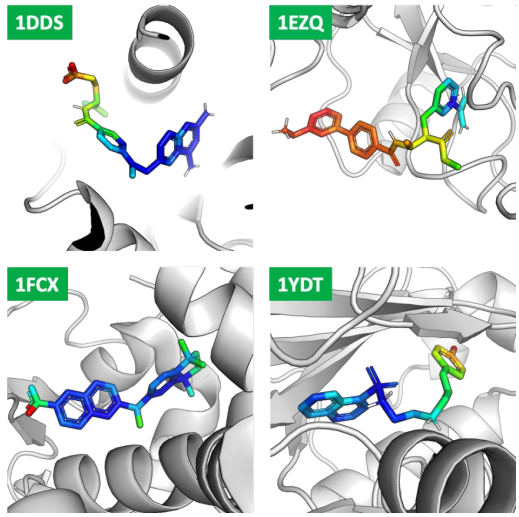

Figure S6. Crystal structures of complexes depicted in Figure 5. The ligands have been coloured based on their relative temperature factors, blue indicating colder (ordered) and red hotter (flexible) regions.

Supplementary Information – Structural stability predicts the binding mode of protein-ligand complexes

Table S2. Error estimation of success rates extracted from Figures 2 and 3. The errors were calculated using bootstrapping. The success rate of each scoring variant was calculated 10 000 times for a random sample with replacement (size of sample 26 for SERAPhiC and 77 for Iridium). Then error was calculated as a standard deviation across all samples.

	SERAPhiC		Iridium
Scoring method	SR (2 Å)	SR (1.5 Å)	SR (2 Å)
rDock	42.3 ± 9.7	38.5 ± 9.5	75.3 ± 4.9
DUck_max	57.7 ± 9.7	50.0 ± 9.8	55.8 ± 5.6
DUck_min	46.2 ± 9.8	30.8 ± 9.1	-
DUck_ave	69.2 ± 9.1	46.2 ± 9.8	66.2 ± 5.4
DUck_sum	69.2 ± 9.1	50.0 ± 9.8	66.2 ± 5.4
DUck_group	-	-	76.6 ± 4.8
random	21.7 ± 7.8	14.0 ± 6.4	23.6 ± 4.7

Chapter 4

Results Summary

4.1 Assessment of Structural Stability

4.1.1 Structural Stability in Biomolecular Complexes

In the first publication, we used Dynamic Undocking to assess the robustness of hydrogen bonds in a set of 79 complexes of proteins with drug-like ligands from Iridium dataset (345 HBs)[119] and a set of 27 protein-fragment complexes from the SERAPhiC dataset (126 HBs).[120] As shown in Figure 4.1, the values of W_{QB} range from 0 to 26 kcal mol^{-1} and more than 50% of bonds are robust ($W_{QB} > 6$ kcal mol^{-1}). Around three-quarters of all complexes possess at least one structurally stable bond.

Surprisingly, fragments behave similarly to drug-like molecules. This behaviour indicates that fragments are more static than standard ligands. It is in agreement with the fact that fragments have in general fewer degrees of freedom, a higher proportion of buried HBs[121] and their binding is driven by enthalpy.[122]

To relate results to experimental observables, we compared W_{QB} values with the normalized B-factor of the ligands atom that makes the hydrogen bond. Atoms forming string HBs tend to have lower normalized B-factors, which means that robust hydrogen bonds are formed in ordered parts of the complex.

Next, we classified all HBs into neutral, mixed (ionic-neutral) and salt bridges and we fund that salt bridges are only very slightly skewed towards more robust interactions than neutral HBs. Ionic interactions have higher desolvation penalty, thus can form a higher energy barrier.

We identified 9 cases (11%) of complexes that did not form any robust HBs. Two cases were low-affinity complexes. For the remaining structures, robustness can be provided by other mechanisms, like water-mediated HBs, or it might be lacking.

The analysis of different types of binding pockets has shown that the type of receptor might dictate binding behaviour. Enzymes and nuclear

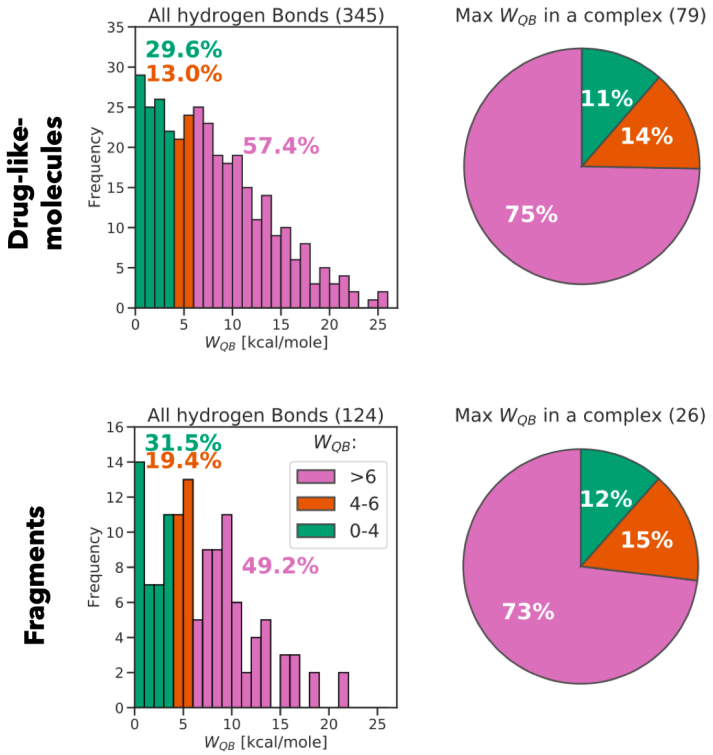

Fig. 4.1 Frequency of robust HBs in protein-ligand complexes (top) and protein-fragment complexes (bottom). On the left - histograms of the frequency of HBs by W_{QB} value. On the right - pie charts showing the share of complexes with at least one robust HB ($W_{QB} > 6$ kcal mol^{-1}, pink), all labile HBs ($W_{QB} < 4$ kcal mol^{-1}, green) or intermediate situations (red).

receptors, where the order is essential for catalysis or stabilization of the optimal conformation, have a higher proportion of robust HBs. On the other hand, ligands occupying secondary pockets are very liable.

4.1.2 Structural Anchors

To see if robust bonds are evenly distributed across the molecules, in each complex we clustered all HBs based on their distance in space into fragment-sized groups of atoms. For most of the complexes (62%), strong HBs are found in a single group, forming a robust structural anchor (Fig.4.2a). Combining a stable anchor with flexible regions minimizes the entropic costs and can be desirable from a binding affinity perspective. 23% of all ligands form two structural anchors in separate regions, and three ligands (4%) form 3 distinct anchors. For two cases of the last group, there might be a functional explanation of such high stability.

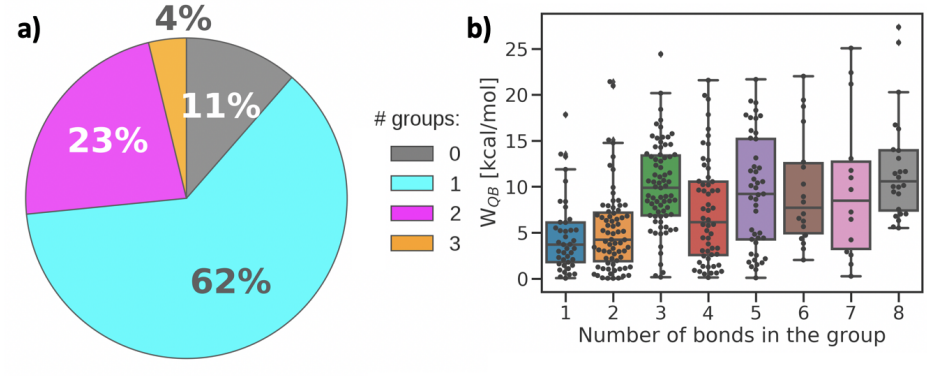

Fig. 4.2 Distribution of complexes based on the number of structural anchors. a) Pie chart presenting the distribution of the number of anchors across the data set. b) Distribution of strength of HBs (W_{QB}) versus the number of HBs per group of atoms. The box shows the quartiles, and the whiskers show the rest of the distribution excluding outliers. The swarmplot showing all data points is placed on the top of the boxplot.

HBs in isolation usually do not form robust interactions. On the other hand, clusters of three or more HBs form robust bonds in the vast majority (Fig.4.2b). The HBs within these clusters present relatively similar W_{QB} values suggesting that they often behave in a concerted-like manner. This synergic behaviour ensures higher barriers during dissociation. It is also well-suited to provide selectivity, as small changes in the composition or geometry of one of the partners may result in significant changes in the stability of the whole network.

4.2 Binding Mode Prediction

4.2.1 Protein-Fragment Complexes

In the second paper, we tested the ability of DUck to predict a binding mode in protein-fragment complexes, collected in SERAPhiC dataset. In the first step, we used rDock to generate poses. Then, we selected the top 5 best-scoring unique poses to simulate with DUck. We evaluated the structural stability of every hydrogen bond from each pose. Finally, the success rate was measured as a percentage of predictions that had RMSD to their corresponding x-ray pose below a threshold value: 2 Åor 1.5 Å.

To assign a single "stability score" to a fragment, we combined W_{QB} values of individual hydrogen bond by taking:

- the maximum of all W_{QB} values (DUck_max),
- the minimum of all W_{QB} values (DUck_min),
- the average of all W_{QB} values (DUck_ave),
- the sum of all W_{QB} values (DUck_sum).

We compared our results to the selection made based on a docking score of rDock and a random choice. Two W_{QB} combinations outperform docking,

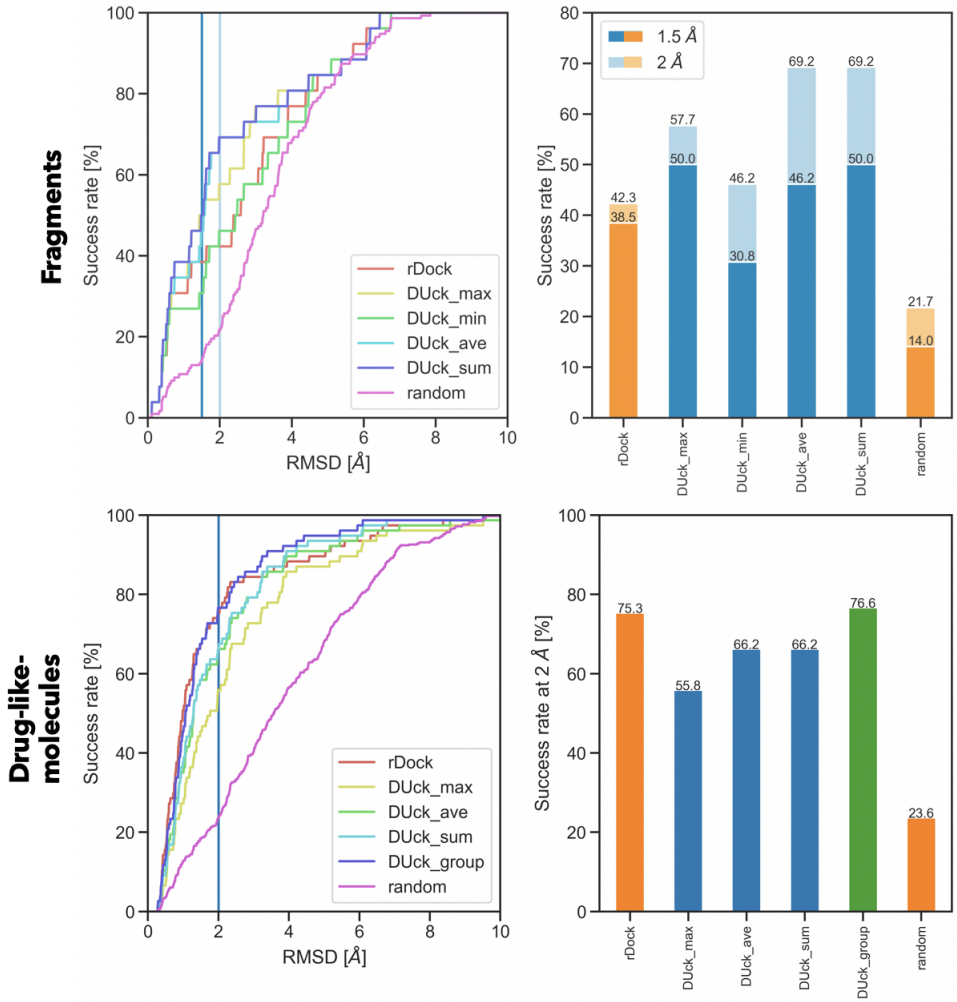

Fig. 4.3 Success rate for binding mode prediction of fragments (top) and drug-like molecules (bottom). On the left, plots representing success rate as a function of the RMSD cut-off between generated binding mode and the reference. On the right, barplots representing success rate at 1.5 Åand/or 2 Å, based on the plot on the left.

with success rates of 46.2% (1.5 Å) and 69.2% (2.0 Å) for DUck_ave and 50% (1.5 Å) and 69.2% (2.0 Å) for DUck_sum (Fig.4.3). The DUck_min combination, on the other hand, performs worse than docking, with success rates of 30.8% (1.5 Å) and 46.2% (2.0 Å).

4.2.2 Protein-Ligand Complexes

We followed up on previous results by predicting binding mode for drug-like molecules, collected in Iridium dataset. The selection based on DUck yields success rates with 2 Åcut-off of 55.8% for DUck_max, 66.2% for DUck_ave and 66.2% for DUck_sum (Fig.4.3). This performance is similar to the fragments and much better than random selection (23.6%), but now the structural stability score underperforms compared to rDock scoring function (75.3%). We did not consider DUck_min in this case due to its poor performance for the fragment data set.

Following the idea of structural anchors from the previous paper, we decided to make a selection that would favour the best-anchored pose. The hydrogen bonds were grouped based on distance, and as a stability score per group, we considered a few simple and more complex combinations:

- the maximum of W_{QB} values in the group (Gr_max),
- the average of W_{QB} values in the group (Gr_ave),
- the sum of W_{QB} values in the group (Gr_sum),
- the maximum of W_{QB} values in the group multiplied by the number of bonds in the group (Gr_max x HB),
- the minimum of W_{QB} values in the group multiplied by the number of bonds in the group (Gr_min x HB).

Then the combined stability score for a complex was set as the sum of values for individual groups.

The success rate as a function of cut-off distance shows that grouping approaches, mainly Gr_ave, Gr_max and Gr_min x HB, outperform whole-molecule scores (Fig.4.4). The optimal cut-off is in the 3 to 4 Årange, allowing to group bonds into fragment-sized structural anchors (Fig.4.4, right panel).

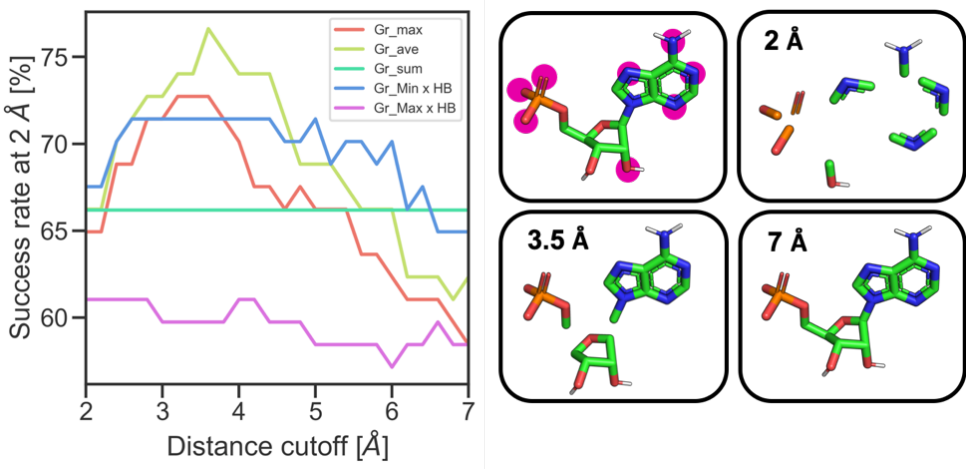

Fig. 4.4 On the left, the success rate at 2 Åas a function of distance cut-off used for different grouping approaches. On the right, fragmentation of the ligand (PDBid: 1UKZ) for distance cut-off of 2, 3.5 and 7 Å. Atoms making hydrogen bonds are highlighted in magenta.

Quite surprisingly for a method that only evaluates hydrogen bonds and has a single fitted parameter (the cut-off distance), DUck with optimal group scoring (DUck_group) has a success rate (76.6%) that is as good as docking, which has multiple adjustable parameters optimized for this task (Fig.4.3).

4.2.3 DUck and Docking Complementarity

In the last stage, we identified the failed cases. Both rDock and DUck had a similar number of failed predictions, with 14 for DUck and 15 for rDock. Only two failures overlapped, which indicates that both methods are complementary, rather than competitive.

We noticed that for half of DUck's failed cases (1dds, 1ezq, 1f0t, 1fcx, 1fcz, 1fm6, 1k1j) the prediction was correct for a part of the molecule. The matching part corresponds to the structural anchor that was identified in the first paper. The remaining part of the ligand causes high RMSD value. In result, DUck predicted the binding mode of structural anchor in 66 cases, increasing the success rate to 87.6%, in comparison to 81.8% for rDock.

Chapter 5

Discussion

The previous chapter presents two papers that summarize the PhD project. Here, we will focus on and expand some of the key concepts presented there.

The Role of Structural Stability in Molecular Design

As described in the introduction and objectives, we wanted to gain a better understanding of structural stability and its role in molecular recognition. We removed the initial knowledge-bias and simulated all hydrogen bond in the structures. This approach revealed interesting insides about the order-disorder balance in ligands and formation of structural anchors, that would otherwise be missed.

It is important to note that the level of structural stability reported here may be overestimated due to the composition of the data set, entirely derived from X-ray crystallography, a technique that relies on order to solve structures. We should also mention that the fraction of well-anchored fragments may be different for fragments hits that fail to crystallize. The overlap between X-ray crystallography and other biophysical screening methods can be rather low.[123]

The extensive assessment of structural stability in protein-ligand complexes has shown that this property is ubiquitous in biomolecular systems. However, not all of the complexes have robust hydrogen bonds. In these cases, the stability can be provided by an accumulative effect of interactions other than hydrogen bonds: water-mediated hydrogen bond, cation-π stacking, or a unique arrangement of hydrophobic interactions (Fig.5.1a,b). Even though some work has been done to adapt DUck to simulate other interactions (e.g. water bridges), at this point, we are not able to reliably evaluate those cases.

On the other hand, the stability of the complex might not always be desirable. Our understanding of its role in molecular recognition remains limited. There are even cases where increased flexibility of the complex might

benefit ligands function. In case of HIV reverse transcriptase, a multiplicity of binding modes might be beneficial to preserve binding affinity when the target is mutated, thus averting resistance.[124, 125] In fact, two complexes of HIV reverse transcriptase that were present in Iridium dataset do not posses any robust hydrogen bond, supporting our suspicion. This observation follows the conclusion about a link between the stability of the complex and its function. As discussed before, tight binding is observed for complexes where there is a functional need, e.g. nuclear receptors and enzymes. To fully confirm this conclusion, further investigation is needed.

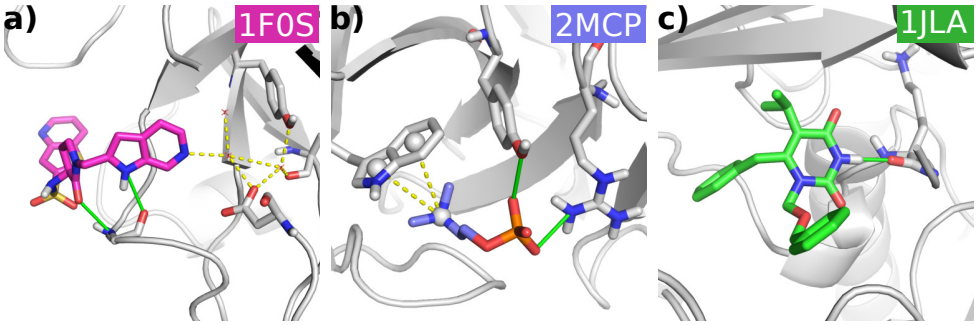

Fig. 5.1 Structures of protein-ligand complexes that form potentially labile structures. Weak hydrogen bonds are marked in green. a) A complex of FXa with inhibitor RPR208707 (PDBid 1F0S; K_i = 18 nM) forms two direct, but labile, HBs with the protein. An additional water-mediated HB with the catalytic residues (yellow dotted lines) might provide structural stability. b) An antibody that recognizes phosphocholine (PDBid 2MCP) forms two charge-reinforced but labile HBs. A cation-π interaction (yellow dotted lines) might provide structural stability. c) Reverse transcriptase inhibitor (PDBid 1JLA; IC50 = 6 nM) forms a single but labile HB with the protein.

An investigation of protein-fragment complexes provides another useful insight for drug design. Their increased stability in comparison to drug-like molecules suggests that despite their low binding affinity, most fragments already have a well-defined binding mode. It serves as a foundation from which it can be evolved into a bigger molecule with higher affinity. We

also believe that a well-anchored fragment is more suitable as a starting point in a drug discovery program. They are more likely to preserve their binding mode, therefore behave more predictable while introducing chemical modifications. Fragments can change their binding mode during evolution into bigger molecules.[126] However, starting a drug discovery campaign with a labile fragment can lead to unpredictable results of chemical modifications.

Now that we have a sense of why structural stability might be desired in the complex, we can think of ways to modify it through molecular design. The wide variety of simulated structures revealed potential strategies to increase structural stability. The first strategy is through a tight network of hydrogen bonds, that act cooperatively (Fig.5.3d). Whenever we break one of the bonds, we need to break the whole network, which means that high W_{QB} values for individual hydrogen bonds are a cumulative effect of the whole network. Another way to increase stability is through shielding from the solvent, thus increasing the desolvation cost and the energy of a transition state. It is best exemplified by the complex of blebbistatin with myosin II (PDBid 1YV3). A single hydroxyl group forms two highly stable bonds (17.2, 24.4 kcal mol^{-1}) (Fig.5.3c). An umbrella-like shape of the ligand efficiently protects the bonds from the solvent.

Summing up, the structural stability of the complex can be modified through molecular design. The desired effect will vary depending on the type of receptor and function of the ligand.

The Origin of Structural Stability

In the first article, we tried to explain the origin of the free energy barrier that causes structural stability. We speculate that it might be linked to binding kinetics, as larger k_{off} values indicate higher transition state (if ΔG_{bind} remains the same; Fig.5.3a). Another factor is thermodynamical stability (if

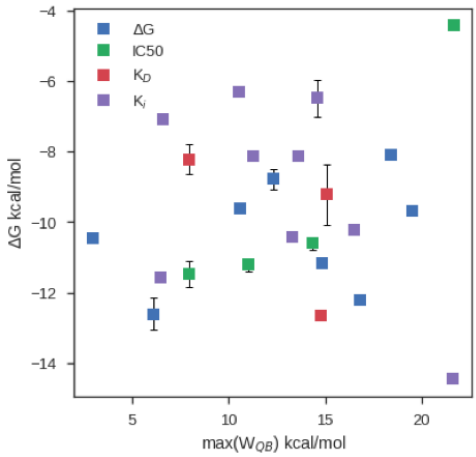

Fig. 5.2 Binding free energy versus maximal W_{QB} value. The plot is based on a set of Iridium complexes with publicly available activity data. Binding energy was calculated based on ΔG (blue), IC50 (green), K_d (red) or K_i (purple) measurements.

k_{on} remains the same; Fig.5.3b). However, most likely structural stability is a combination of both options.

We found that anchoring sites often correspond to binding hot spots, and in those cases, ΔG_{bind} must be a component of W_{QB}. On the other hand, there is no correlation between magnitudes (Fig.5.2). Therefore, we concluded that a transitory dissociation penalty dominates structural stability. Such penalty originates in physical decoupling between HB rupture and resolvation.[25] Both explanations find support in the examples sourced from simulated sets (Fig.5.3c,d).

Expanding the Applicability Domain of Structural Stability

In the second article, we explored the applicability of Dynamic Undocking in a new scenario - binding mode prediction. We have shown that it can perform

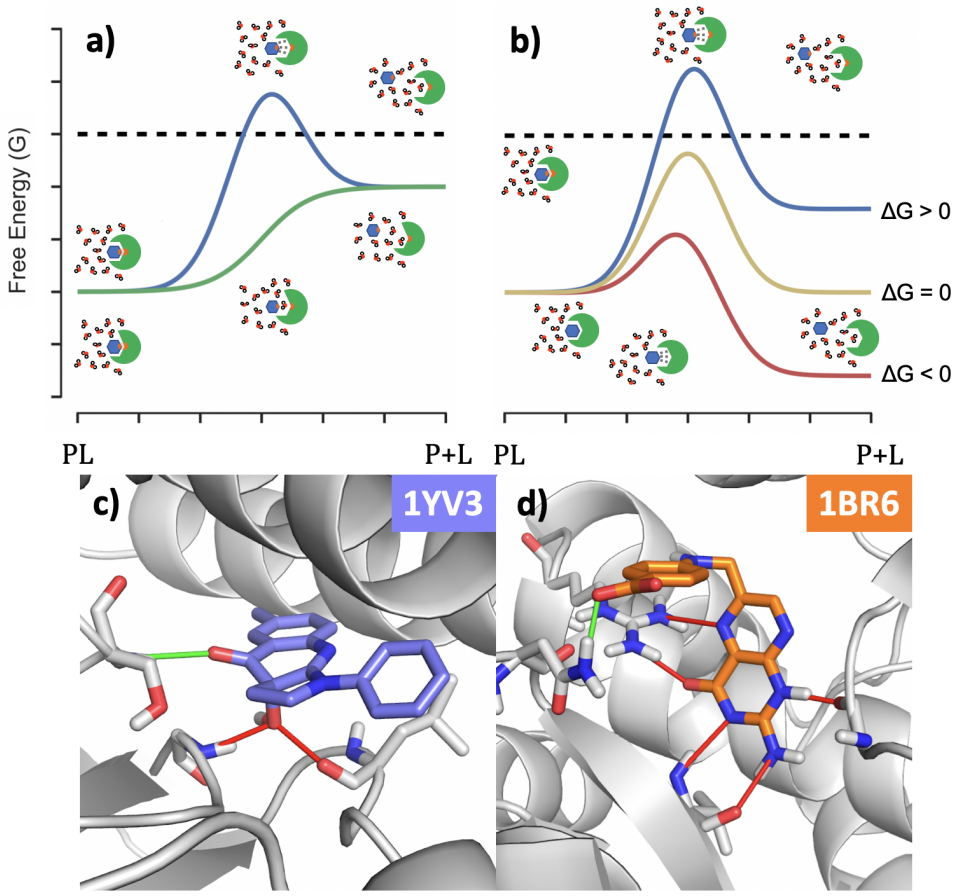

Fig. 5.3 Ways of achieving structural robustness. a) Idealized representation of two dissociation pathways for complexes with the same ΔG_{bind} and different desolvation costs. b) Likewise, for three complexes with the same desolvation cost but different ΔG_{bind}. c) Example of a complex with high dissociation cost due to extreme water-shielding. d) Example of a complex with high dissociation cost due to a tight network of multiple HBs.

as well as docking scoring functions for drug-like ligands. In the challenging cases of fragments, where inaccuracies of scoring functions are amplified due to their small size, DUck outperforms docking.

To make a fair comparison, we need to point out that DUck, being based on MD, is much more computationally demanding than docking. Docking of a single ligand takes a few seconds on a CPU. It takes DUck around 73 GPU hours to perform a similar task. It is a significant difference that affects the throughput of the method. However, DUck is not meant to compete with docking. As mentioned before, structural stability is fundamentally different from binding free energy. Therefore, DUck complements docking by providing new information about the system. It is merely another perspective on biological complexes.

The concept is still very fresh and we do not know all its limitations. For example, it fails for complexes that do not form any robust hydrogen bond. Even though the proportion of such cases is relatively low (10%), we plan to adapt the method to other interaction types, such as water-mediated hydrogen bonds, cation-pi or halogen bonds. The same problem occurs at the substructure level: our approach can predict very well the binding mode of the anchor but is clueless about other parts of the ligand. Better integration with existing docking software should ensure that DUck is applied judiciously, taking the best from each method. We also plan to reduce the computational cost by optimizing of the protocol (e.g. longer integration steps with atom-mass repartitioning, shorter simulations, next-generation hardware), and developing an empirical scoring function (e.g. based on machine learning) to predict W_{QB}.

Chapter 6

Conclusions

Global Conclusions

- We have broadened our knowledge about Hydrogen Bond-based Structural Stability, and we have shown that it is a ubiquitous property in protein-ligand complexes. The design of a ligand can modulate it.
- We speculate that deep and narrow minima, responsible for structural stability if molecules, are highly influenced by desolvation cost, binding free energy and cooperativity of interactions.
- We have expanded the applicability domain of structural stability and shown that it can be used alongside docking in binding mode prediction.

Specific conclusions

- Even though Hydrogen Bond-based Structural, it is not strictly necessary. There are potent complexes that lack structural stability. In some of these cases, stability can be provided by other interactions, and in other increased flexibility can be desirable.
- Fragments are more static than drug-like molecules.
- The comparison with x-ray B-factors has shown that atoms forming robust hydrogen bonds are in more ordered parts of the complex.
- Binding behaviour is dictated by a type of receptor. Highly stable complexes are observed when order is essential for the function of a protein.
- Most of the complexes combine fragment-sized structural anchor with a looser region, thus balancing order with disorder.
- Selecting ligands based on their structural stability outperforms docking scoring functions for fragments.

- Dynamic Undocking has comparable performance to rDock's scoring function at docking drug-like molecules.
- Docking and Dynamic Undocking are complementary to each other and can be successfully applied in drug design.

Bibligraphy

[1] James P Hughes, Stephen Rees, S Barrett Kalindjian, and Karen L Philpott. Principles of early drug discovery. *British journal of pharmacology*, 162(6):1239–1249, 2011.

[2] Janice M Reichert. A guide to drug discovery: Trends in development and approval times for new therapeutics in the united states. *Nature reviews Drug discovery*, 2(9):695, 2003.

[3] Ted T Ashburn and Karl B Thor. Drug repositioning: identifying and developing new uses for existing drugs. *Nature reviews Drug discovery*, 3(8):673, 2004.

[4] Yongliang Yang, S James Adelstein, and Amin I Kassis. Target discovery from data mining approaches. *Drug discovery today*, 17:S16–S23, 2012.

[5] Martin Schneider. A rational approach to maximize success rate in target discovery. *Archiv der Pharmazie: An International Journal Pharmaceutical and Medicinal Chemistry*, 337(12):625–633, 2004.

[6] Ulrich AK Betz. How many genomics targets can a portfolio afford? *Drug discovery today*, 10(15):1057–1063, 2005.

[7] Sandra Fox, Shauna Farr-Jones, Lynne Sopchak, Amy Boggs, Helen Wang Nicely, Richard Khoury, and Michael Biros. High-throughput screening: update on practices and success. *Journal of biomolecular screening*, 11(7):864–869, 2006.

[8] Daniel A Erlanson, Robert S McDowell, and Tom O'Brien. Fragment-based drug discovery. *Journal of medicinal chemistry*, 47(14):3463–3482, 2004.

[9] Mariusz Jaskolski, Zbigniew Dauter, and Alexander Wlodawer. A brief history of macromolecular crystallography, illustrated by a family tree and its nobel fruits. *The FEBS journal*, 281(18):3985–4009, 2014.

[10] Enrique Abola, Peter Kuhn, Thomas Earnest, and Raymond C Stevens. Automation of x-ray crystallography. *Nature Structural & Molecular Biology*, 7(11s):973, 2000.

[11] Marta G Carneiro, AB Eiso, Stephan Theisgen, and Gregg Siegal. Nmr in structure-based drug design. *Essays in biochemistry*, 61(5):485–493, 2017.

[12] Alan Merk, Alberto Bartesaghi, Soojay Banerjee, Veronica Falconieri, Prashant Rao, Mindy I Davis, Rajan Pragani, Matthew B Boxer, Lesley A Earl, Jacqueline LS Milne, et al. Breaking cryo-em resolution barriers to facilitate drug discovery. *Cell*, 165(7):1698–1707, 2016.

[13] Heena Khatter, Alexander G Myasnikov, S Kundhavai Natchiar, and Bruno P Klaholz. Structure of the human 80s ribosome. *Nature*, 520(7549):640, 2015.

[14] John A Christopher, Sarah J Aves, Kirstie A Bennett, Andrew S Dore, James C Errey, Ali Jazayeri, Fiona H Marshall, Krzysztof Okrasa, Maria J Serrano-Vega, Benjamin G Tehan, et al. Fragment and structure-based drug discovery for a class c gpcr: discovery of the mglu5 negative allosteric modulator htl14242 (3-chloro-5-[6-(5-fluoropyridin-2-yl) pyrimidin-4-yl] benzonitrile). *Journal of medicinal chemistry*, 58(16):6653–6664, 2015.

[15] Helen M Berman, John Westbrook, Zukang Feng, Gary Gilliland, Talapady N Bhat, Helge Weissig, Ilya N Shindyalov, and Philip E Bourne. The protein data bank. *Nucleic acids research*, 28(1):235–242, 2000.

[16] Pdb statistics: Overall growth of released structures per year. https://www.rcsb.org/stats/growth/overall. Accessed: 2019-05-20.

[17] Renato Ferreira de Freitas and Matthieu Schapira. A systematic analysis of atomic protein–ligand interactions in the pdb. *MedChemComm*, 8(10):1970–1981, 2017.

[18] Andrew M Davis and Simon J Teague. Hydrogen bonding, hydrophobic interactions, and failure of the rigid receptor hypothesis. *Angewandte Chemie International Edition*, 38(6):736–749, 1999.

[19] Thomas Steiner. The hydrogen bond in the solid state. *Angewandte Chemie International Edition*, 41(1):48–76, 2002.

[20] Eva Nittinger, Therese Inhester, Stefan Bietz, Agnes Meyder, Karen T Schomburg, Gudrun Lange, Robert Klein, and Matthias Rarey. Large-scale analysis of hydrogen bond interaction patterns in protein–ligand interfaces. *Journal of medicinal chemistry*, 60(10):4245–4257, 2017.

[21] Alan R Fersht. The hydrogen bond in molecular recognition. *Trends in Biochemical Sciences*, 12:301–304, 1987.

[22] Brian K Shoichet. No free energy lunch. *Nature biotechnology*, 25(10):1109, 2007.

[23] DudleyáH Williams and MartináS Westwell. Aspects of weak interactions. *Chemical Society Reviews*, 27(1):57–64, 1998.

[24] Jagannath Mondal, Richard A Friesner, and B J Berne. Role of Desolvation in Thermodynamics and Kinetics of Ligand Binding to a Kinase. *Journal of chemical theory and computation*, 10(12):5696–5705, 2014.

[25] Peter Schmidtke, F. Javier Luque, James B. Murray, and Xavier Barril. Shielded hydrogen bonds as structural determinants of binding kinetics: Application in drug design. *Journal of the American Chemical Society*, 133(46):18903–18910, 2011.

[26] E. A. Meyer, R. K. Castellano, and F. Diederich. Interactions with Arenes Interactions with Aromatic Rings in Chemical and Biological Recognition Angewandte. *Angew. Chem. Int. Ed.*, 42(11):1210–50, 2003.

[27] Rubicelia Vargas, Jorge Garza, David A Dixon, and Benjamin P Hay. How strong is the cα- h oc hydrogen bond? *Journal of the American Chemical Society*, 122(19):4750–4755, 2000.

[28] Subrayashastry Aravinda, Narayanaswamy Shamala, Abhishek Bandyopadhyay, and Padmanabhan Balaram. Probing the role of the c- h o hydrogen bond stabilized polypeptide chain reversal at the c-terminus of designed peptide helices. structural characterization of three decapeptides. *Journal of the American Chemical Society*, 125(49):15065–15075, 2003.

[29] Scott Horowitz and Raymond C Trievel. Carbon-oxygen hydrogen bonding in biological structure and function. *Journal of Biological Chemistry*, 287(50):41576–41582, 2012.

[30] Rabi A Musah, Gerard M Jensen, Robin J Rosenfeld, Duncan E McRee, David B Goodin, and Steven W Bunte. Variation in strength of an unconventional c- h to o hydrogen bond in an engineered protein cavity. *Journal of the American Chemical Society*, 119(38):9083–9084, 1997.

[31] Albert C Pierce, Kathryn L Sandretto, and Guy W Bemis. Kinase inhibitors and the case for ch... o hydrogen bonds in protein–ligand binding. *Proteins: Structure, Function, and Bioinformatics*, 49(4):567–576, 2002.

[32] Carey D Waldburger, Joel F Schildbach, and Robert T Sauer. Are buried salt bridges important for protein stability and conformational specificity? *Nature structural biology*, 2(2):122, 1995.

[33] Zachary S Hendsch and Bruce Tidor. Do salt bridges stabilize proteins? a continuum electrostatic analysis. *Protein Science*, 3(2):211–226, 1994.

[34] Dennis A Dougherty. The cation- π interaction. *Accounts of chemical research*, 46(4):885–893, 2012.

[35] Schrödinger, LLC. The PyMOL molecular graphics system, version 1.8. November 2015.

[36] Sebastian Salentin, Sven Schreiber, V Joachim Haupt, Melissa F Adasme, and Michael Schroeder. Plip: fully automated protein–ligand interaction profiler. *Nucleic acids research*, 43(W1):W443–W447, 2015.

[37] Xing Du, Yi Li, Yuan-Ling Xia, Shi-Meng Ai, Jing Liang, Peng Sang, Xing-Lai Ji, and Shu-Qun Liu. Insights into protein–ligand interactions: mechanisms, models, and methods. *International journal of molecular sciences*, 17(2):144, 2016.

[38] Christopher A MacRaild, Antonio Hernández Daranas, Agnieszka Bronowska, and Steve W Homans. Global changes in local protein dynamics reduce the entropic cost of carbohydrate binding in the arabinose-binding protein. *Journal of molecular biology*, 368(3):822–832, 2007.

[39] Agnieszka K Bronowska. Thermodynamics of ligand-protein interactions: implications for molecular design. In *Thermodynamics-Interaction Studies-Solids, Liquids and Gases*. IntechOpen, 2011.

[40] Shu-Qun Liu, Xing-Lai Ji, Yan Tao, De-Yong Tan, Ke-Qin Zhang, and Yun-Xin Fu. Protein folding, binding and energy landscape: A synthesis. In *Protein engineering*. IntechOpen, 2012.

[41] Jack D Dunitz. Win some, lose some: enthalpy-entropy compensation in weak intermolecular interactions. *Chemistry & biology*, 2(11):709–712, 1995.

[42] Tjelvar SG Olsson, John E Ladbury, Will R Pitt, and Mark A Williams. Extent of enthalpy–entropy compensation in protein–ligand interactions. *Protein Science*, 20(9):1607–1618, 2011.

[43] Andrew T Fenley, Hari S Muddana, and Michael K Gilson. Entropy–enthalpy transduction caused by conformational shifts can obscure the forces driving protein–ligand binding. *Proceedings of the National Academy of Sciences*, 109(49):20006–20011, 2012.

[44] Charles H Reynolds and M Katharine Holloway. Thermodynamics of ligand binding and efficiency. *ACS medicinal chemistry letters*, 2(6):433–437, 2011.

[45] Hong Qian. Entropy-enthalpy compensation: Conformational fluctuation and induced-fit. *The Journal of Chemical Physics*, 109(22):10015–10017, 1998.

[46] Chia-En Chang and Michael K Gilson. Free energy, entropy, and induced fit in host guest recognition: calculations with the second-generation mining minima algorithm. *Journal of the American Chemical Society*, 126(40):13156–13164, 2004.

[47] Paola Gilli, Valeria Ferretti, Gastone Gilli, and Pier Andrea Borea. Enthalpy-entropy compensation in drug-receptor binding. *The Journal of Physical Chemistry*, 98(5):1515–1518, 1994.

[48] John D Chodera and David L Mobley. Entropy-enthalpy compensation: role and ramifications in biomolecular ligand recognition and design. *Annual review of biophysics*, 42:121–142, 2013.

[49] Ulf Ryde. A fundamental view of enthalpy–entropy compensation. *MedChemComm*, 5(9):1324–1336, 2014.

[50] Benjamin Breiten, Matthew R Lockett, Woody Sherman, Shuji Fujita, Mohammad Al-Sayah, Heiko Lange, Carleen M Bowers, Annie Heroux, Goran Krilov, and George M Whitesides. Water networks contribute to enthalpy/entropy compensation in protein–ligand binding. *Journal of the American Chemical Society*, 135(41):15579–15584, 2013.

[51] Giovanni Bolcato, Alberto Cuzzolin, Maicol Bissaro, Stefano Moro, and Mattia Sturlese. Can we still trust docking results? an extension of the applicability of dockbench on pdbbind database. *International journal of molecular sciences*, 20(14):3558, 2019.

[52] John D Chodera, David L Mobley, Michael R Shirts, Richard W Dixon, Kim Branson, and Vijay S Pande. Alchemical free energy methods for drug discovery: progress and challenges. *Current opinion in structural biology*, 21(2):150–160, 2011.

[53] Alessandro Borgia, Madeleine B Borgia, Katrine Bugge, Vera M Kissling, Pétur O Heidarsson, Catarina B Fernandes, Andrea Sottini, Andrea Soranno, Karin J Buholzer, Daniel Nettels, et al. Extreme disorder in an ultrahigh-affinity protein complex. *Nature*, 555(7694):61, 2018.

[54] Daria B Kokh, Marta Amaral, Joerg Bomke, Ulrich Gradler, Djordje Musil, Hans-Peter Buchstaller, Matthias K Dreyer, Matthias Frech, Maryse Lowinski, Francois Vallee, et al. Estimation of drug-target residence times by τ-random acceleration molecular dynamics simulations. *Journal of chemical theory and computation*, 14(7):3859–3869, 2018.

[55] Rutger HA Folmer. Drug target residence time: a misleading concept. *Drug discovery today*, 23(1):12–16, 2018.

[56] Sergio Ruiz-carmona, Peter Schmidtke, F Javier Luque, Lisa Baker, Natalia Matassova, Ben Davis, Stephen Roughley, James Murray, Rod Hubbard, and Xavier Barril. Dynamic undocking and the quasi-bound state as tools for drug discovery. *Nature Chemistry*, 9(3):201–206, 2017.

[57] Maciej Majewski, Sergio Ruiz-Carmona, and Xavier Barril. Dynamic Undocking: A Novel Method for Structure-Based Drug Discovery. In Thomas Mavromoustakos and Tahsin F Kellici, editors, *Rational Drug Design: Methods and Protocols*, pages 195–215. Springer New York, New York, 2018.

[58] Albert C Pan, David W Borhani, Ron O Dror, and David E Shaw. Molecular determinants of drug–receptor binding kinetics. *Drug discovery today*, 18(13-14):667–673, 2013.

[59] Caterina Bissantz, Bernd Kuhn, and Martin Stahl. A medicinal chemist's guide to molecular interactions. *Journal of medicinal chemistry*, 53(14):5061–5084, 2010.

[60] Jürgen Bajorath. Integration of virtual and high-throughput screening. *Nature Reviews Drug Discovery*, 1(11):882, 2002.

[61] Douglas B Kitchen, Hélène Decornez, John R Furr, and Jürgen Bajorath. Docking and scoring in virtual screening for drug discovery: methods and applications. *Nature reviews Drug discovery*, 3(11):935, 2004.

[62] Irwin D Kuntz, Jeffrey M Blaney, Stuart J Oatley, Robert Langridge, and Thomas E Ferrin. A geometric approach to macromolecule-ligand interactions. *Journal of molecular biology*, 161(2):269–288, 1982.

[63] Richard A Friesner, Robert B Murphy, Matthew P Repasky, Leah L Frye, Jeremy R Greenwood, Thomas A Halgren, Paul C Sanschagrin, and Daniel T Mainz. Extra precision glide: Docking and scoring incorporating a model of hydrophobic enclosure for protein- ligand complexes. *Journal of medicinal chemistry*, 49(21):6177–6196, 2006.

[64] Richard A Friesner, Jay L Banks, Robert B Murphy, Thomas A Halgren, Jasna J Klicic, Daniel T Mainz, Matthew P Repasky, Eric H Knoll, Mee Shelley, Jason K Perry, et al. Glide: a new approach for rapid, accurate docking and scoring. 1. method and assessment of docking accuracy. *Journal of medicinal chemistry*, 47(7):1739–1749, 2004.

[65] Ruben Abagyan, Maxim Totrov, and Dmitry Kuznetsov. Icm—a new method for protein modeling and design: applications to docking and structure prediction from the distorted native conformation. *Journal of computational chemistry*, 15(5):488–506, 1994.

[66] Sergio Ruiz-Carmona, Daniel Alvarez-Garcia, Nicolas Foloppe, A Beatriz Garmendia-Doval, Szilveszter Juhos, Peter Schmidtke, Xavier Barril, Roderick E Hubbard, and S David Morley. rdock: a fast, versatile and open source program for docking ligands to proteins and nucleic acids. *PLoS computational biology*, 10(4):e1003571, 2014.

[67] Gareth Jones, Peter Willett, and Robert C Glen. Molecular recognition of receptor sites using a genetic algorithm with a description of desolvation. *Journal of molecular biology*, 245(1):43–53, 1995.

[68] Gareth Jones, Peter Willett, Robert C Glen, Andrew R Leach, and Robin Taylor. Development and validation of a genetic algorithm for flexible docking. *Journal of molecular biology*, 267(3):727–748, 1997.

[69] Matthias Rarey, Bernd Kramer, Thomas Lengauer, and Gerhard Klebe. A fast flexible docking method using an incremental construction algorithm. *Journal of molecular biology*, 261(3):470–489, 1996.

[70] David S Goodsell and Arthur J Olson. Automated docking of substrates to proteins by simulated annealing. *Proteins: Structure, Function, and Bioinformatics*, 8(3):195–202, 1990.

[71]

[72] Renee L DesJarlais, Robert P Sheridan, J Scott Dixon, Irwin D Kuntz, and R Venkataraghavan. Docking flexible ligands to macromolecular receptors by molecular shape. *Journal of medicinal chemistry*, 29(11):2149–2153, 1986.

[73] Andrew R Leach and Irwin D Kuntz. Conformational analysis of flexible ligands in macromolecular receptor sites. *Journal of Computational Chemistry*, 13(6):730–748, 1992.

[74] Simon K Kearsley, Dennis J Underwood, Robert P Sheridan, and Michael D Miller. Flexibases: a way to enhance the use of molecular docking methods. *Journal of computer-aided molecular design*, 8(5):565–582, 1994.

[75] David S Goodsell, Hans Lauble, C David Stout, and Arthur J Olson. Automated docking in crystallography: analysis of the substrates of aconitase. *Proteins: Structure, Function, and Bioinformatics*, 17(1):1–10, 1993.

[76] Trevor N Hart and Randy J Read. A multiple-start monte carlo docking method. *Proteins: Structure, Function, and Bioinformatics*, 13(3):206–222, 1992.

[77] Connie M Oshiro, Irwin D Kuntz, and J Scott Dixon. Flexible ligand docking using a genetic algorithm. *Journal of computer-aided molecular design*, 9(2):113–130, 1995.

[78] David R Westhead, David E Clark, and Christopher W Murray. A comparison of heuristic search algorithms for molecular docking. *Journal of Computer-Aided Molecular Design*, 11(3):209–228, 1997.

[79] Carol A Baxter, Christopher W Murray, David E Clark, David R Westhead, and Matthew D Eldridge. Flexible docking using tabu search and an empirical estimate of binding affinity. *Proteins: Structure, Function, and Bioinformatics*, 33(3):367–382, 1998.

[80] Scott J Weiner, Peter A Kollman, Dzung T Nguyen, and David A Case. An all atom force field for simulations of proteins and nucleic acids. *Journal of computational chemistry*, 7(2):230–252, 1986.

[81] Hans-Joachim Böhm. Ludi: rule-based automatic design of new substituents for enzyme inhibitor leads. *Journal of computer-aided molecular design*, 6(6):593–606, 1992.

[82] Sarah L Kinnings, Nina Liu, Peter J Tonge, Richard M Jackson, Lei Xie, and Philip E Bourne. A machine learning-based method to improve docking scoring functions and its application to drug repurposing. *Journal of chemical information and modeling*, 51(2):408–419, 2011.

[83] José Jiménez, Miha Skalic, Gerard Martinez-Rosell, and Gianni De Fabritiis. K deep: protein–ligand absolute binding affinity prediction via 3d-convolutional neural networks. *Journal of chemical information and modeling*, 58(2):287–296, 2018.

[84] Matthew D Eldridge, Christopher W Murray, Timothy R Auton, Gaia V Paolini, and Roger P Mee. Empirical scoring functions: I. the development of a fast empirical scoring function to estimate the binding affinity of ligands in receptor complexes. *Journal of computer-aided molecular design*, 11(5):425–445, 1997.

[85] Didier Rognan, Sanne Lise Lauemøller, Arne Holm, Søren Buus, and Vincenzo Tschinke. Predicting binding affinities of protein ligands from three-dimensional models: application to peptide binding to class i major histocompatibility proteins. *Journal of medicinal chemistry*, 42(22):4650–4658, 1999.

[86] Doree Sitkoff, Kim A Sharp, and Barry Honig. Accurate calculation of hydration free energies using macroscopic solvent models. *The Journal of Physical Chemistry*, 98(7):1978–1988, 1994.

[87] Philippe Ferrara, Holger Gohlke, Daniel J Price, Gerhard Klebe, and Charles L Brooks. Assessing scoring functions for protein- ligand interactions. *Journal of medicinal chemistry*, 47(12):3032–3047, 2004.

[88] Paul S Charifson, Joseph J Corkery, Mark A Murcko, and W Patrick Walters. Consensus scoring: A method for obtaining improved hit rates from docking databases of three-dimensional structures into proteins. *Journal of medicinal chemistry*, 42(25):5100–5109, 1999.

[89] Renxiao Wang, Luhua Lai, and Shaomeng Wang. Further development and validation of empirical scoring functions for structure-based binding affinity prediction. *Journal of computer-aided molecular design*, 16(1):11–26, 2002.

[90] Anthony J Clark, Pratyush Tiwary, Ken Borrelli, Shulu Feng, Edward B Miller, Robert Abel, Richard A Friesner, and BJ Berne. Prediction of protein–ligand binding poses via a combination of induced fit docking and metadynamics simulations. *Journal of chemical theory and computation*, 12(6):2990–2998, 2016.

[91] J Andrew McCammon, Bruce R Gelin, and Martin Karplus. Dynamics of folded proteins. *Nature*, 267(5612):585, 1977.

[92] Bernard R Brooks, Charles L Brooks III, Alexander D Mackerell Jr, Lennart Nilsson, Robert J Petrella, Benoît Roux, Youngdo Won, Georgios Archontis, Christian Bartels, Stefan Boresch, et al. Charmm: the biomolecular simulation program. *Journal of computational chemistry*, 30(10):1545–1614, 2009.

[93] David A Case, Thomas E Cheatham III, Tom Darden, Holger Gohlke, Ray Luo, Kenneth M Merz Jr, Alexey Onufriev, Carlos Simmerling, Bing Wang, and Robert J Woods. The amber biomolecular simulation programs. *Journal of computational chemistry*, 26(16):1668–1688, 2005.

[94] Herman JC Berendsen, David van der Spoel, and Rudi van Drunen. Gromacs: a message-passing parallel molecular dynamics implementation. *Computer physics communications*, 91(1-3):43–56, 1995.

[95] Peter Eastman, Jason Swails, John D Chodera, Robert T McGibbon, Yutong Zhao, Kyle A Beauchamp, Lee-Ping Wang, Andrew C Simmonett, Matthew P Harrigan, Chaya D Stern, et al. Openmm 7: Rapid development of high performance algorithms for molecular dynamics. *PLoS computational biology*, 13(7):e1005659, 2017.

[96] Marco De Vivo, Matteo Masetti, Giovanni Bottegoni, and Andrea Cavalli. Role of molecular dynamics and related methods in drug discovery. *Journal of medicinal chemistry*, 59(9):4035–4061, 2016.

[97] Wendy D Cornell, Piotr Cieplak, Christopher I Bayly, Ian R Gould, Kenneth M Merz, David M Ferguson, David C Spellmeyer, Thomas Fox, James W Caldwell, and Peter A Kollman. A second generation force field for the simulation of proteins, nucleic acids, and organic molecules. *Journal of the American Chemical Society*, 117(19):5179–5197, 1995.

[98] Alex D MacKerell Jr, Donald Bashford, MLDR Bellott, Roland Leslie Dunbrack Jr, Jeffrey D Evanseck, Martin J Field, Stefan Fischer, Jiali Gao, H Guo, Sookhee Ha, et al. All-atom empirical potential for molecular modeling and dynamics studies of proteins. *The journal of physical chemistry B*, 102(18):3586–3616, 1998.

[99] William L Jorgensen and Julian Tirado-Rives. The opls force field for proteins. energy minimizations for crystals of cyclic peptides and crambin. *J. Am. Chem. Soc*, 110(6):1657–1723, 1988.

[100] Junmei Wang, Romain M Wolf, James W Caldwell, Peter A Kollman, and David A Case. Development and testing of a general amber force field. *Journal of computational chemistry*, 25(9):1157–1174, 2004.

[101] Kenno Vanommeslaeghe, Elizabeth Hatcher, Chayan Acharya, Sibsankar Kundu, Shijun Zhong, Jihyun Shim, Eva Darian, Olgun Guvench, P Lopes, Igor Vorobyov, et al. Charmm general force field: A force field for drug-like molecules compatible with the charmm all-atom additive biological force fields. *Journal of computational chemistry*, 31(4):671–690, 2010.

[102] Junmei Wang, Wei Wang, Peter A Kollman, and David A Case. Automatic atom type and bond type perception in molecular mechanical calculations. *Journal of molecular graphics and modelling*, 25(2):247–260, 2006.

[103] Robin M Betz and Ross C Walker. Paramfit: automated optimization of force field parameters for molecular dynamics simulations. *Journal of computational chemistry*, 36(2):79–87, 2015.

[104] Alessandro Laio and Michele Parrinello. Escaping free-energy minima. *Proceedings of the National Academy of Sciences*, 99(20):12562–12566, 2002.

[105] Siewert J Marrink, H Jelger Risselada, Serge Yefimov, D Peter Tieleman, and Alex H De Vries. The martini force field: coarse grained model for biomolecular simulations. *The journal of physical chemistry B*, 111(27):7812–7824, 2007.

[106] Glenn M Torrie and John P Valleau. Nonphysical sampling distributions in monte carlo free-energy estimation: Umbrella sampling. *Journal of Computational Physics*, 23(2):187–199, 1977.

[107] Yuji Sugita and Yuko Okamoto. Replica-exchange molecular dynamics method for protein folding. *Chemical physics letters*, 314(1-2):141–151, 1999.

[108] Barry Isralewitz, Mu Gao, and Klaus Schulten. Steered molecular dynamics and mechanical functions of proteins. *Current opinion in structural biology*, 11(2):224–230, 2001.

[109] Helmut Grubmüller, Berthold Heymann, and Paul Tavan. Ligand binding: molecular mechanics calculation of the streptavidin-biotin rupture force. *Science*, 271(5251):997–999, 1996.

[110] Dario Gioia, Martina Bertazzo, Maurizio Recanatini, Matteo Masetti, and Andrea Cavalli. Dynamic docking: a paradigm shift in computational drug discovery. *Molecules*, 22(11):2029, 2017.

[111] William L Jorgensen and C Ravimohan. Monte carlo simulation of differences in free energies of hydration. *The Journal of chemical physics*, 83(6):3050–3054, 1985.

[112] William L Jorgensen and Laura L Thomas. Perspective on free-energy perturbation calculations for chemical equilibria. *Journal of chemical theory and computation*, 4(6):869–876, 2008.

[113] Daniel Alvarez-Garcia and Xavier Barril. Molecular simulations with solvent competition quantify water displaceability and provide accurate interaction maps of protein binding sites. *Journal of medicinal chemistry*, 57(20):8530–8539, 2014.

[114] Christopher Jarzynski. Nonequilibrium equality for free energy differences. *Physical Review Letters*, 78(14):2690, 1997.

[115] Sergio Ruiz-Carmona, Peter Schmidtke, F Javier Luque, Lisa Baker, Natalia Matassova, Ben Davis, Stephen Roughley, James Murray, Rod Hubbard, and Xavier Barril. Dynamic undocking and the quasi-bound state as tools for drug discovery. *Nature chemistry*, 9(3):201, 2017.

[116] Michael M Mysinger, Michael Carchia, John J Irwin, and Brian K Shoichet. Directory of useful decoys, enhanced (dud-e): better ligands and decoys for better benchmarking. *Journal of medicinal chemistry*, 55(14):6582–6594, 2012.

[117] Sergio Ruiz-Carmona and Xavier Barril. Docking-undocking combination applied to the d3r grand challenge 2015. *Journal of computer-aided molecular design*, 30(9):805–815, 2016.

[118] I-Jen Chen and Roderick E Hubbard. Lessons for fragment library design: analysis of output from multiple screening campaigns. *Journal of computer-aided molecular design*, 23(8):603–620, 2009.

[119] Gregory L Warren, Thanh D Do, Brian P Kelley, Anthony Nicholls, and Stephen D Warren. Essential considerations for using protein–ligand structures in drug discovery. *Drug Discovery Today*, 17(23-24):1270–1281, 2012.

[120] Angelo D Favia, Giovanni Bottegoni, Irene Nobeli, Paola Bisignano, and Andrea Cavalli. Seraphic: A benchmark for in silico fragment-based drug design. *Journal of chemical information and modeling*, 51(11):2882–2896, 2011.

[121] Fabrizio Giordanetto, Chentian Jin, Lindsay Willmore, Miklos Feher, and David E Shaw. Fragment hits: What do they look like and how do they bind? *Journal of medicinal chemistry*, 62(7):3381–3394, 2019.

[122] Gyorgy G Ferenczy and Gyorgy M Keseru. Thermodynamics of fragment binding. *Journal of chemical information and modeling*, 52(4):1039–1045, 2012.

[123] Johannes Schiebel, Nedyalka Radeva, Stefan G Krimmer, Xiaojie Wang, Martin Stieler, Frederik R Ehrmann, Kan Fu, Alexander Metz, Franziska U Huschmann, Manfred S Weiss, et al. Six biophysical screening methods miss a large proportion of crystallographically discovered fragment hits: a case study. *ACS chemical biology*, 11(6):1693–1701, 2016.

[124] Kalyan Das, Arthur D Clark, Paul J Lewi, Jan Heeres, Marc R De Jonge, Lucien MH Koymans, H Maarten Vinkers, Frederik Daeyaert, Donald W Ludovici, Michael J Kukla, et al. Roles of conformational and positional adaptability in structure-based design of tmc125-r165335 (etravirine) and related non-nucleoside reverse transcriptase inhibitors that are highly potent and effective against wild-type and drug-resistant hiv-1 variants. *Journal of medicinal chemistry*, 47(10):2550–2560, 2004.

[125] Won-Gil Lee, Albert H Chan, Krasimir A Spasov, Karen S Anderson, and William L Jorgensen. Design, conformation, and crystallography of 2-naphthyl phenyl ethers as potent anti-hiv agents. *ACS medicinal chemistry letters*, 7(12):1156–1160, 2016.

[126] Shipra Malhotra and John Karanicolas. When does chemical elaboration induce a ligand to change its binding mode? *Journal of medicinal chemistry*, 60(1):128–145, 2017.

Additional Publications

Dynamic Undocking: A Novel Method for Structure-Based Drug Discovery

Maciej Majewski[1], Sergio Ruiz-Carmona[1], and Xavier Barril[1,2]

In *Rational Drug Design (**2018**). Humana Press, New York, NY, pp. 195-215*

1. Institut de Biomedicina de la Universitat de Barcelona (IBUB) and Facultat de Farmacia, Universitat de Barcelona, Av. Joan XXIII 27-31, 08028 Barcelona, Spain.
2. Catalan Institution for Research and Advanced Studies (ICREA), Passeig Lluis Companys 23, 08010 Barcelona, Spain.

Chapter 11

Dynamic Undocking: A Novel Method for Structure-Based Drug Discovery

Maciej Majewski, Sergio Ruiz-Carmona, and Xavier Barril

Abstract

Computer-aided methods have been broadly used in pharmaceutical research to identify potential ligands and design effective therapeutics. Most of the approaches rely on the binding affinity prediction and approximate thermodynamic properties of the system. Our alternative approach focuses on structural stability, provided by native protein–ligand interactions, in particular hydrogen bonds. Based on this idea, we designed new fast computational method, called dynamic undocking (DUck), that evaluates stability by calculating the work necessary to break the most important native contact in a ligand-receptor complex. This property is effective in distinguishing true ligands from decoys and is orthogonal to currently existing docking methods, thus making it exceptionally useful in virtual screening. Here, we present a protocol suitable for DUck's application in drug design strategy, as well as notes that will help to solve common problems addressed by users.

Key words Drug discovery, Molecular docking, Molecular dynamics, Structure-based drug design, Virtual screening, Hydrogen bonds, Structural stability

1 Introduction

There is a continuous need for new methods that increase the efficacy and efficiency of rational drug design. Structure-based approaches aim to predict the binding free energy of protein–ligand complexes, but this is an elusive property that is extremely difficult to calculate in a rigorous manner. As a result, commonly used tools apply various layers of approximations, and the resulting estimates carry a large, and often unknown, absolute error. Recently, we have postulated that protein–ligand complexes could be evaluated, not only by their binding free energy but also by their ability to form a precise and stable binding mode. Structural stability is relatively easy to compute, as one can start with the bound state, introduce minor perturbations, and measure the resistance that the system opposes to that change.

Thomas Mavromoustakos and Tahsin F. Kellici (eds.), *Rational Drug Design: Methods and Protocols*, Methods in Molecular Biology, vol. 1824, https://doi.org/10.1007/978-1-4939-8630-9_11,

In this book chapter, we describe a particular computational approach, termed dynamic undocking (DUck) [1], that we have implemented to assess the robustness of protein–ligand interactions. DUck is fast and automatic and, thus, amenable to high-throughput applications. The method is very effective in distinguishing active from inactive compounds and is virtually free from false negatives. At the same time, it is orthogonal to existing approaches as they focus on fundamentally different properties. In this introduction, we will present the conceptual basis for DUck and summarize the most important results validating the method. Then we will present and discuss all the methodological details involved in the practical application of DUck.

1.1 Structural Stability and Binding

In target-based drug design, K_D is the parameter that defines efficacy. The thermodynamic equilibrium constant (or other parameters that are easier to determine experimentally—IC_{50}, AC_{50}, K_I—and are used as proxy) informs about the potency of a ligand for its macromolecular target and is the main parameter under optimization. Not surprisingly, structure-based drug design has always focused on predicting K_D (or mathematical transformations of the same, such as ΔG_{BIND}) in order to guide and accelerate the discovery of new bioactive molecules. Inevitably, this involves a comparison of the bound (protein–ligand complex in solution) and unbound states (independently solvated entities). These states are difficult to characterize, and their comparison leads to an accumulation of errors. In spite of the economic and intellectual incentives in solving this problem, accurate solutions are—at best—impractical, and common methods offer very qualitative estimates [2].

We propose to consider a different property of protein–ligand complexes, which is not related to a thermodynamic constant but appears to be ubiquitous. Most protein–ligand complexes are structurally robust (i.e., they have a single binding site that is preserved under dynamic conditions). This implies that active ligands—irrespective of their ΔG_{BIND}—must present a deep and narrow free energy minimum around the bound state (Fig. 1). As this is a local magnitude, it would be relatively straightforward to predict, simply starting from the bound state and measuring the resistance that the ligand opposes to small perturbations. Note, however, that (1) structural stability is not an essential condition for binding (consider, i.e., the case of a lipid inside a bilayer), but—empirically—most protein–ligand complexes form robust complexes, and (2) a priori, structural stability should not correlate with any thermodynamic constant (K_D, k_{off}).

1.2 Hydrogen Bonds as Structural Anchors

The calculation of structural stability could be realized in many different ways. Here we postulate that hydrogen bonds are privileged anchoring motifs and decide to monitor specifically this

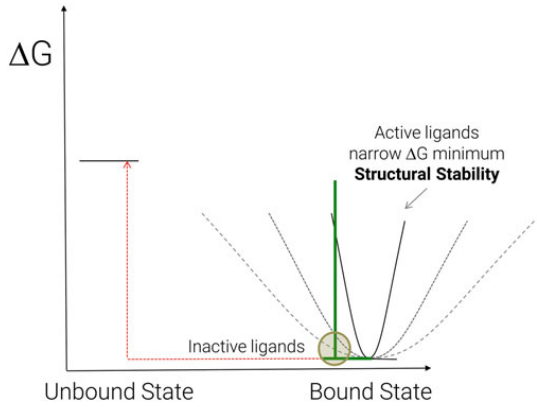

Fig. 1 Graphical representation of the quasi-bound state (green lines and circle) in relation to bound and unbound states

type of interactions. The choice is based on the fact that hydrogen bonds have very strict geometric requirements (maximal fluctuation ~0.5 Å). Additionally, we have observed that protein–ligand complexes can form water-shielded hydrogen bonds, which create steep barriers to dissociation [3]. Hydrogen bonds are an essential feature of most protein–ligand complexes, including fragment-sized ligands [4], and most well-studied binding sites present a polar interaction point that is fulfilled by all known ligands. In the initial implementation of the method, we have decided to consider only the single most important hydrogen bond, as defined by a pharmacophore analysis of known ligands. In the future, we will investigate the use of multiple hydrogen bonds and also other types of molecular interactions. The designated hydrogen bond is then pulled from 2.5 Å to 5.0 Å, which covers the whole range from a very strong hydrogen bond to a water-mediated interaction. In order to exclude effects that are unrelated to the hydrogen bond under investigation, we use a small portion of the receptor. The judicious definition of this subsystem is essential, as it must preserve the local environment that modulates the rupture of the hydrogen bond while removing interactions that may preclude displacement by unrelated mechanisms (e.g., steric blockage). Simulating only a subset of the system offers the additional advantages of simplifying the dissociation pathway and speeding up the calculations, which scale linearly with the number of particles. Having defined the system and the scope of the simulation, we have designed a computational protocol to realize it.

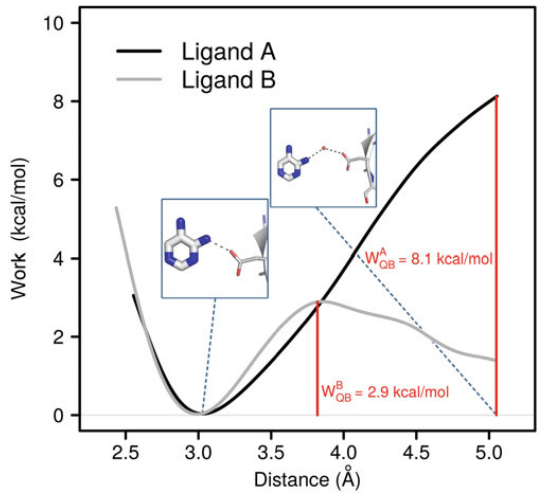

Fig. 2 Representative work profiles obtained from DUck simulations for a strong (black) and a weak (gray) ligand. The QB state is defined as the point with the highest energy relative to the ideal hydrogen-bond geometry

1.3 Dynamic Undocking and the Quasi-Bound State

Dynamic undocking per se is a particular type of steered molecular dynamics (SMD) simulation, where we force the rupture of an intermolecular hydrogen bond formed between a predefined interaction point in the receptor and a complementary atom in the ligand. The distance between the said two atoms is the reaction coordinate, and steering is carried out at constant velocity, monitoring the force (and thus the work) needed to proceed at each point along the reaction coordinate. Then, we define the quasi-bound state as the point where work reaches a maximum (Fig. 2). The work needed to reach the quasi-bound state (W_{QB}) is used as a measure of structural stability. If our hypothesis is correct, potent ligands must present relatively large W_{QB} values, while weak ligands or inactive molecules should oppose little resistance to dissociation. Initial experiments were devised to test the hypothesis and to identify a relationship between W_{QB} and binding that could be used in virtual screening applications.

1.4 Hypothesis Validation

Figure 3 shows the distribution of W_{QB} values observed for a set [5] of strong CDK2 binders ($IC_{50} < 1$ μM), weak CDK2 binders ($IC_{50} > 1$ μM), and decoys (i.e., molecules that have similar properties and can dock to CDK2 but have no reported activity against this protein). Strikingly, all strong binders present high W_{QB} (>5 kcal/mol) values, while the vast majority of decoys present no or very low W_{QB} values (<3 kcal/mol). Weak binders present larger dispersion on the low end of the distribution but must also

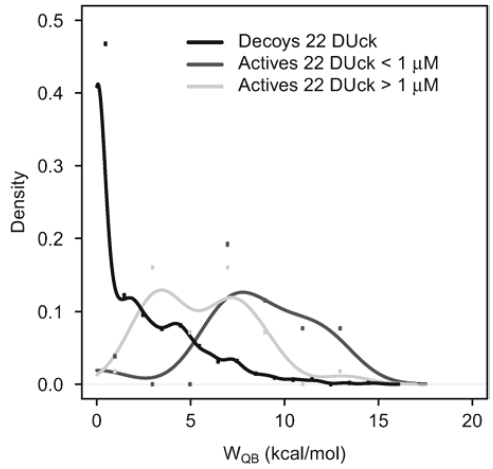

Fig. 3 Distribution of W_{QB} values of potent CDK2 ligands (IC50 $<$ 1 μM, dark gray), weak CDK2 ligands (IC50 $>$ 1 μM, light gray), and non-binding decoys (black). Points indicate population values from which the smooth lines are extrapolated

offer strong resistance to dissociation. This result is a strong indication that, as we hypothesized, true ligands form hydrogen bonds that make the protein–ligand complex structurally robust. It also indicates that this property can be used to separate active compounds from inactive ones. In consequence W_{QB} can be used in virtual screening applications. This is shown in the ROC curves plotted in Fig. 4. Here we considered one member of each of the following protein families: kinases (CDK2), GPCRs (adenosine A2A receptor), and proteases (trypsin). As shown, a selection based on this metric produces a clear enrichment in true active compounds (curves well above the diagonal). It is important to appreciate that W_{QB} offers a completely new, yet complementary, perspective on binding. While existing methods, such as docking score, try to capture the overall complementarity between two molecules in their bound state, DUck evaluates the resistance that a particular interaction opposes to geometrical perturbation. It is not surprising then that both parameters are uncorrelated (Fig. 5). Using both methods together increases the effectiveness of virtual screening over each individual method. DUck has also proven its worth in prospective validation, confirming that it can multiply the efficacy of docking-based virtual screening by detecting many of the false positives that this method produces, without introducing any false negatives [1].

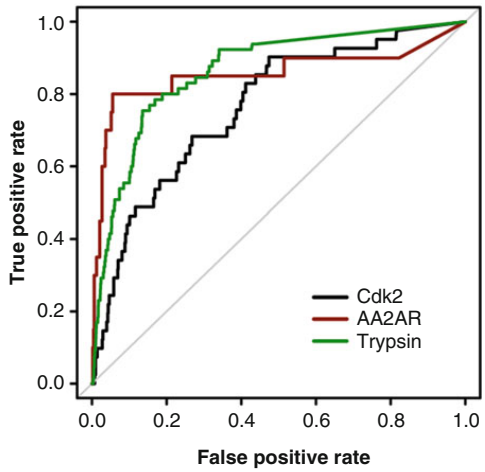

Fig. 4 ROC curves for the CDK2 (black), AA2AR (red), and trypsin (green) sets from the directory of useful decoys. The plotted results correspond to two DUck runs per ligand

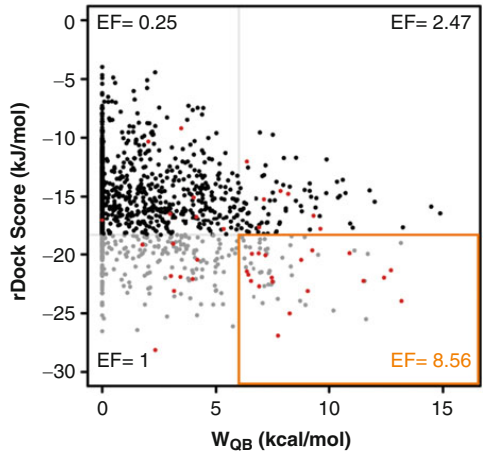

Fig. 5 Docking score (rDock) versus W_{QB} values for active (red) and inactive (black or gray) compounds in the CDK2 retrospective virtual screening dataset. The quadrant in orange highlights the area that corresponds to the top 25% docking score and top 25% W_{QB} values in which the optimal enrichment factors (EFs) are achieved

In the following sections, you will find a detailed explanation about how to prepare and run dynamic undocking. A step-by-step guide will walk you through the whole process, and a final section of "Notes" will help you in case any issues or errors arise.

2 Materials

1. Molecular Operating Environment (MOE) [6]. Download MOE (versions 2015, 2016, and above). License is required. Open MOE installer, and follow the instructions.
2. Molecular dynamics package (AMBER) [7]. Download Amber and AmberTools (version 16) from their website (http://ambermd.org/), and follow the installation instructions for your platform. AmberTools is free, but you will need a license for running Amber. Make sure AmberTools is installed locally and their binaries are visible (adapt $PATH variable if needed) so MOE can run them.
3. PyMOL [8]. Download the PyMOL molecular viewer at http://www.pymol.org/. Click on "Download." On the next page, fill out the information according to your status. Follow the instructions to download and install PyMOL.
4. R [9]. Download R software from https://cran.r-project.org/ for your platform. Follow the instructions, and make sure that R and Rscript binaries are visible during production stage.
5. DUck scripts. Download the public DUck scripts from https://github.com/CBDD/duck. Make sure $MOE_SVL_LOAD variable is declared and pointing to the DUck scripts directory (MOE2015). Make sure all scripts are located in $HOME/moefiles/svl directory (MOE2016 and newer).
6. Hardware: a computer workstation with Linux or MAC OS for DUck preparations; a computational cluster with Linux-based OS for parallelization, and GPUs for MD simulations (DUck is compatible with SGE and SLURM queuing systems).

3 Methods

3.1 Dynamic Undocking

Dynamic undocking is a particular type of molecular dynamics (MD). As such, the system must get parameters from an existing molecular mechanics force field (protein) or must be parameterized according to a compatible protocol (ligands). The protein–ligand complex must also be solvated and treated as a periodic system. Ultimately, running the dynamic undocking is just a matter of creating certain files that contain the parameters describing the system (topology file); the initial atomic positions (coordinate

files); the parameters that control execution of the MD software (input files); and, finally, the sequence of commands that establish how, where, and in which order the various simulations and analysis scripts will be executed (execution files). Preparation of these files could be done in different ways, and the expert user may choose to adopt their own protocols. Equally, most MD software packages have the capability of running steered MD and could be used to carry out DUck. However, here we will describe the current protocols developed in our group. They have the advantage of being automatic and computationally efficient, but they rely on commercial software (MOE and AMBER). We are currently working to provide an open-source solution, which will follow a similar workflow to the one described herein.

3.2 Ligand Preparation

For running the dynamic undocking, we first need a collection of small molecules, or ligands, which will be subjected to the simulation. In order to correctly create this collection, the following steps should be carried out:

1. Starting from a file with all ligand structures (we use the MDL SD file format (sdf)), open it with MOE, and save it as an mdb (molecular database) file. The structure of the ligands should already be in the binding site, either from a crystallographic structure or from a binding mode predicted by docking (*see* **Note 1**).
2. All the ligands must have a well-defined protonation and tautomeric state, as parameterization and DUck simulations will use the ligands as provided by the user (*see* **Note 2**). Also, hydrogen atoms must be explicit for all molecules: to add them to all the ligands with MOE, click on Compute > Molecule > Wash. Unmark all the options, and set the Hydrogens value to Add Explicit, and name the destination field "mol" (*see* **Note 3**).

3.3 Identification of H-Bond

Dynamic undocking relies on the presence of a key interaction, specifically a hydrogen bond, which is considered fundamental for binding. Almost all protein–ligand complexes form at least one hydrogen bond. On the other hand, most systems form more than one hydrogen bond, and each of them could potentially be used as the key interaction point for DUck simulations. In practice, we use a single hydrogen bond formed between the ligand and a particular atom on the protein side. Depending on the existing data, different approaches can be used in order to identify the key interaction.

3.3.1 Case A: Multiple Protein–Ligand Complexes Are Known

1. Align the protein structures to obtain a 3D superimposition of the ligands. Then a pharmacophore can be elucidated. There are plenty of options (free and licensed software such as Maestro [10] or MOE) that allow the user to identify a

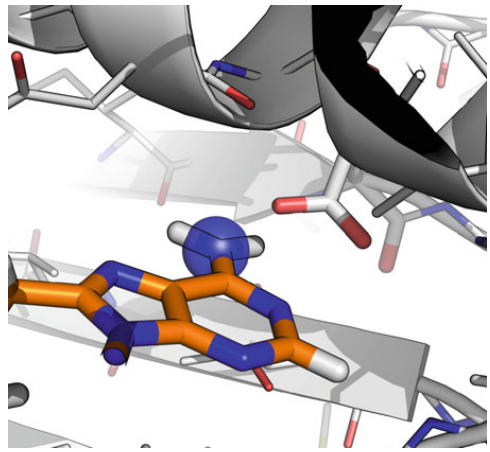

Fig. 6 An example of a complex with a single key interaction

pharmacophore for a specific protein from a given set of known binders (and non-binders).

2. From this pharmacophore identification, hydrogen bonds are detected and applied for DUck simulations, as detailed in Subheading 3.5.
3. The cases where only 1 hydrogen bond is identified, DUck will only be run for this key interaction (Fig. 6). On the other hand, there might be protein–ligand complexes with more than one hydrogen bond (Fig. 7). In this case, if there is not any additional information to identify which of these hydrogen bonds should be selected, independent DUck simulations for each of these interactions should be carried out (*see* **Note 4**).

3.3.2 Case B: Novel Binding Sites

If a pharmacophore definition can't be obtained due to a lack of known protein–ligand complexes, other approaches should be followed in order to identify possible key interaction points:

1. The structure can provide valuable hints, as the interaction will usually occupy a central position in the binding site. Further, the polar group in the protein will likely display the characteristics of an almost buried polar atom (low SASA, convex local surface curvature) and generally corresponds to a low mobility area.
2. Empirical data, especially the effect of point mutations on substrate recognition, may also be useful. On enzymes, the residues that are important for ligand recognition are often the ones that define the most important interaction with the inhibitors.

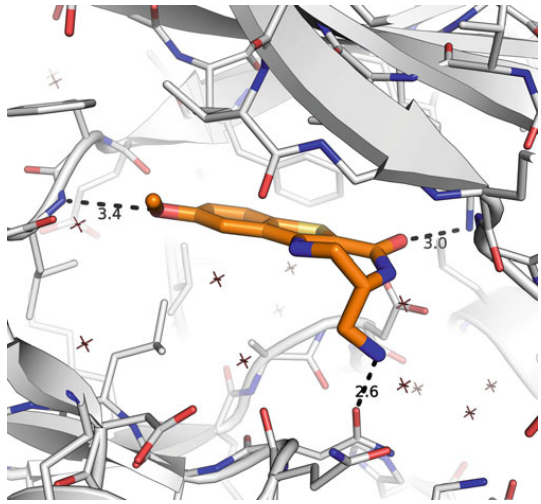

Fig. 7 An example of a complex with multiple hydrogen bonds

3. Computational methods that identify binding hot spots can be used to select a candidate interaction point. We find MDmix (MD simulations with mixed cosolvents) very useful to prioritize interaction points based on the relative strength of their binding hot spots. Other methods exist, but it's out of the scope of this book chapter to list or compare the alternatives, so we recommend the user to look to the bibliography for more details on the technique [11, 12].

3.4 Chunk Creation

One of the most important steps in system preparation is chunk selection. "Chunk" is a minimal subset of residues that preserve the local environment around the key hydrogen bond (Fig. 8).

Selection of residues is essential for the accurate result of dynamic undocking; thus very careful visual inspection is required (*see* **Note 5**). Excess residues will slow down calculation and can potentially block the ligand from leaving the pocket, resulting in very high W_{QB} values that do not reflect the strength of the hydrogen bond. An incomplete structure will result in artificially high solvent exposure, which will render the hydrogen bond more labile and cause to underestimate W_{QB} value. The following steps describe chunk preparation process:

1. If dynamic undocking was preceded by docking, it is best to use the same protonated structure. In any other case, e.g., X-ray structure, the protein structure must be prepared by protonation with a standard protocol implemented in MOE software or other protonation methods. Essential water molecules for complex stability must be identified and preserved in the

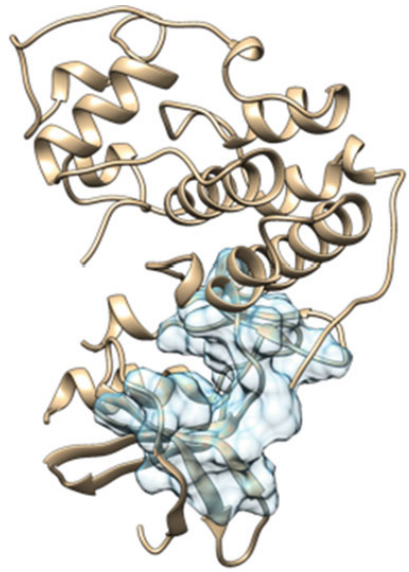

Fig. 8 Chunk of protein, constructed from pocket residues, compared to whole protein structure

structure (*see* **Note 6**). The rest of water molecules, ions, and other ligands must be removed from the system.

2. Initially, chunk is created by selecting residues within 6 Å of the atom of reference. To complete the base selection further, visual inspection is needed. Additional residues must be added, based on following rules:
   (a) Residues important for protein–ligand interaction.
   (b) Residues blocking the channels in the structure, preventing solvent molecules from accessing the key H-bond through holes created when carving the chunk out of the protein matrix.
   (c) Residues connecting parts of the chunk, if sequence gap between two selected parts of the protein is less than three residues.
   (d) Preserve interstitial water molecules that may be essential for complex stability.
3. Unselected residues are eliminated. Typically, this causes polypeptide chains to split into separate chains. To prevent charged ends and unnatural electrostatic forces, chains must be capped with acetyl and N-methyl groups.
4. Final structure has to be saved in MOE format, with names of residues adjusted to AMBER force field (*see* **Note 7**).

3.5 Simulation Preparation

In this step that has to be run in MOE, the system and simulation parameter files are generated automatically by a MOE SVL script. Before proceeding further, make sure that the MOE format file with the prepared chunk and the mdb file with ligand/poses library are located in the same directory.

1. First, the chunk structure has to be opened in MOE, and the atom defining the key protein–ligand hydrogen bond has to be selected.
2. The duck.svl script must be loaded in MOE (from $MOE_SVL_LOAD directory in MOE2015 and previous versions, for newer versions see details in **Note 8**). It opens a window with parameters for the simulation (Fig. 9).
   (a) "load additional params"—field is useful in cases of structures of ligands with metal ions (Zn^{2+}, Ca^{2+}, or Mn^{2+}), since the force field parameters for metal ions are not included in the standard force field.
   (b) The other variable is a queue system that will be used for the simulation, either SGE or SLURM. However, it is also possible to run calculations on local UNIX. Appropriate *.sh files are created when the box is marked.

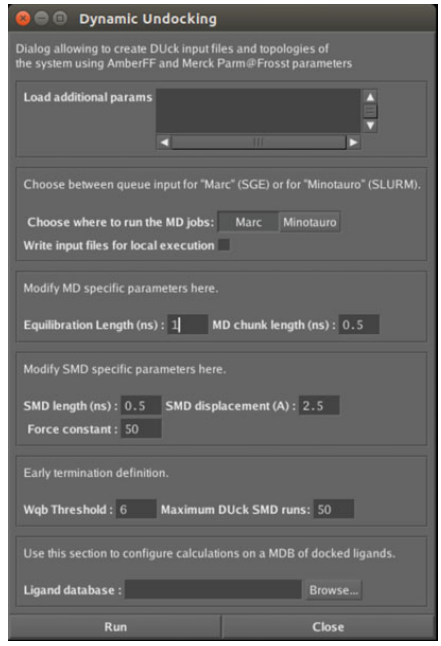

Fig. 9 Duck.svl graphical window in MOE

(c) In the next section, MD parameters can be modified:
- "Equilibration Length" (default 1 ns).
- "MD chunk length" (default 0.5 ns)—length of free MD between consecutive SMD simulations in order to generate different starting points for SMD.

(d) In the next section, SMD parameters can be modified:
- "SMD length" (default 0.5 ns)—length of each SMD step.
- "SMD displacement" (default 2.5 Å)—the distance that the ligand is going to be displaced, starting at the distance of 2.5 Å from reference atom in ligand, finishing at 5 Å by default.
- "Force constant" (default 50 kcal/mol $Å^2$)—force constant of the spring that is pulling the ligand out of the pocket.

(e) In the "Early termination definition" section, following actions can be done:
- "W_{QB} threshold" (default 6 kcal/mol)—establishes threshold of work value, below which calculations will be terminated. Optimal value depends on the system and set of ligands. For most cases, the threshold 6 kcal/mol is sufficient. If, for your system, known ligands bind with weak forces, a lower W_{QB} threshold may be necessary (*see* **Note 9**).
- "Max DUck SMD runs" (default 50)—sets the maximum number of calculations (*see* **Note 10**).

(f) In the last section, the ligand database must be selected. Ligands have to be in the binding site, as mentioned in previous sections.

3. Executed script performs the following steps:

(a) Calculates AM1-BCC charges [13] for all the ligands (*see* **Note 11**).

(b) Assigns Parm@Frosst [14], atom types, and nonbonded parameters to the ligands.

(c) Identifies the atom of each ligand that makes the hydrogen bond with the protein's reference atom (based on the distance).

(d) Writes input and execution files to carry out the MD simulations with AMBER.

(e) Calls AMBER's tleap to generate valid topology and coordinate files for each individual receptor–ligand complex (*see* **Note 12**).

4. The script creates a series of files that will perform the dynamic undocking, which can be later transferred to a server. For the protein, AMBER force field 99SB is used. Each system is placed in a cuboid box spanning at least 18 Å more than the furthest atom in each direction. The box is then filled with TIP3P water molecules to create periodic boundary conditions. When needed, Na^+ or Cl^- are added to force the neutrality of the whole system. As an output, the duck.svl script creates series of files:
   (a) submit_duck_smd_gpu.csh – calls *.q files in subdirectories and submits SMDs to the queue system.
   (b) getWqbValues.R – R script that calculates the value of W_{QB}. More details are given in "Result Analysis" section.
   (c) The rest of the files are collected in LIG_target_* folders, separated for every ligand:
      - duck_template_gpu.q and duck_template_gpu_325K.q—submit the SMD to queue system.
      - equil.q, md*.q—equilibration file submits a job with equilibration of the system to the server queue; the md*q files submit jobs that perform the SMDs (both in 300 K and 325 K), preceded by 0.5 ns of unbiased molecular dynamics, to increase the sampling.
      - 1_min.in, 2_eq.in, 3_eq_200.in, 3_eq_250.in, 3_eq_300.in, 4a_eq.in, 4b_eq.in—AMBER input files for the equilibration stage.
      - md.in—AMBER input files containing the parameters for the MD stage.
      - duck.in and duck_325K.in—AMBER input files with parameters for the SMD stage at 300 K and 325 K, respectively. The different temperature is simply used to ensure that both SMDs follow different trajectories even though they start from the same restart file.
      - dist_md.rst—file needed for MD simulations. It includes the indexes of the atoms that form the defined hydrogen bond and the parameters of restraints applied to ligand during MD.
      - dist_duck.rst—file needed for SMD simulations. It includes the indexes of the atoms that form the defined hydrogen bond and the initial and final distance between key atom in the receptor and end of the string that applies the force to the ligand during the SMD.
      - lib/—directory that gathers the files with coordinates and topology of the solvated system in the simulation box that will be used as input for the simulation.

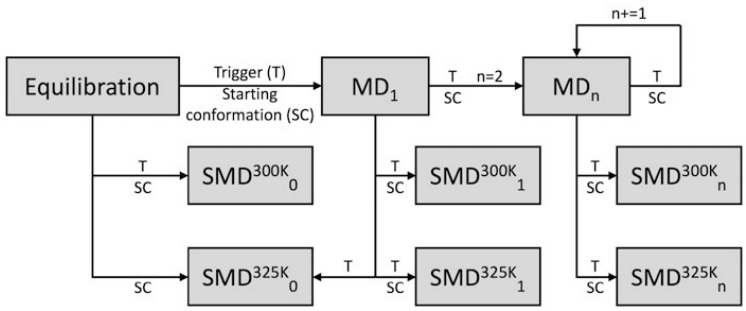

Fig. 10 Scheme of the DUck workflow

3.6 Production Stage

In the production stage, a series of MD and SMD simulations using AMBER are performed for every ligand in the library. All files required for proper execution are generated in previous stage, and they are located in LIG_target_* folders (Fig. 10).

The process is comprised by different parts:

1. First, the system is equilibrated in the following steps:
   (a) Energy minimization for 1000 cycles.
   (b) Assignment of random velocities at 100 K and gradual warming to 300 K for 400 ps in the NVT ensemble.
   (c) Equilibration of the system for 1 ns in the NPT ensemble (1 atm, 300 K).
2. Equilibration stage produces:
   (a) *.rst—restart files for the next step of calculations.
   (b) *.out—standard AMBER output files.
   (c) equil.q.e equil.q.o—files helping identifying process and errors in the simulation.
3. Equilibration stage is followed by a series of MDs and SMDs with conditions as follows:
   (a) At all stages, harmonic restraints with a force constant of 1 kcal/mol Å^2 are placed on all non-hydrogen atoms of the receptor to prevent structural changes.
   (b) Spontaneous rupture of the key hydrogen bond during non-steered simulations is prevented with a gradual restraint for distances beyond 3 Å (parabolic with $k = 1$ kcal/mol, Å^2 between 3 Å and 4 Å, and linear with $k = 10$ kcal/mol Å^2 beyond 4 Å).
   (c) All equilibration and simulation steps were run using Langevin thermostat with a collision frequency of 4 ps^{-1}, and the cutoff for nonbonded interactions was set to 12 Å.
   (d) Bonds involving hydrogen are constrained using SHAKE.

4. The first step of SMD is executed in 300 K. The SMD lasts 500 ps, during which time the distance between the atoms forming the key hydrogen bond is steered, by default, from 2.5 Å to 5.0 Å (this distance, however, can be changed in the parameters, as explained in Subheading 3.5), with constant velocity of 5 Å/ns and spring constant of 50 kcal/mol Å^2. Once the first SMD is completed, W_{QB} is evaluated, which can trigger the continuation of the process or stop the simulation altogether if W_{QB} is lower than the predefined threshold. Thus, running the first SMD only at one temperature saves calculation time. Results of SMD are gathered in DUCK_* folder:
   (a) duck.dat—file with four columns (*see* **Note 13**):
      - Distance between reference atom in chunk and place where the additional potential is applied.
      - Distance between key atom in chunk and equivalent atom in ligand.
      - Value of force applied to ligand.
      - Value of work.
   (b) duck_*.q.e duck_*.q.o—files that help the identifying process and errors in the simulation.
5. The first step of MD follows the trajectory generated by equilibration stage in the previous step.
6. The MD stage produces:
   (a) *.rst—restart files for the next step of calculations.
   (b) *.out—standard AMBER output files.
   (c) md.q.e md.q.o—files helping identifying process and errors in the simulation.
7. The first MD triggers the first SMD in 325 K and two new SMDs in both temperatures. The first SMD in higher temperature starts from the same restart file as the first SMD in 300 K (**step 4**). The two subsequent SMDs follow the trajectory generated by first MD and proceed at different temperatures (300 K and 325 K) to ensure different trajectories.
8. To generate diverse starting points for SMD trajectories, we perform 0.5 ns of unbiased MD simulation, and repeat the process as many times as set in the SVL window (e.g., 50 steps of unbiased MD simulations are needed to execute 100 SMD trajectories). Fifty is enough repetitions to satisfactory evaluate W_{QB} value. To decrease time of calculation for virtual screening, 5 SMDs runs are recommended.
   (a) Before and after performing every DUck step, getWqbValues.R script calculates the W_{QB} value, and if it is greater than established threshold, md{n + 1}.q will be submitted.

Jobs must be submitted to server queue manager.

(a) SLURM queue system:

- $ sbatch equil.q.

(b) SGE queue system:

- $ qsub equil.q.

3.7 Analysis

Once the production stage is finished, the work necessary to reach the quasi-bound state can be calculated:

1. In the simulation preparation stage, the script for calculating the W_{QB} is created and stored in the main folder of the DUck project. To run it, enter the desired folder, and run it as Rscript ../getWqbValues.R that will return the W_{QB} value on standard output. It will read the output from all completed SMDs that have finished, and return the lowest value of all W_{QB} values calculated for each replica.
2. To visualize the results, the same script can be called with the flag "plot" that will generate a summary plot, "wqb_plot.png" (Fig. 11), and a file, "wqb_final.txt," with the calculated W_{QB} in the first and only line (8.29 for the example in Fig. 11).
3. This script can be called at any time, so it might happen that some SMD simulations are still running or they have finished earlier than they should. These and other types of errors are taken into account by the script. More details on how these errors are managed are provided in **Note 14**.

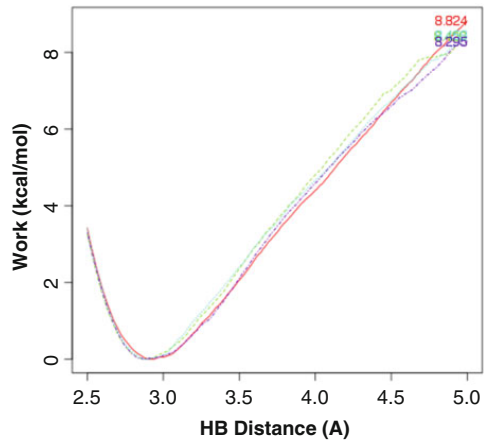

Fig. 11 Example of summary plot of W_{QB} obtained by running Rscript ../getWqbValues.R plot

4 Notes

1. Dynamic undocking needs a starting pose of the ligand in the binding site. This starting pose can be obtained from a crystallographic structure, ideally, but also from binding mode prediction programs such as docking. In the latter case, the user needs to be sure that the starting pose is representative of true pose; otherwise dynamic undocking calculations might be wrong.
2. Having the correct protonation and tautomeric states is something that has been widely discussed in the past years. For docked poses, the different stereoisomers should be generated prior to running docking, i.e., with programs like Schrödinger's ligprep or Chemaxon suite. On the other hand, most of the ligands that come from crystallographic structures of the PDB are correct. However, some of them have incorrectly assigned topologies, or the tautomeric state is not well defined. Double checking the structure by digging in the publication could avoid problems in the following stages.
3. After washing the molecules to add the explicit hydrogen atoms, be sure that the field is called mol. Dynamic undocking will use the "mol" field to prepare the simulations and parametrize the ligands. If no "mol" field is found, the first field with "molecule" format will be used.

   In order to avoid problems regarding this issue, it is strongly recommended to change the field name of the unwashed molecule to "mol_unwashed," for example, and then save the washed molecules in a field named "mol."
4. One common problem in the identification of the key hydrogen bond is the case where more than one hydrogen bond could be selected. In ref. 1, there is a specific example addressing this issue: a ligand had three different hydrogen bonds, and it turned out that the one used for the rest of the ligands in the dataset was not the key interaction point for this ligand. After running two more DUck simulations with the other possibilities, the key interaction was identified. The suggested approach when the user happens to be in such scenario is to run independent runs for each of the possible hydrogen bonds and select the one with higher W_{QB}.
5. In case of multiple interaction points (hydrogen bonds) are selected, individual chunks of protein must be created for each key atom separately.
6. Water molecules can have a big influence on complex stability. Some water molecules mediate interactions between ligand and protein. It is worth inspecting the structure more closely and preserving important water molecules. For example, in

complexes of Hsp90, water molecules are crucial in mediating interactions between protein and ligand.

7. If the structure of the chunk contains ASH residue, duck.svl will crash during tleap system preparation stage. Crash is caused by different namings of residues in MOE and AMBER. To fix the problem, remove HD2 hydrogen from the structure, and run duck.svl script on modified system.
8. Preparation process described in the chapter is adjusted to MOE2015. In MOE2016, developer changed the way that environmental variables are handled. In the new version of MOE, copy the svl files /scripts and /tleap to the $HOME/moefiles/svl directory, and run svl as described in the chapter.
9. If structures of protein with ligands are available, the best way to estimate W_{QB} threshold value is to run DUck for the known complexes. Use exhaustive sampling (20–50 SMDs).
10. 50 SMD runs are recommended for precise estimation of W_{QB} value. For accurate estimation, 20 runs is enough. For virtual screening purposes, 5–7 runs with threshold-based early termination are recommended.
11. SVL script might crash during calculation of AM1-BCC charges for the ligand. If so, the script will not create systems for invalid ligands, leaving a gap in LIG_target_* folders numbering. The easiest way to avoid the problem is calculating partial charges in MOE. Load *.mdb file with ligand/pose library, and calculate partial charges (Compute > Molecule > Partial charges...) with "AM1-BCC" selected in the "Method" field. If charges are calculated for all of ligands without problem, SVL script should run smoothly. Otherwise, discard or fix the problematic ligands. Sometimes crash is caused by the initial 3D geometry (e.g., internal clash), and slight changes of atomic positions (e.g., bond rotation) can fix the issue.
12. Another problem with system preparation might be caused by tleap. In case system cannot be created, the following error will be displayed:

    Error, tleap did not manage to build the system.
    There might be a couple of reasons for such error:

    (a) tleap cannot be run from the terminal. Make sure that AmberTools is properly installed and can be executed in the terminal. Loading appropriate module might be necessary.

    (b) If the chunk contains ASH residue. For solution look at **Note 7**.

    (c) Wrong force field file pointed in SVL script. For new version of AmberTools (16), FF file is named leaprc.

ff99Bild; however for older versions, this file may be in oldFF directory. In this case to fix the error, editing duck.svl script is required.

```
$ sed 's/leaprc\.ff99Bild/oldFF\/leaprc\.ff99Bild/' duck.svl
> tmp.
$ mv tmp duck.svl
```

13. Checking duck.dat is the best way to ensure that the step of the simulation is completed. With the default parameters, this file should be exactly 5000 lines long. If something went wrong during the simulation, e.g., the server crashed, for some of the ligands, this file will be shorter.
14. The script to calculate the W_{QB} can be run at any point of the DUck simulation. This can lead to error where some SMD simulations are not over or have been abruptly terminated, which is of particular importance when the script is used to decide whether more steps of MD + SMD simulations need to be carried or not.

A correctly finished SMD simulation will have a duck.dat file similar to:

2.50000	2.92018	−42.01769	0.00000
2.50050	2.78965	−28.91455	−0.01097
2.50100	2.55078	−4.97794	−0.02026
2.50150	2.71974	−21.82384	−0.02933
2.50200	2.63421	−13.22120	−0.03907
[...]			
4.99700	5.02624	−2.92401	0.30579
4.99750	5.09999	−10.24863	0.30125
4.99800	4.98177	1.62251	0.30058
4.99850	5.00014	−0.16448	0.29868
4.99900	5.06074	−6.17372	0.29649
4.99950	5.04282	−4.33195	0.29338

where 2.5 and 5.0 are the defined starting and final point of the hydrogen bond distance. The script will check that the final line is actually the defined final point (±0.001 A); otherwise it will return a W_{QB} of 100.

References

1. Ruiz-Carmona S, Schmidtke P, Luque FJ et al (2017) Dynamic undocking and the quasi-bound state as tools for drug discovery. Nat Chem 9(3):201–206. https://doi.org/10.1038/nchem.2660
2. Chodera JD, Mobley DL, Shirts MR et al (2011) Alchemical free energy methods for drug discovery : progress and challenges. Curr Opin Struct Biol 21(2):150–160. https://doi.org/10.1016/j.sbi.2011.01.011
3. Schmidtke P, Luque FJ, Murray JB, Barril X (2011) Shielded hydrogen bonds as structural determinants of binding kinetics: application in drug design. J Am Chem Soc 133 (46):18903–18910. https://doi.org/10.1021/ja207494u
4. Ferenczy GG, Keseru GM (2012) Thermodynamics of fragment binding. J Chem Inf Model 52(4):1039–1045. https://doi.org/10.1021/ci200608b
5. Huang N, Shoichet BK, Irwin JJ (2006) Benchmarking sets for molecular docking. J Med Chem 49(23):6789–6801. https://doi.org/10.1021/jm0608356
6. Molecular Operating Environment (MOE), 2013.08 (2016) Chemical Computing Group Inc., 1010 Sherbooke St. West, Suite #910, Montreal, QC, Canada, H3A 2R7
7. Case DA et al (2016) Amber 16. University of California, San Francisco
8. DeLano WL (2014) The PyMOL Molecular Graphics System, Version 1.8. Schrödinger LLC. http://www.pymol.org. https://doi.org/10.1038/hr.2014.17
9. R Core Team (2017) R: a language and environment for statistical computing. R Foundation for Statistical Computing, Vienna, Austria https://www.R-project.org/
10. Schrödinger Release 2017-3: Maestro, Schrödinger, LLC, New York, NY, 2017
11. Seco J, Luque FJ, Barril X (2009) Binding site detection and druggability index from first principles. J Med Chem 52(8):2363–2371. https://doi.org/10.1021/jm801385d
12. Álvarez-García D, Barril X (2014) Molecular simulations with solvent competition quantify water displaceability and provide accurate interaction maps of protein binding sites. J Med Chem 57(20):8530–8539. https://doi.org/10.1021/jm5010418
13. Jakalian A, Jack DB, Bayly CI (2002) Fast, efficient generation of high-quality atomic charges. AM1-BCC model: II. Parameterization and validation. J Comp Chem 23(16):1623–1641. https://doi.org/10.1002/jcc.10128
14. Bayly CI, McKay D, Truchon J-F (2011) An Informal AMBER Small Molecule Force Field: parm@Frosst. Computational Chemistry Ltd.